Summer 2015

Classification of Digital Communication Signal Modulation Schemes in Multipath Environments Using Higher Order Statistics

Meena Sreekantamurthy
Old Dominion University

CLASSIFICATION OF DIGITAL COMMUNICATION SIGNAL MODULATION SCHEMES IN MULTIPATH ENVIRONMENTS USING HIGHER ORDER STATISTICS

by

Meena Sreekantamurthy
B.S. May 2011, Virginia Commonwealth University

A Thesis Submitted to the Faculty of
Old Dominion University in Partial Fulfillment of the
Requirements for the Degree of

MASTER OF SCIENCE

ELECTRICAL AND COMPUTER ENGINEERING

OLD DOMINION UNIVERSITY
August 2015

Approved by:

_____
Ravindra P. Joshi (Director)

_____
Linda L. Vahala (Co-Director)

_____
Duc Nguyen (Member)

ABSTRACT

CLASSIFICATION OF DIGITAL COMMUNICATION SIGNAL MODULATION SCHEMES IN MULTIPATH ENVIRONMENTS USING HIGHER ORDER STATISTICS

Meena Sreekantamurthy
Old Dominion University, 2015
Director: Dr. Ravindra P. Joshi
Co-Director: Dr. Linda L. Vahala

Automatic identification and classification of modulation schemes in communication signals and decoding of information from the captured signals has assumed great importance recently in the wireless communication industry. Advancements in communications have introduced a large variety of modulation schemes in the transmitted signals; consequently, reliable detection of the modulation scheme in the intercepted signal has become an important issue in communications. It is the aim of this thesis to address this issue of reliable detection. Therefore, this research is focused on modeling and simulation of an automatic modulation classifier and, in particular, on the development of algorithms to use higher order statistical characteristics detected in the communication signals received. This research began with an understanding of commonly used digital modulation schemes, such as Phase Shift Keying (PSK), Frequency Shift Keying (FSK), and Quadrature Amplitude Modulation (QAM). A basic framework for a numerical modeling and simulation of wireless communication systems was developed first to serve as a building block for the development of an automatic modulation classifier. Since signal noise plays an important role in the detection of signals received, the channel model of the wireless system was enhanced to allow signals with Additive White Gaussian Noise (AWGN) and multipath Rayleigh fading and multipath Ricean fading channels at various levels of Signal to Noise Ratios. In this study, an algorithm was developed to identify the modulation schemes used in the signals that is based on the eighth order cumulants extracted from the signals.

The functions and characteristics of the wireless communication transmitter, channel and receiver with an automatic modulation are modeled using user developed functions of the MATLAB® program and the associated MATLAB® Communication's Toolbox. Simulated digitally modulated signals were processed in the receiver to extract the signal's statistical moments and cumulants. Supplementary mathematical simulations have been performed to demonstrate the effect of communication channel disturbance in the detection of the signals at the receiver. These simulation experiments also recognized the benefits of a receiver with an automatic modulation classifier that could identify a range of modulation signals that may be received from multiple transmitters. The classification algorithm coded in the MATLAB® functions performs the threshold decisions to identify and classify the modulation schemes. The automatic classification modulation algorithm has helped to identify the modulation schemes in the signals by evaluating eighth order cumulants in the modulated signal. The modulation classifier algorithm developed is capable of detecting the signal modulation scheme even in the presence of noisy signals. The robustness and capabilities of the modulation classification algorithm were determined for reliable detection of the communication signals. Under various noise and multipath fading channel conditions, the classification modulation algorithm was able to successfully identify the modulation scheme of the transmitted signals with a success of 79.21% among all the trial cases of signals passed through the system.

In the memory of my late grandmother and grandfather.

ACKNOWLEDGMENTS

First and foremost, I would like to express my sincere gratitude to Old Dominion University for letting me fulfill my educational dream in higher studies. I am extremely grateful to Dr. Joshi for assistance and suggestions throughout my project. My deep appreciation also goes out to my co-advisor Dr. L. Vahala. Furthermore, I would like to thank Dr. Popescu, who has taught me many courses in the field of communication engineering, increasing my interest and broadening my knowledge in this area. My sincere thanks also to Dr. D. Nguyen for serving on my thesis committee. The time, effort, helpful comments and suggestions from my entire thesis committee are greatly appreciated.

I am grateful to my parents' for their love and unwavering support. Their encouragement and blessings helped me reach where I am today. I would also like to thank my sister with whom I can share all of my aspirations and feelings. I am extremely thankful for my friends and colleagues who have made my experience at Old Dominion memorable. I am beyond appreciative for their support and motivation. I am grateful for Newport News Shipbuilding, a Division of Huntington Ingalls Industries for sponsoring my M.S. graduate education.

NOMENCLATURE

AM	Amplitude Modulation
ASK	Amplitude Shift Keying
AWGN	Additive White Gaussian Noise
BER	Bit Error Rate
BPSK	Binary Phase Shift Keying (same as 2-PSK)
CDF	Cumulative Distribution Function
CW	Continuous Wave
dB	decibel
FM	Frequency Modulation
FSK	Frequency Shift Keying
GMSK	Gaussian Minimum Shift Keying
LOS	Line of Sight
MAP	Maximum A Posteriori Probability
MATLAB®	Matrix Laboratory, Software
ML	Maximum-Likelihood
M-FSK	M-ary Frequency-Shift Keying
M-PAM	M-ary Phase Amplitude Modulation
M-PSK	M-ary Phase-Shift Keying
MSK	Minimum Shift Keying
M-QAM	M-ary Quadrature Amplitude Modulation
PDF	Probability Density Function
PM	Phase Modulation
PAM	Pulse Amplitude Modulation
PSK	Phase Shift Keying
QAM	Quadrature Amplitude Modulation
QPSK	Quadrature Phase Shift Keying
SNR	Signal to Noise Ratio

TABLE OF CONTENTS

Page

Chapter Page

Chapter Page

LIST OF FIGURES

Figure Page

Figure Page

Figure Page

LIST OF TABLES

Table Page

Table Page

Table Page

CHAPTER 1

INTRODUCTION

1.1 Primary Purpose of Thesis Work

Modulation is an essential part of the telecommunications signal processing for conveying a message or information over a carrier signal wave that can readily transmit across a communication network. Digital modulation involves mapping information bits onto an analog signal for transmission over the communication network. The bits are binary digits taking on the values of either zero or one of the digital state. The digital modulation process usually accompanies the detection process where the bit sequence mapped onto the received signal is decoded to retrieve the message or information that was transmitted by the sender. The digital modulation therefore involves transfer of the digital bits stream over an analog bandpass channel constrained by a limited frequency bandwidth. A good digital signal modulation scheme along with good information recognition or a good decoding system is necessary for effective transfer of the communication signal, especially in the presence of noise. An efficient modulation scheme can achieve information transfer at a high data/bit rate, with minimum frequency bandwidth, with maximum power efficiency, and with minimum probability of bit error.

A digital signal communication system consists of three major components - a receiver, a channel and a transmitter. The transmitter generates random bits of information that represent the message in the form of a digital signal; they are modulated using one of the many available schemes for modulation. The modulated signal often passes through multipath channels having various levels of Signal to Noise Ratios (SNR). At the receiver end, the noisy signal is received and has to be analyzed or decoded to extract the original signal.

A wide variety of modulation methods currently exists, and the methods are generally grouped into either linear modulation methods or nonlinear modulation methods. The

first group of methods, linear modulation methods, includes several variations of phase-shift keying (PSK). The keying simply means signaling, and this term comes from telegraph terminology. The second group of methods include frequency-shift keying (FSK) and many of its variations [1, Ch. 5]. Besides these two modulation methods, there exist other methods, which can be viewed as either variants of phase-shift keying method or variants of frequency shift keying method. The commonly identified digital modulation methods are Phase Shift Keying (PSK) and its variants 2-PSK, 4-PSK and 8-PSK; Frequency Shift Keying (FSK) and its variants 4-FSK and 8-FSK. Other modulation schemes include Quadrature Amplitude Modulation (QAM) and its variants 16-QAM, 64-QAM and 256-QAM.

Automatic classification of modulation schemes in the communication signals has become an important theme in wireless communications [2]. Interest in this area has increased recently due to the urgent need to develop more intelligent and reliable communication systems. Automatic classifiers of modulation schemes assume great importance in both civilian and military applications [3]. Commercial applications of automatic modulation classifiers pertain to implementation of devices capable of identifying a range of modulation schemes that may be used in the intercepted signal without *a priori* knowledge of the modulation scheme coded into the signal. A few examples of commercial applications of digital modulation schemes classifiers pertain to software radio and reconfigurable systems, interference identification, and spectrum management [4]. In defense applications, receivers with an automatic modulation classifier are capable of automatically capturing and decoding the noisy signal received, thereby eliminating the complexity of preprocessing of the signal prior to the signal detection [5].

The importance of automatic modulation recognition has increased considerably over the past several years. Advancements in the telecommunication industry have introduced a large variety of modulation schemes and have reduced the ability of receivers to reliably detect the modulation scheme of the intercepted signal. As a result, numerous approaches have been proposed to enhance digital modulation classifiers [2]. Automatic classifiers can be distinctively grouped into two main subsets. These two types of

automatic modulation classifiers are (a) decision directed classifiers and (b) statistical pattern recognition classifiers. The decision directed classifiers are based on probabilistic and hypothesis arguments that are integrated to form a modulation classification scheme. This classification approach is optimal when the specific performance measures of the communication system are known. The statistical pattern recognition classifier is broken up into two subsystems: feature extraction and pattern recognition. The feature extraction classifier extracts useful information from the incoming signal and maps it to a chosen feature space. On the other hand, statistical pattern recognition extracts prominent statistical characteristics of the received signal and then decides the modulation scheme. In this thesis a decision directed automatic modulation classifier is implemented which uses the predetermined channel hypothesis to identify the signal modulation scheme. This type of classification model is easy to implement in receivers [2].

In the identification of modulation schemes used in the received signals, the presence of noise in the signals further complicates the development of modulation classification systems. Uncertainty in the signal must be accounted for by suitable statistical models derived from measurements on continuous signals as well as from the discrete sampled signals. Hence there is a need for appropriate statistical tools for carrying out these operations in real time. Statistical tools such as mean function or first moment of random process, cumulative distribution functions, probability density function, and second moments are needed for statistical specification of the random process. In this regard, higher-order statistics such as higher order-moments and cumulants bring out promising features of signal characteristics to enable classification of unknown modulation types. The reason that the higher order moments and cumulants are promising is because they appear to be particularly forgiving in very noisy signals. Whether these higher-order statistical features of the noisy signal can be favorably used in the classification of the modulation schemes used in the signal received remains to be investigated and, hence, is the purpose of this thesis.

This research study demonstrates that the higher order statistical features can be used in the classification of the modulation scheme in a received signal. First, the classification

of commonly used digital modulation types, such as PSK, FSK, and QAM are studied. Then, the receiver, the channel, and the transmitter functions and their characteristics are modeled using user-developed functions of the MATLAB® program so that the various modulation schemes can be evaluated. In this study, a particular modulation classification algorithm is developed that is based on the eighth order cumulants to identify the modulation scheme. The eighth order cumulants algorithm is implemented in the user developed algorithm. The Additive White Gaussian Noise (AWGN) and multipath channels at various levels of SNR are implemented in the MATLAB® program. Computations are made with the noisy signal coded into the receiver model to extract the higher order moments and cumulants. The higher order statistical characteristics of the noisy signal are passed on to the classification algorithm coded in the MATLAB® functions, which can make threshold decisions to identify and classify the modulation scheme. Finally, the robustness and capabilities of a modulation classification algorithm are investigated. The modulation classifier algorithm is capable of detecting the signal modulation scheme even in the additive white Gaussian noisy signal passed through Rayleigh [1, Ch. 3] and Ricean [1, Ch. 3] multipath at various SNR levels.

1.2 Scope

A high-level description of the fundamental elements of a communication system is studied first to understand the process of transmitting and receiving a wireless signal. The conventional receiver is examined to recognize the importance of an automatic modulation classifier. Usually a wireless system uses a modulation scheme best suited for the channel characteristics in order to ensure that the transmitted signal is adequately replicated at the user end. A literature survey is performed to list some of the contributions that have been made to assist in developing automatic modulation classifiers. In this study, a modulation classification algorithm is designed to investigate the ability to determine the modulation scheme of the received signal without *a priori* information on the modulation type of the transmitted signal.

A wireless communication system is modeled to develop and simulate an automatic modulation classifier that will identify the modulation scheme of the received signal. In the simulation model of the communication system, various modulated signals are transmitted through the communication channel to extract the received signal's moments and cumulants. The statistical characteristics of higher order moment and cumulant have been studied to design an automatic modulation classifier. MATLAB® software has been used to design a modulation classification algorithm that identifies the modulation scheme of the received signal based on eighth order cumulants. In this research, the signals are propagated through the AWGN channel, Rayleigh multipath fading channel, and Ricean multipath fading channel to observe the robustness of the classification algorithm developed.

Supplementary mathematical simulations are performed to demonstrate the effect of communication channel disturbance on the signal detection at the receiver. Signals are modulated using M-ary Phase Amplitude Modulation (M-PAM) and M-ary Phase Shift Keying (M-PSK) to compare the performance and tradeoffs of these modulated signals when propagated through various levels of noisy channels. These experiments are performed to recognize the benefits of a receiver with an automatic modulation classifier that could identify a range of modulation signals that may be received from multiple transmitters or a transmitter using a range of modulation schemes.

The scope of the communication system model generated is limited to 20,000 bits of random data to represent an information signal. Each signal is modulated 1,000 times with a particular modulation scheme and taken to be transmitted through a noisy communication channel. Higher order statistics on this noisy signal were computed and passed to the modulation classifier to examine the ability of the algorithm to correctly identify the modulation scheme. The modulation classification algorithm identifies the modulation scheme of a signal by evaluating whether the received signal's statistical features lie within a predefined cumulant threshold range. These predefined cumulant threshold ranges were determined upon higher order statistical analysis of modulated signals that propagated through an AWGN channel at various levels of SNRs.

The scope of this research is limited to signals that are modulated using Binary Phase Shift Keying (BPSK) or 2-PSK, 4-PSK, 8-PSK, 2-FSK, 4-FSK, 8-FSK, 8-QAM, 16-QAM, 64-QAM and 256-QAM schemes. The modulation classification algorithm is able to distinguish among four modulation schemes, namely, BPSK, 4-PSK, 8-PSK, 8-QAM. It is also able to identify the signal class formats of FSK (2-FSK, 4-FSK, 8-FSK) as M-ary Frequency Shift Keying (M-FSK) and signal class formats of QAM (16-QAM, 64-QAM and 256-QAM) as M-ary Quadrature Amplitude Modulation. The ability of the modulation classification algorithm to detect the modulation scheme of the transmitted signal is evaluated on modulated signals that are passed through Rayleigh and Ricean multipath channels with AWGN at various levels of SNRs. Section 1.3 outlines some of the literature on this topic and presents the contributions made in this thesis to assist in advancement of the modulation classification algorithm.

1.3 Previous Work

Research work has been reported on using selected features of intercepted signals to successfully detect the digital modulation scheme. The following sections describe some of the publications made in this field.

Le Martret and M. Boiteau [6] used a combination of fourth order and second order moments to classify 4-PSK and 16-QAM modulation schemes using a pattern recognition approach. The classification system developed in this research was able to detect close to 100% of the modulated signal at SNR levels equal to 0 dB or higher. However, since modern telecommunications consist of several modulation types, this classifier would not be able to recognize other schemes. Additionally, the classification algorithm did not take into consideration multipath channels.

Marchand [7] later extended this research in a dissertation which proposed a computationally simple and inexpensive scheme that could classify M-PSK and M-QAM signals by using cyclical statistics of higher order. The robustness of the designed classification algorithm was also evaluated at various levels of AWGN and at various

number of information symbols. However, this study did not evaluate the performance of the classification algorithm on signals propagated through multipath channels.

Taira and Murakami [4] proposed an automatic classification procedure that discriminated between analog modulation and digital modulation signals. Amongst the analog modulation signals, phase-continuous FSK signals could be identified using statistical parameters of the signal envelope. However, this research did not attempt to classify the various digital modulation schemes, and only a variety of analog modulation schemes were classified using the algorithm developed. Nowadays, since communication systems are mostly digital based, designing an analog modulation classifier does not have practical value.

Soliman and Hsue [8] approached the modulation classification problem in terms of hypothesis testing. The classification algorithm used signal moments to identify the M-PSK modulation schemes. This research simulated successful modulation identification for SNR levels greater than 15 dB. However, performance of the modulation classifier was not evaluated based on any real world propagation models.

Dobre, Bar-Ness and Su [9], [10] proposed a robust automatic recognition algorithm that could classify PSK and QAM signals based on higher order cyclic cumulants. The advantage to this algorithm was that it could detect the modulation scheme on intercepted signals that had carrier phase and frequency offsets. A hierarchical classification scheme was developed to first identify the signal class format (i.e., M-QAM, M-PSK) and then choose the modulation order (M) within the selected signal class. Even though the simulated data matched the theoretical calculations, this classifier would not be able to identify the other vast quantities of modulation schemes in the world of digital communications.

Kalinin and Kavalov [11] used a neural network processor to automatically recognize two types of digital passband modulations. A feed-forward network with six hidden neurons was trained to recognize BPSK and Minimum Shift Keying (MSK) signals in the presence of AWGN. Simulation results showed that the neural network processor was able to correctly identify 95-99% of the modulation schemes correctly for SNR levels of

10 dB to 12 dB. This publication did not report classification results for higher levels of SNRs. Additionally, this research did not evaluate classification of FSK and QAM signals. Further, the propagation channel was not appropriately modeled to represent realistic channels such as urban or rural environments.

Baarrij, Nasir and Masood [12], developed a real time modulation classifier to detect digitally modulated signals without any prior knowledge of the intercepted signal parameters. The classifier was hierarchical and used linear approximations to detect FSK, PSK, Amplitude Shift Keying (ASK), QAM and Gaussian Minimum Shift Keying (GMSK) modulation types. Simulation results showed that the classifier was able to accurately recognize nearly 99% of the signals for SNR levels as low as 5 dB. However, their study only evaluated the classifier on signals propagated through a AWGN channel propagation and did not consider the effects due to signals intercepted from multipath channels.

Hatzichristos [13] developed a modulation classification scheme based on neural networks. However, the higher order moments and cumulants for FSK and other modulation schemes did not match the theoretical calculations. As a result, the data in some of their tables may be inaccurate. Furthermore, Young [14] performed similar research in parallel to Hatzichristos. Young developed a decision directed classifier that used higher order cumulants to distinguish all modulation schemes. Signal generation and propagation were modeled using Simulink®, and MATLAB® software tools to simulate the receiver with the modulation classification algorithm. Simulation results showed that at low levels of SNRs, the classifier was able to distinguish only 72.3% of the signals distorted by an AWGN channel. This research also had similar errors in the theoretical calculations of the modulation schemes. This in turn motivated the need to reevaluate the work of Hatzichristos and Young. In this thesis, higher order cumulants thresholds are used to show that the accuracy of the classification decision can be greatly improved for lower levels of SNRs.

1.4 Thesis Contributions and Organization

In this thesis, an automatic modulation scheme classifier algorithm is developed based on eighth order cumulants to identify the modulation type of the intercepted signal. The digital signals are taken to pass through the AWGN channel to extract cumulant threshold decisions for the classification algorithm. The robustness of the modulation classifier is tested by evaluating the ability of the algorithm to identify the modulation scheme of the signal passed through the Rayleigh and Ricean fading channels.

Chapter 2 provides a high level description of the fundamental elements of a communication system. The characteristics of the various modulation schemes such as PSK, FSK, and QAM are described in Section 2.13. Additionally, in this section both the conventional signal modulation and demodulation process are described to motivate the necessity of an automatic modulation classifier.

An introduction to the AWGN channel and the Ricean and Rayleigh multipath fading channels is given in Chapter 3. Chapter 4 introduces moments and cumulants and derives the higher order moments and cumulants that are then used to identify modulation schemes in this study.

Chapter 5 describes the modeling efforts that were made to simulate the wireless communication system. The design and implementation of the automatic modulation classifier algorithm is described in this section as well. Chapter 6 provides a summary of results describing the accuracy of the modulation classification algorithm developed in this research. Supplementary experiments are performed in this section to show the effect of noise on the accuracy of the signal detection at the receiver. Finally, the thesis research carried out is summarized with an overall conclusion. and recommendations of relevant future work that may be conducted in this field are provided.

CHAPTER 2

DIGITAL COMMUNICATION SYSTEMS

2.1 Introduction

In this chapter, a high level description of the fundamental elements involved in a communication system is introduced. This is an important step in understanding the process of transmitting and receiving a wireless signal. The method used manually to detect the signal modulation scheme at the receiver is presented. Based on this presentation, an argument is made to recognize the benefits of an automatic modulation classifier. The proposed method can detect a diverse range of modulation schemes almost instantaneously. Also presented in this chapter are the digital modulation techniques studied in this research work.

2.2 Brief Overview of Digital Communication Systems

Wireless systems differ from wired systems because in the former mode signals propagate through a wireless medium and experience random fluctuations in time due to the unpredictable and noisy wireless communication channel. The design of a wireless system should be optimized for the channel in order to ensure that information transmitted will be accurately replicated at the receiving (i.e., user) end. A wireless system includes a transmitter and receiver to send the source of information and to extract the intercepted information accurately at the receiving end, respectively. The transmitter consists of a modulator, which encodes digital information into analog waveforms prior to transmitting over the channel [15, Ch. 1]. At the user end of the communication system, a receiver will detect the transmitted signal by observing the received noisy signal. Included within the receiver are the demodulator and detector that convert the received analog signal into a vector form to estimate the message signal. Depending on the physical characteristics of the communication medium, the choice of a modulation

scheme will affect the detectability of the received signal and, more largely, the performance of a wireless system [16, Ch. 5]. This chapter presents the architecture of the signal detection process and recommends a robust modulation classifier that can differentiate a range of modulation schemes, reducing the complexity of the traditional receiver.

2.3 Fundamental Elements of a Communication System

A wireless communication system is composed of interdependent elements that are designed to send information through a medium that supports unguided electromagnetic propagation. Figure 1 shows the basic elements of a digital communication system. The communication system is grouped into three parts: 1) transmitter, 2) channel and 3) the receiver [15, Ch. 1]. The purpose of the transmitter is to convert the message signal into a form suitable for transmission over the channel. The channel is a physical medium used to transmit the message signal to the receiver. The function of the receiver is to recover the transmitted message signal [15, Ch. 1].

The transmitter and the receiver are divided into functional block diagrams, as shown in Figure 1. The functional blocks of the transmitter include the information source and input transducer, source encoder, channel encoder and digital modulator. The receiver contains functional blocks that mirror those of the transmitter. The functional blocks of the receiver include the digital demodulator, source decoder and output transducer, which output the message signal to the end user. The transmitter, receiver and its functional blocks are described in detail in Sections 2.4 to 2.11.

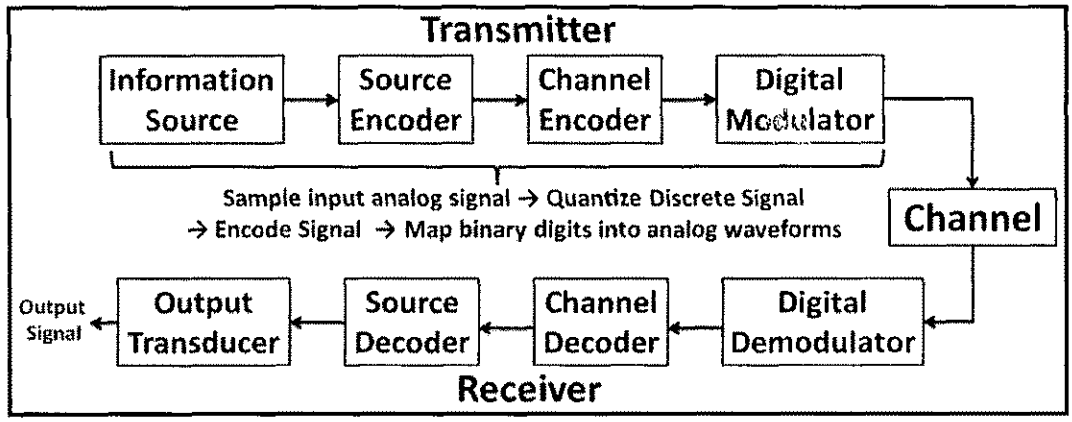

Figure 1: Fundamental Elements of a Digital Communication System.

2.4 The Transmitter

The task of the transmitter is to convert the message signal into a form suitable for transmission through the channel. If the information source is analog, the transmitter samples the analog signal into a digital form. Then the transmitter embeds the digital bits of information into the sinusoidal carrier waveforms through a process called digital modulation. Usually, in digital signal modulation, the bits of information are embedded within the amplitude, frequency or phase of a sinusoidal carrier signal [15, Ch. 1]. The advantage to transmitting an analog signal by means of digital modulation is that signal fidelity is better controlled. Additionally, digital systems are easier to implement and are cheaper designs of the wireless system. The digital modulator details are discussed in Section 2.7.

2.5 Information Source

Transducers are used to convert the information source into an electrical signal. For example, a microphone serves as a transducer; it converts a sound signal into an electrical signal. Similarly, at the receiver an output transducer converts the received electrical signal into a form that is suitable for interpretation by the end user (i.e., sound signal) [15, Ch. 1].

2.6 Source Encoder and Channel Encoder

In a digital communication system, the input message signal is sampled and quantized to convert it into a discrete form. Next, the discrete message signal is fed into the source encoder. For efficient representation of the message signal, it is ideal to have minimum or no redundancy of the data. The digital signal is converted into a compact sequence of non-redundant binary digits through a process called source encoding. The compressed binary digits are then passed to the channel encoder which introduces some redundancy of the digital signal in a controlled manner to overcome anticipated noise and interference effects experienced over the channel [15, Ch. 1].

2.7 Digital Modulator

The transmitter includes a digital modulator, which maps digital bits of information into analog signals suitable for transmission over a channel through a process called modulation. Modulation involves embedding the digital information into the amplitude, frequency or the phase of the sinusoidal carrier signal. Depending on the characteristics of the channel, amount of allocated bandwidth, or the parameters of the electronic appliances of the communication design, a modulation scheme is chosen which provides the best replica of the transmitted signal [15, Ch. 1].

The input to the digital modulator is a stream of binary bits from the information source. The digital modulator takes blocks of k binary digits of information at a time and maps it into M analog waveforms, given by the relationship $M = 2^k$. Equation (2.1), given below, shows the bandpass carrier signal that is used to impress the message signal prior to transmission [16, Ch. 5].

$$s_i(t) = g(t)A_i \cos[2\pi f_c t + 2\pi(i-1)\Delta f t + \phi_i(t)] \qquad (2.1)$$

Blocks of binary digits may be embedded within the amplitude A_i, frequency $(i-1)\Delta f$, phase $\phi_i(t)$ or a combination of the three, of the bandpass carrier signal. The shape of the bandpass carrier signal is given by $g(t)$. For efficient bandwidth utilization, a raised cosine pulse carrier signal is used to transmit the message signal [16, Ch. 5].

Equation (2.1) can be written in terms of the in-phase and quadrature components as

$$s_i(t) = g(t)A_i \cos\phi(t) \cos(2\pi f_c t) - g(t)A_i sin\phi(t) \sin\phi(t) \qquad (2.2)$$
$$= s_I(t) \cos(2\pi f_c t) - s_Q(t) \sin(2\pi f_c t)$$

where $s_I(t) = g(t)A_i(cos\ \phi(t))$ is the in-phase component of $s_i(t)$ and where $s_Q(t) = g(t)A_i(\sin\phi(t))$ is the quadrature component. The carrier signal $s_i(t)$ can also be written in terms of its equivalent lowpass representation as

$$s_i(t) = Re\{u(t)e^{j2\pi f_c t}\}, \qquad (2.3)$$

where $u(t) = s_I(t) + js_Q(t)$. The carrier signal is written in this representation because it is useful at the receiver where it processes the in-phase and quadrature components of the signal separately [16, Ch. 5].

In order to transmit multiple modulated signals over the same bandwidth and avoid signal interference, signals need to be orthogonal, and to have zero cross correlation. This means signals are time and band limited and, hence, do not interfere over the channel. Orthogonal signals are represented by a set of basis functions. Basis functions are a linear combination of energy type (message) signals. The cross correlation of any two orthogonal basis functions is zero, which effectively avoids signal interference. A communication system uses bandwidth, *B*, for signal transmission with digital symbol duration given by *T*. The maximum number of orthogonal signals, *N*, which can be transmitted over a channel is given by the time bandwidth product, *2BT*. Orthogonal information barring signals are used for transmission in order to be distinguished by the receiver hardware [16, Ch. 5].

In order to estimate the transmitted signal at the receiver, signal constellation diagrams are used for geometric representation of the analog waveforms in terms of its basis function. Signal constellation diagrams are signal space representations in which signal points are mapped to particular combinations of binary digits. Each point on the constellation represents the orthogonal information barring signals. The digital modulator is designed to encode the predetermined possible blocks or combines binary digits into orthogonal signals that can be mapped to points on the signal constellation diagram. The transmitter and receiver both know the mapping between the binary digits

to the orthogonal signal points in signal representation. Therefore, the receiver will look at the signal received and will map it to points on the signal constellation diagram [15, Ch. 7].

Signal points are mapped to particular combinations of binary digits using the Grey encoding method [16, Ch. 5]. In the Grey encoding method, the difference between neighboring bits (i.e., bits which are closest to each other) on the signal constellation diagram, should differ by at least one bit [16, Ch. 5]. Grey encoding is performed because if an error occurs at the decoder (due to noise), the error will be limited to one bit in the sequence of k bits [16, Ch. 5]. If larger amounts of bits (increased k) are encoded at a time, then the average error rate will be lower during the decoding process at the receiver [16, Ch. 5].

2.8 The Channel

Most wireless communication channels include atmosphere or free space [15, Ch. 1]. In physical worlds, digital message signals are embedded within analog carrier signals, which are then transmitted through the channel. Analog message signals can be directly transmitted over the wireless medium with the aid of a carrier signal. However, signal fidelity is better controlled if the analog message signal is converted into a digital form and processed via digital modulation prior to transmitting over the channel. Therefore, for optimal performance, analog message signals are sampled and quantized to represent the source of information in a digital form prior to transmission [15, Ch. 1].

2.9 The Receiver

Based on the received stream of bits, the task of the receiver is to reproduce the original transmitted signal that was fed through a channel that may have altered or degraded the message signal. Demodulation and detection is performed at the receiver to extract the digital message signal embedded within the analog sinusoidal carrier signal [15, Ch. 1].

The demodulator and detector convert the received noisy signal into an equivalent sequence of vectors and decide the possible M waveforms that was actually transmitted. Basically, the receiver knows the predetermined type of modulation scheme that was used to transmit the message signal. Hence, the demodulator uses a filtering operation wherein it uses the basis function of the signal representation to determine the corresponding vectors of the received signal. These filters are analog devices, which sample the data at the output of the filter to produce a stream of bits for the input of the detector [16, Ch. 5].

2.10 Digital Demodulator

The digital demodulator within the receiver implements inverse mapping from the transmitted waveforms to digital bits of information. Demodulation is a process wherein a vector form of the received signal is obtained by taking the basis function of the signal representation and correlating it with the received signal. Generally, two types of techniques are used by the demodulator to convert the received analog signal into an equivalent vector of bits. These are: 1) correlation-type demodulator and 2) the matched filter demodulator. A correlation type demodulator projects the received signal onto the orthonormal basis function of the signal space to obtain the vector form of the received analog waveform. A matched filter type demodulator passes the received signal through linear filters that are matched to the orthonormal basis functions of the signal space. Regardless of the type of demodulator used the receiver, both the correlation and the matched filter demodulator produce the same vector output to be fed into the input of the detector [15, Ch. 7].

The detector is a decision making device which looks at the received vector of bits and decides the message bit that was transmitted. Assuming the detector receives a sufficient amount of bits for each received signal vector, the detector uses an optimum decision rule to maximize the probability of correct decision. An optimum detector uses the maximum *a posteriori* probability (MAP) criterion wherein it decides the specific bit that was transmitted by comparing the probability a signal was transmitted so that the observed

received signal is maximized. In other words, the MAP criterion bases its decision on the probability that the received signal is greater than any other probability that a signal was transmitted given that received vector was observed. The MAP criterion is also known as the maximum-likelihood (ML) criterion [15, Ch. 7].

An alternative decision practice used by the detector is the minimum distance decoding. In minimum Euclidian distance decoding, the received signal constellation diagram is compared with the transmitted signal constellation diagram constructed by the modulator. The received point (bit) which closely maps to the point on the transmitted signal constellation diagram is chosen as the received waveform. The results obtained from minimum distance decoding are equivalent to MAP criterion [16, Ch. 5]. Chapter 3 describes the effect of noise on the decision process of the detector.

2.11 Channel Decoder, Source Decoder and Output Signal

After the received signal is uncovered from the carrier signal, the channel decoder is used to remove bit redundancy, similar to the channel encoder. The compact sequence of output bits from the channel decoder is then passed to the source decoder which attempts to reconstruct the original signal from the source [15, Ch. 1]. Channel decoding and source decoding is performed to eliminate errors during the demodulation process. Hence, the output signal is an approximation of the original source output [15, Ch. 1].

2.12 Conventional Demodulator Versus Automatic Modulation Classifier

For a signal to be demodulated at the user end, the conventional receiver must have a priori knowledge on modulation type of the transmitted signal. The transmitter and receiver both use the same mapping scheme to represent the digital signal on the constellation diagram [16, Ch. 5]. At the receiver, this mapping process is performed by either the matched filter, or a correlation type demodulator. These use the basis function of the known modulation scheme to project the received signal to the orthonormal basis functions of the signal space.

Conventional receivers and transmitters are compatible as long as both the transmitter and the receiver are using the same modulation scheme. Most transmitter and receivers only operate a limited number of modulation schemes. Developing a generic receiver that could operate with any transmitter is beneficial because it would be able to demodulate signals from a range of transmitters using various modulation schemes. An automatic modulation classifier could be used to detect the modulation scheme of the intercepted signal in-situ, reducing the complexity of the demodulator.

2.13 Digital Modulation Schemes

Sections 2.13.1 through 2.13.5 present various digital modulation techniques, including the schemes studied in this work.

2.13.1 Pulse Amplitude Modulation (PAM)

PAM is one of the methods used to encode digital information into sinusoidal carrier waveforms for transmission over a channel. The scheme, in which the digital modulator maps each binary bit of the message signal into the amplitude of the analog carrier waveform, is referred to as 2-PAM. In 2-PAM, each binary bit, 0 and 1, is represented by analog waveform, $s_1(t)$ and $s_2(t)$. The digital modulator takes each binary digit and maps it into two analog waveforms ($M = 2^1$), with different amplitudes in order to distinguish between the bits (0 and 1) of transmitted information over the channel [15, Ch. 7], [16, Ch. 5]. Equation (2.4) shows the analog waveform expression for a PAM scheme in Figure 2.

$$s_i(t) = A_i g(t)\cos(2\pi f_c t) \text{ where } i = 1, \ldots, M. \qquad (2.4)$$

The scheme in which the digital modulator maps a pair of binary bits of the message signal onto the amplitude of the analog of the carrier signal is referred to as 4-PAM. In 4-PAM, four analog waveforms ($M = 2^4$), $s_1(t)$, $s_2(t)$, $s_3(t)$, and $s_4(t)$ with different amplitudes are used for distinguishing between the bits 00, 01, 11 and 10 of information transmitted over the channel [15, Ch. 7], [16, Ch. 5].

In PAM, signal points (signal amplitudes) are placed on a one dimensional line since all of the waveforms can be represented in terms of a single basis function. Equation (2.5) below shows the basis function of a PAM, where $E_g$is the energy of the signal:

$$\phi(t) = \sqrt{\frac{2}{E_g}}\, g(t)\cos(2\pi f_c t) \ . \qquad (2.5)$$

Figure 2 shows the 2-PAM and 4-PAM signal constellation diagram. Notice that the distance between the two signal points will vary depending on the amplitude or energy E_g of the carrier signal [15, Ch. 7], [16, Ch. 5].

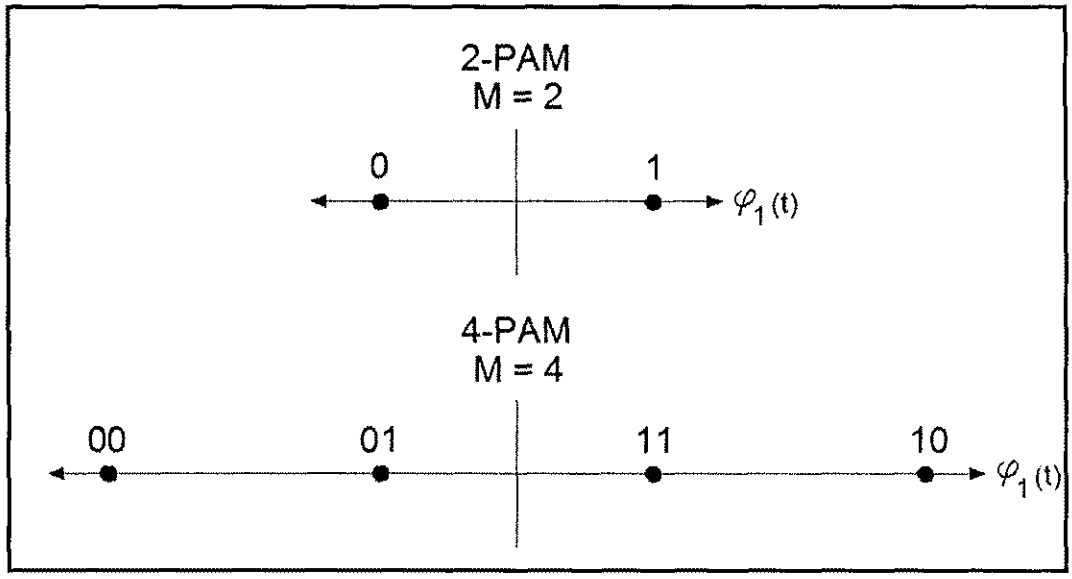

Figure 2: 2-PAM and 4-PAM Signal Constellation Diagram.

2.13.2 Phase Shift Keying Modulation (PSK)

PSK is another method used to encode digital information into analog waveforms for transmission over a channel. In PSK, digital information is encoded into the phase of an analog waveform. The scheme in which the digital modulator maps a pair of binary bits of the message signal into four different phase angles of the carrier signal is referred to as 4-PSK. Therefore, in 4-PSK, four analog waveforms ($M = 2^4$) with four different phase

angles, 0, $\frac{\pi}{2}$, π, and $\frac{3\pi}{2}$, are used for distinguishing between the bits 00, 01, 11 and 10 of transmitted information over the channel. Equations (2.6), (2.7), (2.8) and (2.9) given below show the analog waveform expressions for a PSK scheme [15, Ch. 7], [16, Ch. 5].

$$s_1(t) = g(t)\cos(2\pi f_c t), \tag{2.6}$$

$$s_2(t) = -g(t)\sin(2\pi f_c t), \tag{2.7}$$

$$s_3(t) = -g(t)\cos(2\pi f_c t), \tag{2.8}$$

$$\text{and, } s_4(t) = g(t)\sin(2\pi f_c t). \tag{2.9}$$

Quadrature Phase Shift Keying (QPSK) modulation is applied by shifting the original 4-00PSK constellation by $\frac{\pi}{4}$. In QPSK, four analog waveforms with four different phase angles $\frac{\pi}{4}$, $\frac{3\pi}{4}$, $\frac{5\pi}{4}$ and $\frac{7\pi}{4}$ are used for distinguishing between the bits 00, 01, 11 and 10 of transmitted information over the channel. Equations (2.10), (2.11), (2.12) and (2.13) show the analog waveform expressions for a QPSK scheme [15, Ch. 7], [16, Ch. 5].

$$s_1(t) = g(t)\cos\left(2\pi f_c t + \frac{\pi}{4}\right), \tag{2.10}$$

$$s_2(t) = g(t)\cos\left(2\pi f_c t + \frac{3\pi}{4}\right), \tag{2.11}$$

$$s_3(t) = g(t)\cos\left(2\pi f_c t + \frac{5\pi}{4}\right), \tag{2.12}$$

$$\text{and, } s_4(t) = g(t)\cos(2\pi f_c t + \tfrac{7\pi}{4}). \tag{2.13}$$

In 4-PSK and QPSK, signal points are places on two dimensional lines since all of the waveforms can be represented in terms of two basis functions. Equations (2.14) and (2.15) show the basis functions of a 4-PSK or QPSK, where E_g is the energy of the signal.

$$\phi_1(t) = \sqrt{\frac{2}{E_g}}\, g(t)\cos(2\pi f_c t), \tag{2.14}$$

$$\text{and, } \phi_2(t) = \sqrt{\tfrac{2}{E_g}}\, g(t)\sin(2\pi f_c t). \tag{2.15}$$

Figure 3 shows the 4-PSK and QPSK signal constellation diagrams [15, Ch. 7], [16, Ch. 5].

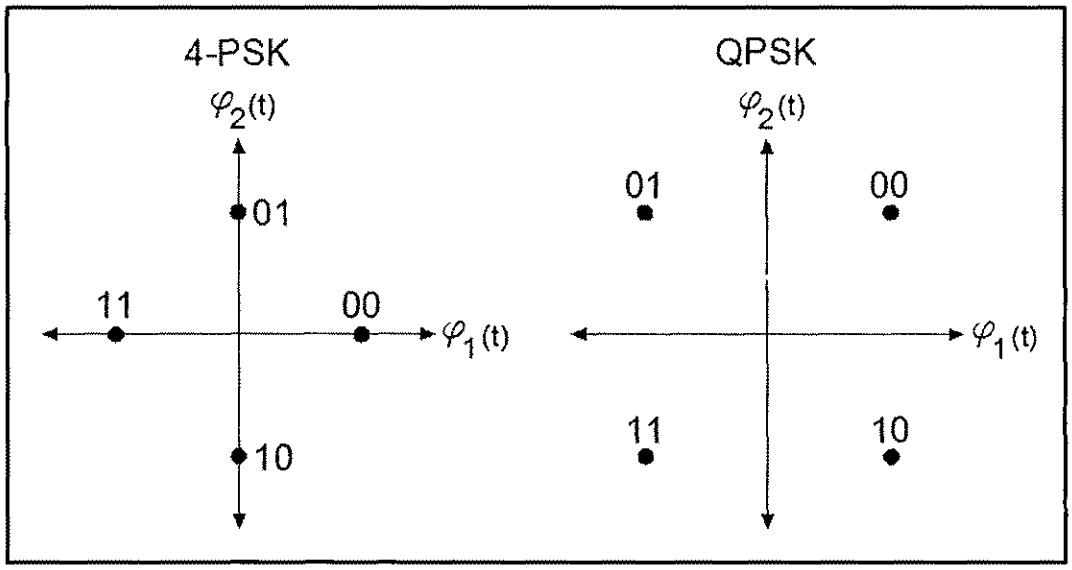

Figure 3: 4-PSK and QPSK Signal Constellation Diagram.

QPSK is used in practice because it is easier in the signal detection process at the receiver. In QPSK, the signal points are placed in the first, second, third and fourth quadrants, whereas, in 4-PSK and 2-PSK points are placed on the axis, and it may become complicated to make decisions in the signal decoding process at the receiver. The distance between signal points will vary depending on the energy E_g of the carrier signal [15, Ch. 7], [16, Ch. 5].

In 8-PSK, the digital modulator maps three groups of binary bits onto an analog waveform. Therefore, in 8-PSK eight analog waveforms ($M = 2^3$) $s_1(t)$, $s_2(t)$, $s_3(t)$, $s_4(t)$, $s_5(t)$, $s_6(t)$, $s_7(t)$, and $s_8(t)$ with different phase angles are used for distinguishing between the bits (000, 001, 011, 010, 110, 111, 101, 100) of information transmitted over the channel. Figure 4 shows an 8-PSK signal constellation diagram.

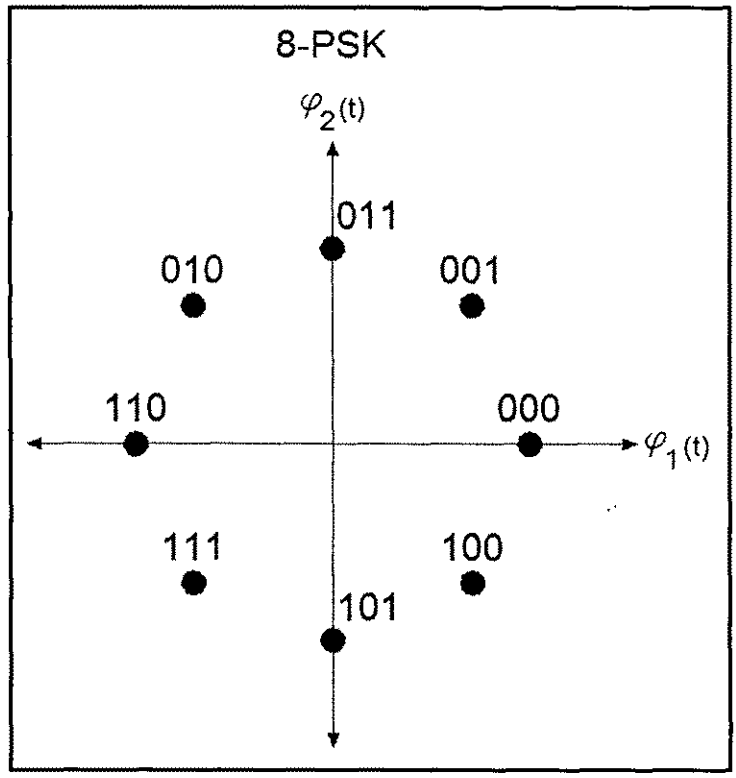

Figure 4: 8-PSK Signal Constellation Diagram.

The simplest form of phase modulation is BPSK, also known as 2-PSK. In BPSK the carrier phase has only two signal phases $+\frac{\pi}{2}$ and $\frac{\pi}{2}$ [15, Ch. 7], [16, Ch. 5]. Notice that 2-PSK is equivalent to 2-PAM (when the two signal phases are 0 and π). Both these representations have only one basis function and have the same distance between points in the signal constellation diagrams [15, Ch. 7]. In this thesis, the BPSK modulation scheme is evaluated in the modulation classification algorithm.

2.13.3 Quadrature Amplitude Modulation (QAM)

QAM is a hybrid form of a modulation scheme in which both the phase and the amplitude levels contain embedded information. QAM can be obtained by superimposing multiple PSK constellations shifted 45 degrees and with different amplitudes. Information bits are impressed on the phase and amplitude of the quadrature carriers, $\cos(2\pi f_c t)$ and $\sin(2\pi f_c t)$. The transmitted signal waveforms have the following form:

$$s(t) = A_{ic} g(t) \cos(2\pi f_c t) \cos(\theta_{ic}) - A_{is} g(t) \sin(2\pi f_c t) \sin(\theta_{is}), \qquad (2.16)$$
$$where \quad i = 1, 2, \ldots, M.$$

where A_{ic} and A_{is} are the sets of amplitude levels and θ_{ic} and θ_{is} are the phase levels that are obtained by mapping k-bit sequences onto signal amplitudes and phase levels, respectively. Figure 5 shows the signal representation of combined PAM-PSK for the cases when M is equal to 8 (8-QAM) and 16 (16-QAM) [15, Ch. 7].

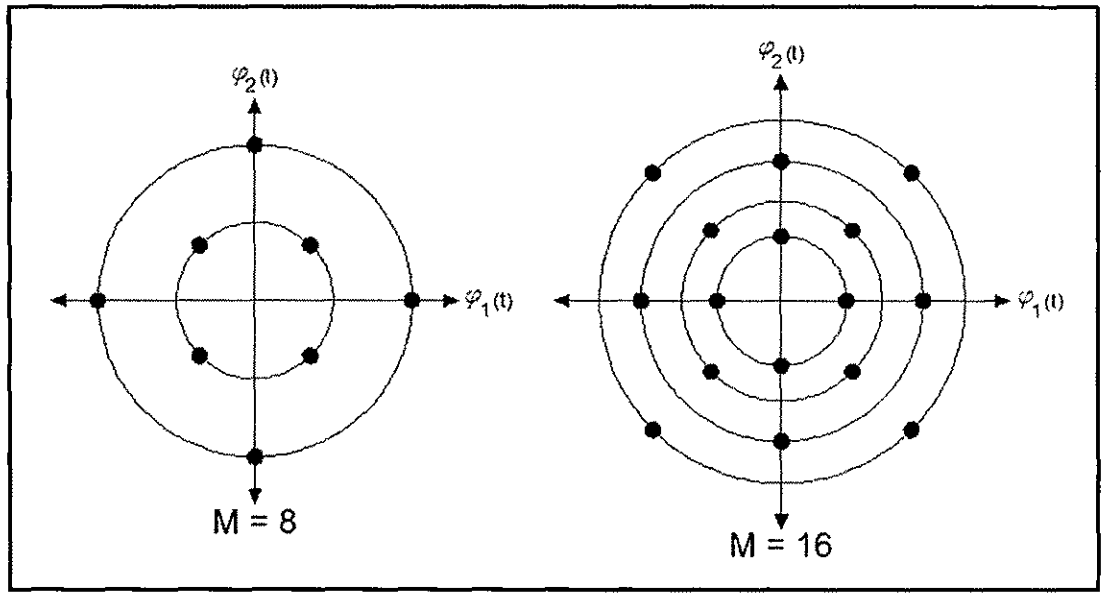

Figure 5: 8-QAM and 16-QAM Signal Constellation Diagram.

2.13.4 Rectangular Quadrature Amplitude Modulation (QAM)

Rectangular QAM is a form of a modulation scheme in which the amplitude levels contain only embedded information. Information bits are impressed on the amplitude of the carriers, $\cos(2\pi f_c t)$ and $\sin(2\pi f_c t)$. The transmitted signal waveforms have the form

$$s(t) = A_{ic} g(t) \cos(2\pi f_c t) - A_{is} g(t) \sin(2\pi f_c t), \qquad (2.17)$$
$$where \quad i = 1, 2, \ldots, M.$$

A_{ic} and A_{is} are the sets of amplitude levels that are obtained by mapping k-bit sequences into signal amplitudes. Figure 6 shows the signal constellations result when two carriers are each modulated by QAM [15, Ch. 7], [18].

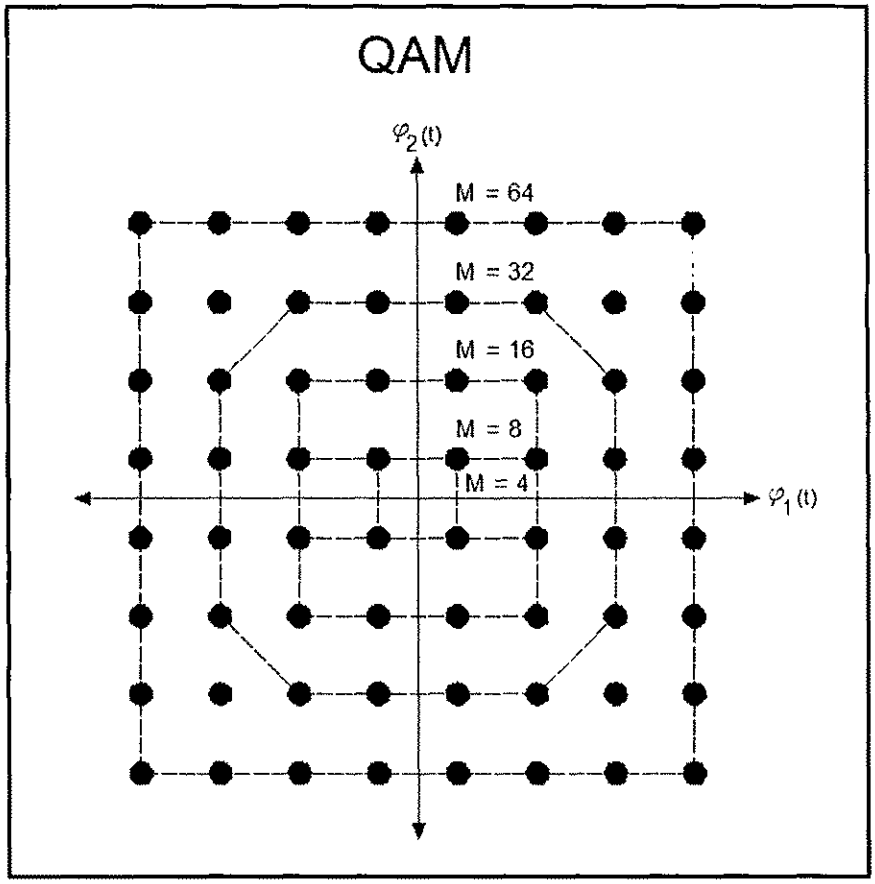

Figure 6: Rectangular QAM Signal Constellation Diagram.

2.13.5 Frequency Shift Keying (FSK)

In FSK each of the M information waveforms is encoded into the carrier signal in terms of different frequencies. The frequency at which information is encoded within is given by Equation (2.18):

$$f_i = f_c + (i+1) * \Delta f \text{ where } i = 1, \ldots, M. \tag{2.18}$$

The carrier frequency f_c is the band of frequencies at which the signal is transmitted, and Δf is the frequency increment between each transmitted signal ($\Delta f \sim \frac{1}{T}$). In order to ensure that any two signals are orthogonal, f_c must be a multiple of Δf. Alternate assignments of carrier frequencies in terms of negative increments can be made in which f_c occurs in the middle of the band, and the assigned frequencies can occur to the left and to the right to the band of frequencies. Equation (2.19) shows analog waveform expression for FSK scheme, where E_g is the energy of the signal [15, Ch. 7], [16, Ch. 5].

$$\begin{aligned} s_i(t) &= \sqrt{\frac{2E_g}{T}}\cos(2\pi f_i t), \\ &= \sqrt{\frac{2E_g}{T}}\cos(2\pi f_c t + (i+1)2\pi\Delta f t), \\ &\text{where } i = 1, \ldots, M. \end{aligned} \tag{2.19}$$

Equation (2.20) shows the basis functions of a FSK modulation scheme [15, Ch. 7], [16, Ch. 5].

$$\phi_i(t) = \sqrt{\frac{2}{T}}\cos(2\pi f_i t) \text{ where } i = 1, \ldots, M. \tag{2.20}$$

Figure 7 shows the 3-FSK orthogonal signals [15, Ch. 7], [16, Ch. 5].

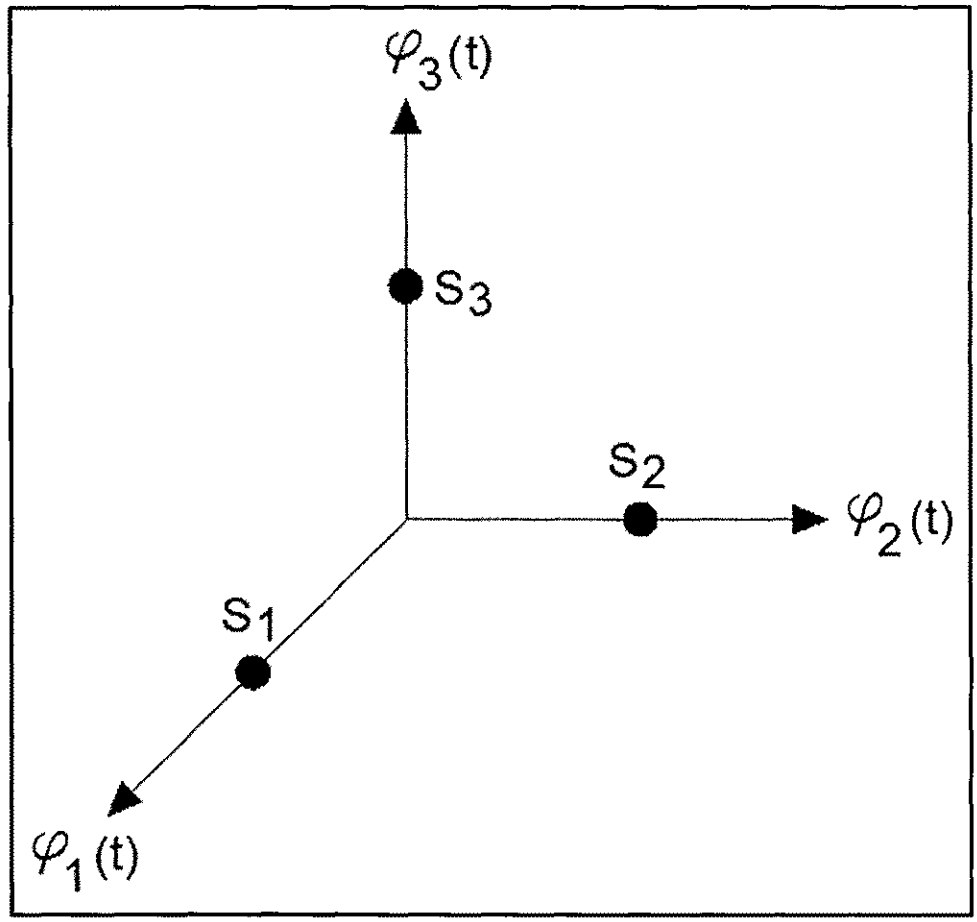

Figure 7: 3-FSK Orthogonal Signals.

Figure 8 shows a 2-FSK signal constellation diagram [15, Ch. 7], [16, Ch. 5].

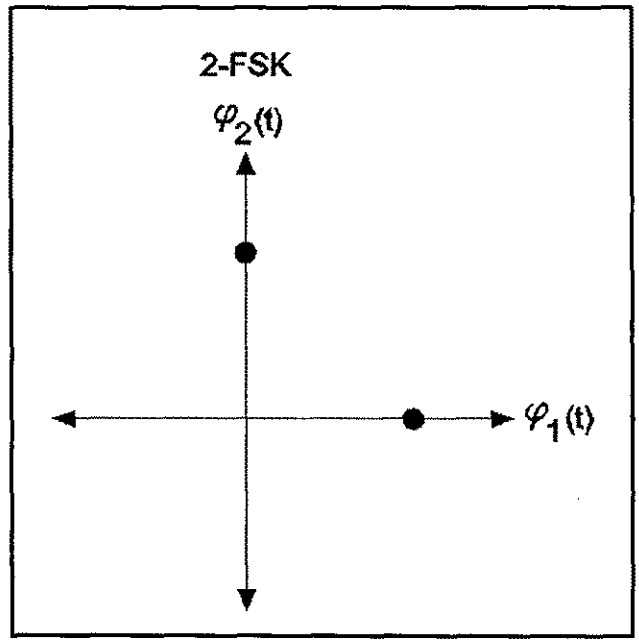

Figure 8: 2-FSK Signal Constellation Diagram.

Equations (2.21) and (2.22) show the basis functions of the 2-FSK modulation scheme.

$$\phi_1(t) = \sqrt{\frac{2}{T}}\cos(2\pi f_2 t)\ , \tag{2.21}$$

$$\text{and, } \phi_2(t) = \sqrt{\frac{2}{T}}\cos(2\pi f_1 t)\ . \tag{2.22}$$

In 4-PSK, the two axes (basis functions) correspond to cosine and sine of the same frequencies. Even though 2-FSK is represented as a two-dimensional signal constellation, the basis functions will not correspond to the sine and cosine of the same frequency but rather to two cosines of different frequencies which are both multiples of Δf. Also, for a given signal energy (or amplitude) FSK points on a signal constellation are closer than PSK points. Points which are closer on the signal constellation have a higher likelihood of decoding error at the receiver [15, Ch. 7].

CHAPTER 3

WIRELESS TRANSMISSION CHANNELS

3.1 Introduction

This chapter introduces wireless transmission channels including AWGN, Rayleigh fading, and Ricean fading multipath channels. Modern telecommunications has introduced a large variety of modulation schemes in order to transmit a signal that is compatible with the characteristics of the channel. Wireless systems differ from wired systems. In the former system, transmitted signals propagate through a wireless medium and experience random fluctuations due to the unpredictable and complex nature of the wireless communication channel. The wireless medium contains noise and interference affecting the fidelity of the received signal. Channel noise occurs as a result of atmospheric disturbances, extraterrestrial radiation and/or random motion of electrons of the electromagnetic wave. Unintentional radiations that produce noise in signals come from sources, such as power generators, electronic instruments, and microwave ovens [1, Ch. 1]. Sometimes, large objects existing in the path between the transmitter and the receiver may cause reflections of the signal and affect the quality of the message signal. Additionally, variations in the geographic locations in the path of signal propagation may alter or degrade the signal. A variety of modulation schemes are introduced into the modulated signal so that the transmitted signal is compatible with the characteristics of the channel. Wireless transmission channels evaluated in this research, namely, AWGN channel, multipath Rayleigh fading channel, and multipath Ricean fading channel are described in this chapter.

3.2 Additive White Gaussian Noise (AWGN) Channel

The AWGN is a basic noise model that is used in the analysis of communication system channels. The AWGN channel mimics many of the random processes that occur in nature. AWGN has a power spectrum that is constant at all frequencies. The word

"white" in the phrase additive white Gaussian noise is comparable to white light, which has a constant power spectrum at all wavelengths. The word "Gaussian" is due to the Gaussian distribution of the amplitude of the noise [1, Ch. 2]. The power spectrum density of AWGN is given as:

$$S(f) = \frac{N_0}{2} \tag{3.1}$$

where N_0 is a constant and the $\frac{1}{2}$ factor indicates that half the power is associated with positive frequencies and half with negative frequencies. Figure 9 shows the power spectral density of the AWGN.

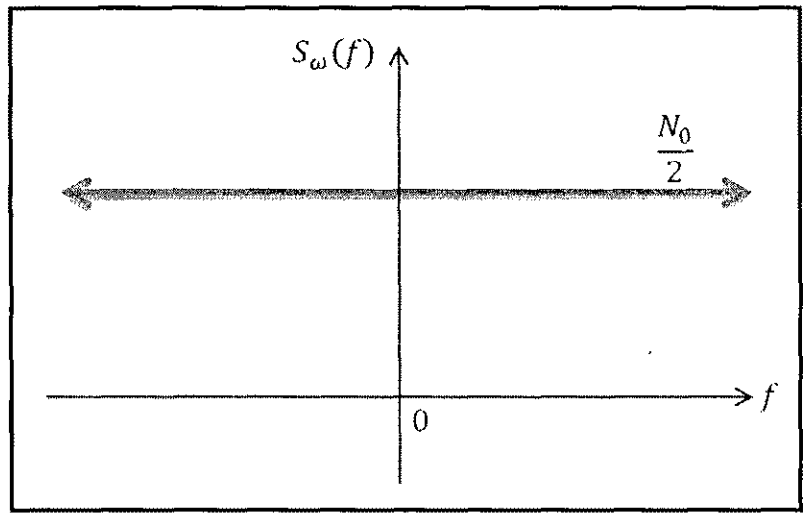

Figure 9: AWGN Power Spectral Density.

3.3 Signal to Noise Ratio (SNR)

The SNR is defined as the ratio of the average power of the received signal to the average power of the noise and is given in the units of decibels (dB). If the signal has zero mean, the SNR can also be written in terms of the ratio between the variance of the received

signal to the variance of the channel noise [1, Ch. 2]. In this thesis, the noise of the channel will be described in terms of the SNR of the received signal or the variance of the channel noise.

3.4 Bit Error Rate (BER)

Quality of service of a digital communication system can be measured by the bit error rate (BER). The BER measures the performance of the optimum receiver in terms of how often a bit is interpreted incorrectly by the receiver [15, Ch. 7]. The performance of the optimum receiver depends on several factors such as the energy per transmitted signal, AWGN variance, number of transmitted signals, and the distance between points on the signal constellation diagram. The BER is used to compare the various types of modulation schemes for optimal performance of the detector in the presence of AWGN [18]. A successful wireless communication design relies on predictions and assumptions made on the channel [15, Ch. 7]. Choosing a modulation scheme that will transmit signals efficiently to the end user with minimum error would be desirable in the system. Hence, it would be convenient to have a general receiver that can demodulate a range of modulated signals that may be received from multiple transmitters.

Figure 10 throughFigure 15 show the constellation diagrams of BPSK, 4-PSK, and 16-QAM signals passed through AWGN channel. Figure 10, Figure 12 and Figure 14 show a perfectly transmitted BPSK, 4-PSK and 16-QAM with zero signal to noise ratio, respectively. Figure 11, Figure 13 and Figure 15 show distortion of these modulated signals due to AWGN channel. In the distorted constellation diagram, each of the bits are overlapped, thereby increasing the BER.

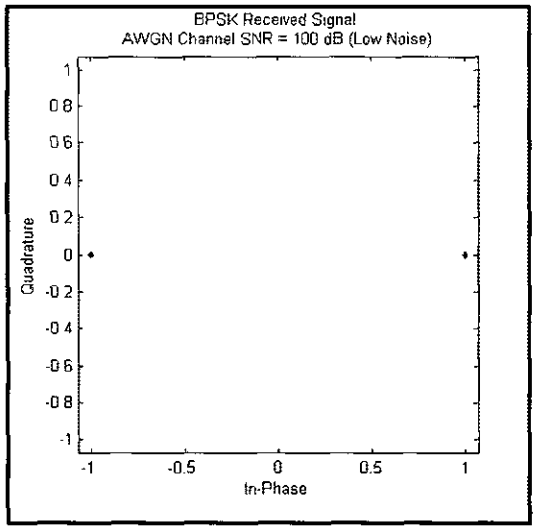

Figure 10: Perfectly Transmitted BPSK Signal.

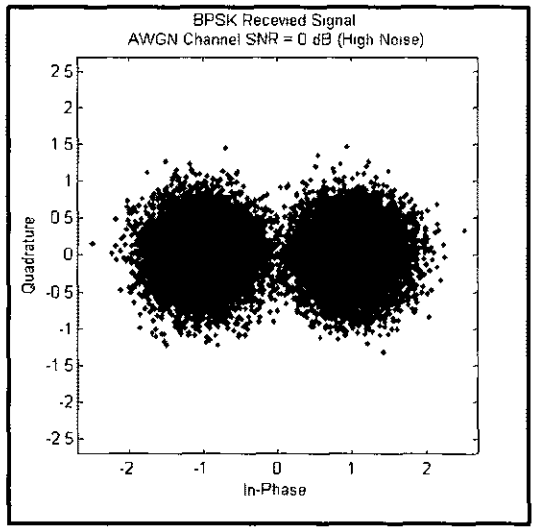

Figure 11: Effect of AWGN Channel on BPSK Signal.

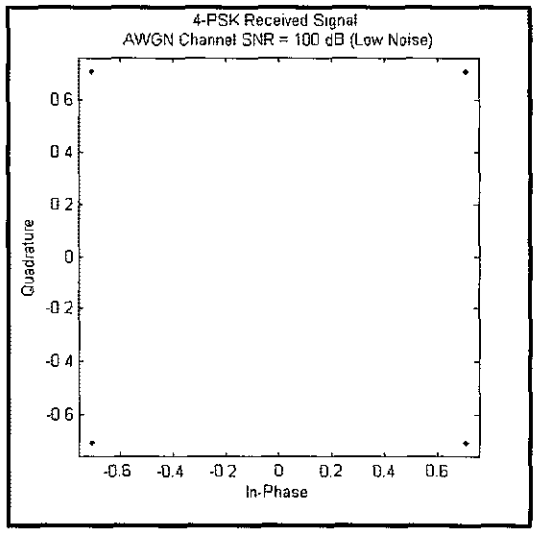

Figure 12: Perfectly Transmitted 4-PSK Signal.

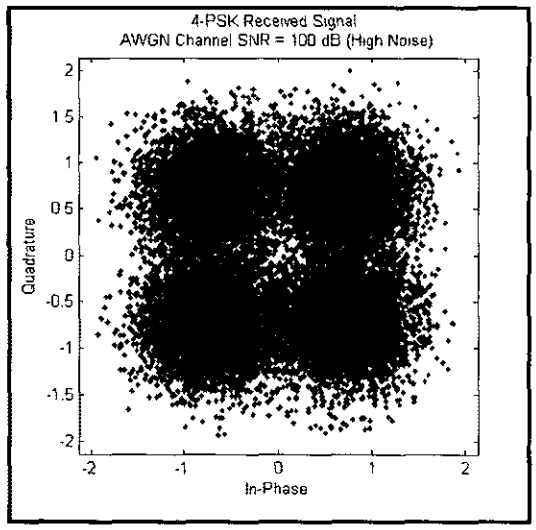

Figure 13: Effect of AWGN Channel on 4-PSK Signal.

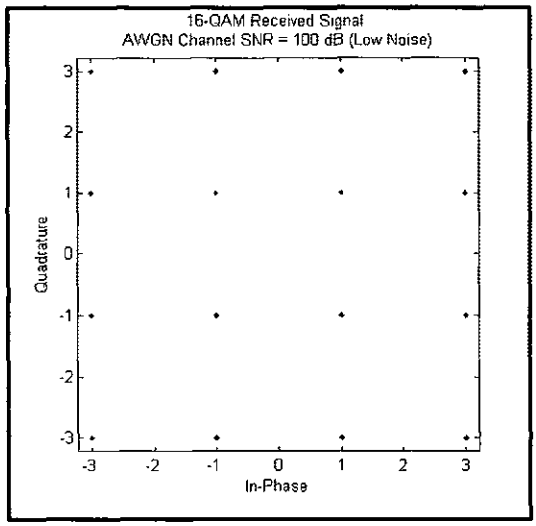

Figure 14: Perfectly Transmitted 16-QAM Signal.

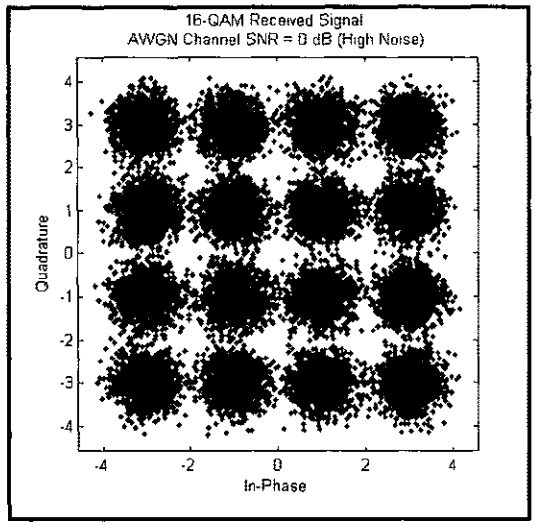

Figure 15: Effect of AWGN Channel on 16-QAM Signal.

A wireless communication system should be designed with a modulation technique to best provide high data rate, occupy minimum bandwidth, require minimum signal transmit power, result in minimum probability of error and, lastly, require low cost to implement the design [15, Ch. 1]. One of the reasons a particular modulation scheme is selected to transmit a signal is based on the characteristics of the propagation channel [15, Ch. 7]. In a conventional receiver both the digital modulator and the receiver know the modulation mapping between the binary bits to the analog waveform [16, Ch. 5]. Designing a generic receiver should be able to identify the modulation scheme of the transmitted signal so that the complexity of the wireless communication system is reduced. Particularly, the receiver preprocessing functions, such as the matched filter or correlation type demodulation, could be eliminated with the addition of the modulation scheme identifier [5]. Hence, an automatic modulation classifier should be able to identify a range of modulation schemes of the intercepted signal without a priori knowledge of the modulation type of the signal. The effects on signals when propagated through multipath fading channels are described in Section 3.5.

3.5 Fading Channels

The propagation path of wireless signals to describe the propagation loss in the channels can be modeled using two different methods: 1) using the free space propagation model, and 2) using the multipath propagation model. When dealing with satellite and other communication systems, where there is a line of sight (LOS) between the transmitter and the receiver, the free space propagation model can be used to describe the propagation loss. In dense urban environments where there is no direct line of sight path, objects in the propagating path of the wireless signal may reflect, refract, diffract, scatter or absorb the transmitted signal causing the information to become attenuated or corrupt. This phenomenon is known as multipath propagation where the transmitted signal travels in multiple paths to combine at the receiver. A signal transmitted through a wireless multipath channel will experience random variations due to blockage from objects causing delayed versions of the signal to arrive at slightly different times at the receiver. This phenomenon is known as fading [1, Ch. 3].

3.6 Rayleigh Multipath Channel

Signals transmitted through an environment with moving objects (such as vehicles) will be subject to Rayleigh fading resulting in multiple phase shifts of a single transmitted signal [1, Ch. 3]. A Rayleigh fading multipath channel would be useful in modeling signal propagation in larger city environments where there is no line of sight between the transmitter and the receiver.

The probability density function (PDF) of a received signal that experienced Rayleigh fading will have the following form:

$$p(r) = \begin{cases} \frac{r}{\sigma^2} e^{\left(-\frac{r^2}{2\sigma^2}\right)} & 0 \leq r \leq \infty \\ 0 & r \leq 0 \end{cases}, \tag{3.2}$$

where r models the power of each time delayed signal generated by the multipath distortion, σ^2 is the time average of the received power and σ is the Root Mean Square

(RMS) of the received voltage [1, Ch. 3]. Figure 16 shows the probability density function for a Rayleigh fading signal with unit variance.

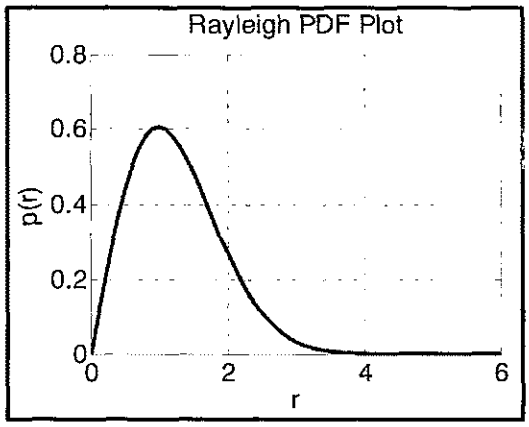

Figure 16: PDF of Rayleigh Distribution.

The cumulative distribution function (CDF) of the Rayleigh faded signal is expressed as follows [1, Ch. 3]:

$$c(r) = \begin{cases} 1 - e^{\left(-\frac{r^2}{2\sigma^2}\right)} & 0 \leq r \leq \infty \\ 0 & r \leq 0 \end{cases} . \tag{3.3}$$

Figure 17 shows the cumulative distribution function for a Rayleigh fading signal with unit variance.

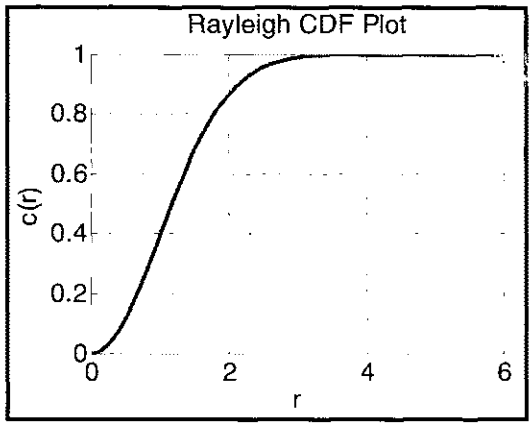

Figure 17: CDF of Rayleigh Distribution.

Figure 18 through Figure 23 show the constellation diagrams of BPSK, 8-PSK and 64-QAM signal passed through a multipath Rayleigh fading channel with AWGN noise. Figure 18, Figure 20 and Figure 22 show a perfectly transmitted BPSK, 8-PSK and 64-QAM signal (no noise). Figure 19, Figure 21 and Figure 23 show distortion of these modulated signals due to multipath Rayleigh fading channel with AWGN noise. In the distorted constellation diagram, each of the bits are overlapped increasing the BER.

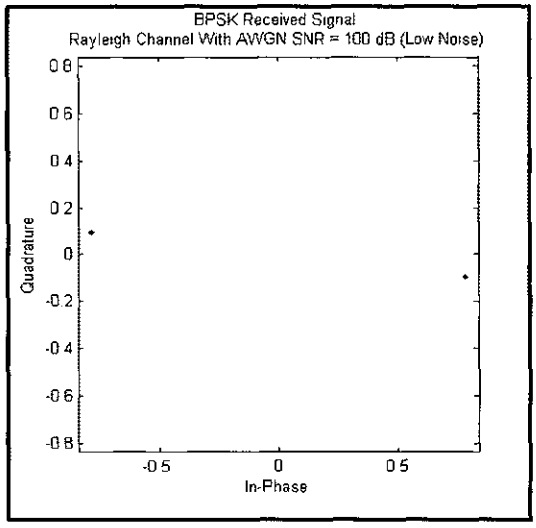

Figure 18: Perfectly Transmitted BPSK Signal.

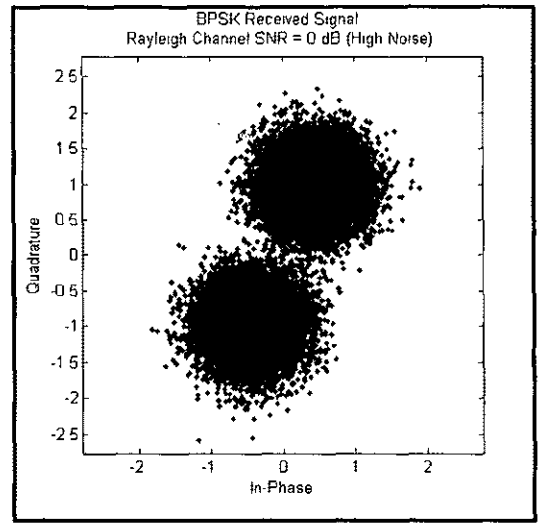

Figure 19: Effect of Rayleigh Fading With AWGN Channel on BPSK Signal.

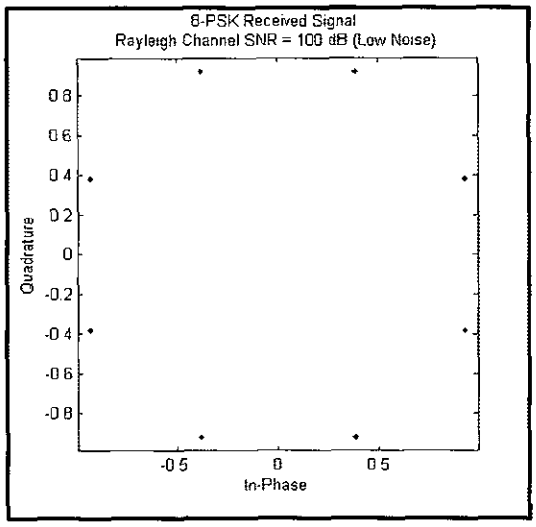

Figure 20: Perfectly Transmitted 8-PSK Signal.

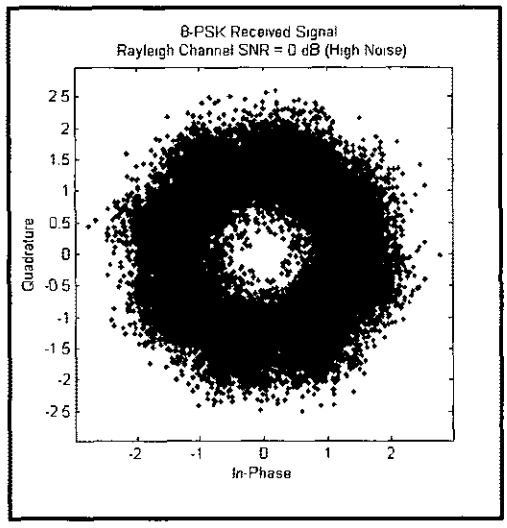

Figure 21: Effect of Rayleigh Fading With AWGN Channel on 8-PSK Signal.

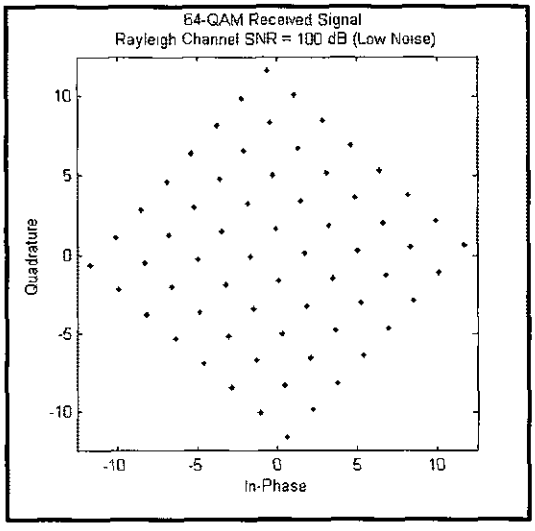

Figure 22: Perfectly Transmitted 64-QAM Signal.

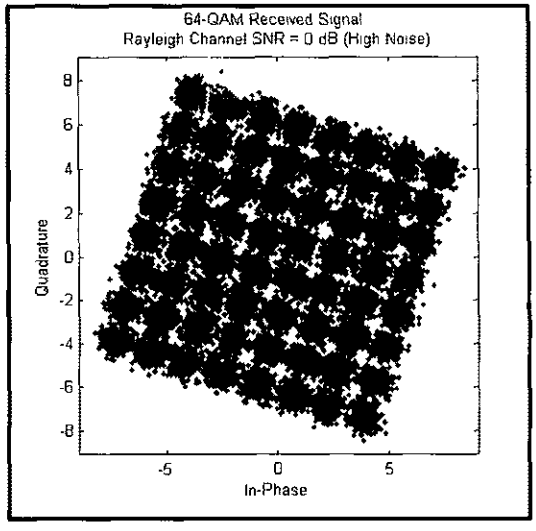

Figure 23: Effect of Rayleigh Fading With AWGN Channel on 64-QAM Signal.

3.7 Ricean Multipath Channel

A Ricean fading model is used to describe a channel where there is both a dominant Line of Sight (LOS) wave component between the transmitter and the receiver in addition to multiple waves that experience random multipath fluctuations that cause fading. Therefore, the Ricean fading model is a combination of the Rayleigh fading and LOS component [1, Ch. 3].

The probability density function (PDF) of a received signal that experienced Ricean fading will have the following form:

$$p(r) = \begin{cases} \frac{r}{\sigma^2}\exp\left(-\frac{r^2+A^2}{2\sigma^2}\right) I_0\left(\frac{Ar}{\sigma^2}\right), & A \geq 0, 0 \leq r \leq \infty \\ 0, & r < 0 \end{cases}, \tag{3.4}$$

where A is the peak amplitude of the dominant signal, I_0 is the modified Bessel function of the first kind and zero-order, and σ^2 is the time average received power of the non-dominant components [1, Ch. 3].

The ratio between the deterministic signal power and the power of the non-dominant wave is defined as the Ricean factor, K. The K factor is given as follows [1, Ch. 3]:

$$K = \frac{A^2}{\sigma^2} \rightarrow K(dB) = 10\log\left(\frac{A}{\sigma^2}\right). \tag{3.5}$$

Figure 24 throughFigure 29 show the constellation diagrams of BPSK, 4-PSK and 256-QAM signal passed through a multipath Ricean fading channel with AWGN noise. Figure 24, Figure 26 and Figure 28 show a perfectly transmitted BPSK, 4-PSK and 256-QAM signal (no noise). Figure 25, Figure 27 and Figure 29 show distortion of these modulated signals due to multipath Rayleigh fading channel with AWGN noise. In the distorted constellation diagram, each of the bits are overlapped increasing the BER.

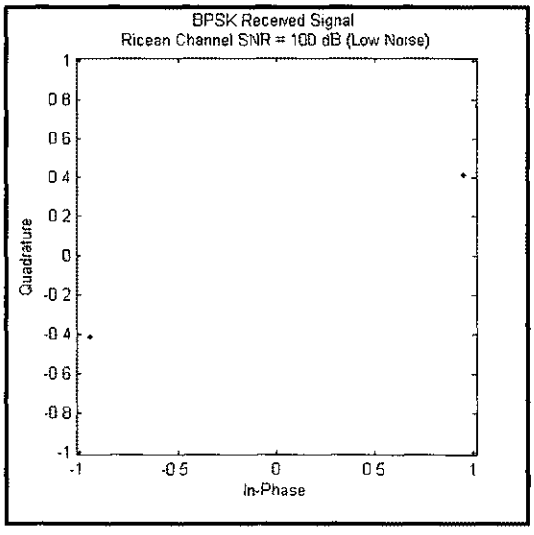

Figure 24: Perfectly Transmitted BPSK Signal.

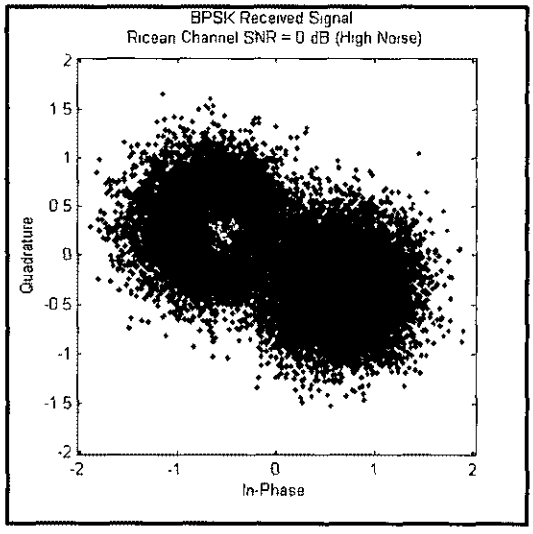

Figure 25: Effect of Ricean Fading With AWGN Channel on BPSK Signal.

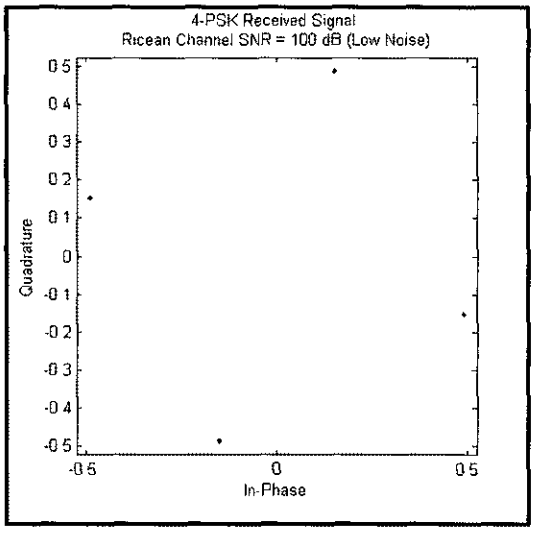

Figure 26: Effect of Ricean Fading With AWGN Channel on 4-PSK Signal.

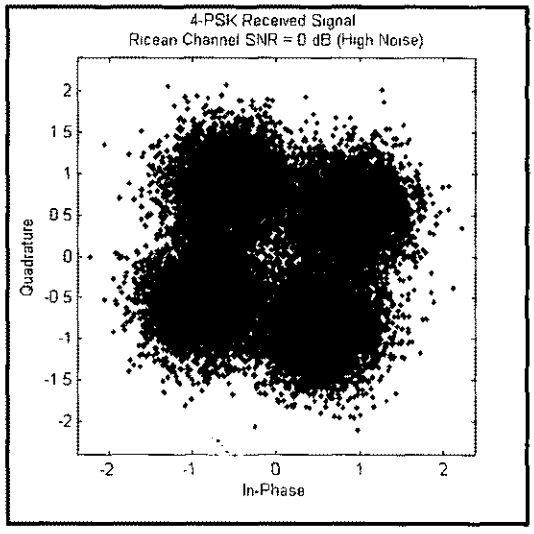

Figure 27: Effect of Ricean Fading With AWGN Channel on 4-PSK Signal.

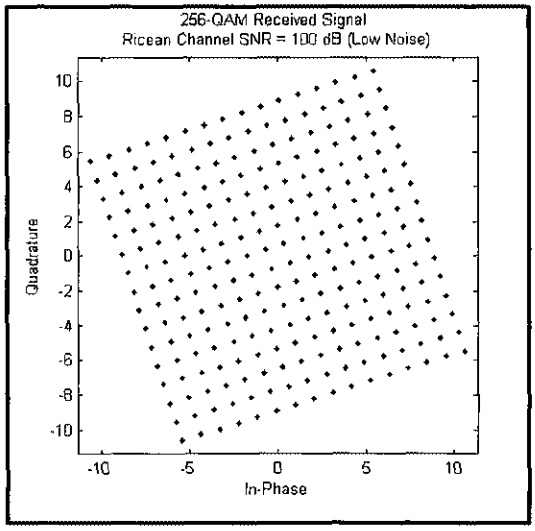

Figure 28: Perfectly Transmitted 256-QAM Signal.

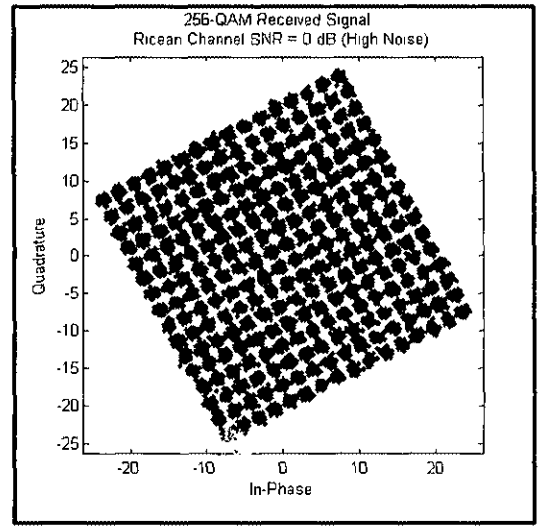

Figure 29: Effect of Ricean Fading With AWGN Channel on 256-QAM Signal.

Various characteristics of the channel will affect the performance of the detectability of the signal at the receiver. A wireless system should be designed to best prohibit those factors in the channel which may alter or degrade the transmitted signal [16, Ch. 5]. In this research, random signals will be modulated and propagated through the AWGN channel, multipath Rayleigh fading channel and multipath Ricean fading channel at various levels of SNRs. The moments and cumulants of the received signal will be computed to correctly identify the modulation scheme of the transmitted signal and, thus, evaluate the capability of the classification modulation algorithm.

CHAPTER 4

MOMENTS AND CUMULANTS

4.1 Introduction

This chapter presents the higher order moments and cumulants calculations, which are used to distinguish between the modulation schemes of the received signal. These moments and cumulants are used to identify the modulation type of the received noisy signal. The reason that moments and cumulants are used is that they are resilient to noise effects of the propagation channel [14]. The automatic modulation classification algorithm designed in this thesis uses a combination of eight order moments and cumulants to distinguish between the modulation schemes of an intercepted signal.

As mentioned in the introduction, uncertainty in the signal must be accounted for by suitable statistical models derived from measurements on continuous signals as well as from the discrete sampled signals; hence, there is a need for appropriate statistical tools for carrying out these operations in the real-time. Statistical tools such as mean function or first moment of random process, cumulative distribution functions, probability density function, second moments are needed for statistical specification of the random process. In this regard, higher-order statistics such as higher order-moments and cumulants bring out promising features of signal characteristics to enable classification of unknown modulation types. The reason that the higher order moments and cumulants are promising is because they appear to be particularly forgiving in very noisy signals. Whether these higher-order statistical features of the noisy signal can be favorably used in the classification of the modulation schemes is investigated here.

The first order moment is equivalent to the mean of a signal and the second order moment provides the variance. The third and fourth order moment measure the skew and the kurtosis of the signal, respectively. Moments beyond the fourth order moment are higher order moments. Higher order moments are considered further in this thesis in designing an automatic modulation classifier that will be described later in Chapter 5.

The thresholds for the modulation classification algorithm were determined by evaluating the higher order statistics of each of the modulated signals transmitted through an AWGN channel at low and high levels of SNRs. Based on the moments and cumulants evaluated at each of the SNR levels, an overall maximum and minimum 2nd order moment, 4th order moment, 6th order moment and 8th order moment were extracted for each of the modulation schemes. Similarly, an overall maximum and minimum 2nd, 4th, 6th and 8th order cumulants were extracted for each of the modulation schemes evaluated in this study. In particular, eighth order cumulants are used in the automatic classification algorithm designed, as described later.

4.2 Moments Definition

Random signals are used this study, and the signals are discrete and finite. Discrete implies that the signals are digital, and finite means that the signals are of certain length and not infinite. In this study, the random signal to be transmitted are generated with zero mean, and are of the form $s = a + jb$. Further, the random signal data is modulated using various modulation schemes implemented in the model of communication system as will be described later in Chapter 5.

Moments are the statistical average or expected value of a modulated random signal data set. For complex discrete random variables, s, the moments of s are defined as:

$$E_{s,a,b} = E[s^a \cdot (s^*)^b] \tag{4.1}$$

where s and s^* represent the number of non-conjugated and conjugated terms, respectively and $a + b$ is the moment order. As examples: (1) if $a = 1$, and $b = 1$, then $E_{s,1,1}$ is second order moment, (2) if $a = 4$, $b = 0$, then $E_{s,4,0}$ is the fourth order moment. The moments are computed by statistical average of the discrete points of the random signal data set. Therefore, the second order moment is defined as $E[s^2]$. The second order moment is the average signal power because s^2 is the power of the signal. The m^{th} order moment is defined as $E[s^m]$.

The moments for M-PSK, M-FSK and M-QAM can be derived by applying Equation (4.1) for various orders of a and b and keeping the real part only [20]. Table 1 shows the derivation of the second and fourth order moments. Table 2 shows the derivation of sixth order moments. Table 3 shows the derivation of eighth order moments.

Table 1: Derivation of 2nd and 4th Order Moments.

Order	Moment	Expression of Moments
2	$E_{s,2,0}$	$E[s^2(s^*)^0] = E[(a+jb)^2]$ $= E[(a^2 - b^2)]$
2	$E_{s,1,1}$	$E[s^1(s^*)^1] = E[(a+jb)(a-jb)]$ $= E[(a^2 + b^2)]$
4	$E_{s,4,0}$	$E[s^4(s^*)^0] = E[(a+jb)^4] = E[(a+jb)^2(a+jb)^2] \rightarrow$ $= E[a^4 + 4a^3bj + 4ab^3j + 6a^2b^2j^2 + jb^4]$ $= E[a^4 + b^4 - 6a^2b^2]$
4	$E_{s,3,1}$	$E[s^3(s^*)^1] = E[(a+jb)^3(a-jb)] \rightarrow$ $= E[(a^3 + 3a^2bj + 3ab^2j + b^3j^3)(a-jb) \rightarrow$ $= E[a^4 + 2a^3bj - 3ab^3j - ab^3j - b^4]$ $= E[a^4 - b^4]$
4	$E_{s,2,2}$	$E[s^2(s^*)^2] = E[(a+jb)^2(a-jb)^2] \rightarrow$ $= E[(a^2 - b^2 + 2abj)(a^2 + b^2 - 2abj)] \rightarrow$ $= E[a^4 + b^4 - 2a^2b^2j^2]$ $= E[a^4 + b^4 + 2a^2b^2]$

Table 2: Derivation of 6th Order Moments.

Order	Moment	Expression of Moments
6	$E_{s,6,0}$	$E[s^6(s^*)^0] = E[(a+jb)^6] = E[(a+jb)^3(a+jb)^3] \rightarrow$ $= E[(a^3+3a^2bj+3ab^2j^2+b^3j^3)(a^3+3a^2bj+3ab^2j^2+b^3j^3)] \rightarrow$ $= E[(a^3+3a^2bj-3ab^2-b^3j)(a^3+3a^2bj-3ab^2-b^3j)]$ $= E[a^6+6a^5bj-6a^4b^2-20a^3b^3j+9a^4b^2j^2-6a^2b^4j^2+9a^2b^4+6ab^5j+b^6j^2] \rightarrow$ $= E[a^6-b^6+15a^2b^4-15a^4b^2]$
6	$E_{s,5,1}$	$E[s^5(s^*)^1] = E[(a+jb)^5(a-jb)] \rightarrow$ $= E[(a^5+5a^4bj+10a^3b^2j^2+10a^2b^3j^3+5ab^4j^4+b^5j^5)(a-bj)] \rightarrow$ $= E[a^6+4a^5bj+5a^4b^2j^2-5a^2b^4j^4-4ab^5j^5-b^6j^6] \rightarrow$ $= E[a^6-5a^4b^2-5a^2b^4+b^6]$
6	$E_{s,4,2}$	$E[s^4(s^*)^2] = E[(a+jb)^4(a-jb)^2] \rightarrow$ $= E[a^4+4a^3bj+6a^2b^2j^2+4ab^3j^3+b^4j^4)$ $(a^2-2abj-b^2)] \rightarrow$ $= E[a^6+2a^5bj-a^4b^2j^2-4a^3b^3j^3-a^2b^4j^4+2ab^5j^5+b^6j^b] \rightarrow$ $= E[a^6+a^4b^2-a^2b^4-b^6]$
6	$E_{s,6,3}$	$E[s^3(s^*)^3] = E[(a+jb)^3(a-jb)^3] \rightarrow$ $= E[a^3+3a^2bj+3ab^2j^2+b^3j^3)(a^3-3a^2bj+3ab^2j^2-b^3j^3)] \rightarrow$ $= E[a^6-3a^4b^2j^2+3a^2b^4j^4-b^6j^6] \rightarrow$ $= E[a^6+3a^4b^2+3a^2b^4+b^6]$

Table 3: Derivation of 8th Order Moments.

Order	Moment	Expression of Moments
8	$E_{s,8,0}$	$E[s^8(s^*)^0] = E[(a+jb)^8] \rightarrow$ $= E[a^8 + 8a^7bj + 28a^6b^2j^2 + 56a^5b^3j^3 + 70a^4b^4j^4 +$ $56a^3b^5j^5 + 28a^2b^6j^6 + 8ab^7j^7 + b^8j^8] \rightarrow$ $= E[a^8 - 28a^6b^2 + 70a^4b^4 - 28a^2b^2 + b^8]$
8	$E_{s,7,1}$	$E[s^7(s^*)^1] = E[(a+jb)^7(a-jb)] \rightarrow$ $= E[(a^7 + 7a^6bj + 21a^5b^2j^2 + 35a^4b^3j^3 + 35a^3b^4j^4 +$ $21a^2b^5j^5 + 7ab^6j^6 + b^7j^7)(a-jb)] \rightarrow$ $= E[a^8 + 6a^7bj + 14a^6b^2j^2 + 14a^5b^3j^3 - 14a^3b^5j^5 -$ $14a^2b^6j^6 - 6ab^7j^7 - b^8j^8] \rightarrow$ $= E[a^8 - 14a^6b^2 + 14a^2b^6 - b^8]$
8	$E_{s,6,2}$	$E[s^6(s^*)^2] = E[(a+jb)^6(a-jb)^2] \rightarrow$ $= E[a^6 + 6a^5bj + 15a^4b^2j^2 + 20a^3b^3j^3 + 15a^2b^4j^4 +$ $6ab^5j^5 + b^6j^6)(a^2 - 2abj + b^2j^2) \rightarrow$ $= E[a^8 + 4a^7bj + 4a^6b^2j^2 - 4a^5b^3j^3 - 10a^4b^4j^4 -$ $4a^3b^5j^5 + 4a^2b^6j^6 + 4ab^7j^7 + b^8j^8] \rightarrow$ $= E[a^8 - 4a^6b^2 - 10a^4b^4 - 4a^2b^6 + b^8]$
8	$E_{s,5,3}$	$E[s^5(s^*)^3] = E[(a+jb)^5(a-jb)^3] \rightarrow$ $= E[(a^5 + 5a^4bj + 10a^3b^2j^2 + 10a^2b^3j^3 + 5ab^4j^4 +$ $b^5j^5)(a^3 - 3a^2bj + 3ab^2j^2 - b^3j^3)] \rightarrow$ $E[a^8 + 2a^7bj - 2a^6b^2j^2 - 6a^5b^3j^3 + 6a^3b^5j^5 + 2a^2b^6j^6 -$ $2ab^7j^7 - b^8j^8)] \rightarrow$ $= E[a^8 + 2a^6b^2 - 2a^2b^6 - b^8]$
8	$E_{s,4,4}$	$E[s^4(s^*)^4] = E[(a+jb)^4(a-jb)^4] \rightarrow$ $= E[(a^4 + 4a^3bj + 6a^2b^2j + 4ab^3j^3 + b^4j^4)(a^4 - 4a^3bj +$ $6a^2b^2j - 4ab^3j^3 + b^4j^4] \rightarrow$ $= E[a^8 - 4a^6b^2j^2 + 6a^4b^4j^4 - 4a^2b^6j^6 + b^8j^8] \rightarrow$ $= E[a^8 + 4a^6b^2 + 6a^4b^4 + 4a^2b^6 + b^8]$

4.3 Cumulants Definition

Cumulants are defined using the cumulant generating function, which is an extension of the moment generating function. The cumulant generating function is defined as:

$$g(t) = \log(E\{e^{ts}\}) = \sum_{n=1}^{\infty} \kappa_n \frac{t^n}{n!} . \tag{4.2}$$

Taking the derivatives of the expanded series of Equation (4.2) and then evaluating these derivatives at time $t = 0$ will lead to the κ_n values, which correspond to the cumulants [21, Ch. 5]. The first derivative of Equation (4.2) gives the mean of the data. The second derivative gives the variance of the data. Higher order cumulants provide additional statistics measures of central tendency of the data [14].

Even ordered cumulants can be expressed in terms of equal or lower order moments [13]. Table 4 lists the expressions for the second, fourth, sixth and eight order cumulants in terms of moments expressed as given in Table 1 throughTable 3. In Table 4, a higher order cumulant $C_{s,a,b}$ of a complex discrete signal s is given, where a and b represent the number of non-conjugated and conjugated terms, respectively and $a + b$ is the cumulant order.

Table 4: 2nd, 4th, 6th, and 8th Order Cumulants Expressed in Terms of Moments.

Order	Cumulant	Expressed in terms of the Moments
2	$C_{s,2,0}$	$E_{s,2,0} = E[s^2(s^*)^0]$
2	$C_{s,1,1}$	$E_{s,1,1} = E[s^1(s^*)^1]$
4	$C_{s,4,0}$	$E_{s,4,0} - 3(E_{s,2,0})^2$
4	$C_{s,3,1}$	$E_{s,3,1} - 3E_{s,2,0} \cdot E_{s,1,1}$
4	$C_{s,2,2}$	$E_{s,2,2} - (E_{s,2,0})^2 - 2(E_{s,1,1})^2$
6	$C_{s,6,0}$	$E_{s,6,0} - 15E_{s,2,0}E_{s,4,0} + 30(E_{s,2,0})^3$
6	$C_{s,5,1}$	$E_{s,5,1} - 10E_{s,2,0}E_{s,3,1} - 5E_{s,1,1}E_{s,4,0} + 30(E_{s,2,0})^2E_{s,1,1}$
6	$C_{s,4,2}$	$E_{s,4,2} - E_{s,2,0}E_{s,4,0} - 8E_{s,1,1}E_{s,3,1} - 6E_{s,2,0}E_{s,2,2} + 6(E_{s,2,0})^3 + 24(E_{s,1,1})^2E_{s,2,0}$
6	$C_{s,3,3}$	$E_{s,3,3} - 6E_{s,2,0}E_{s,3,1} - 9E_{s,1,1}E_{s,2,2} + 18(E_{s,2,0})^2E_{s,1,1} + 12(E_{s,1,1})^3$
8	$C_{s,8,0}$	$E_{s,8,0} - 35(E_{s,4,0})^2 - 630(E_{s,2,0})^4 + 420(E_{s,2,0})^2E_{s,4,0}$
8	$C_{s,7,1}$	$E_{s,7,1} - 35E_{s,4,0}E_{s,3,1} - 630(E_{s,2,0})^3E_{s,1,1} + 210E_{s,4,0}E_{s,2,0}E_{s,1,1} + 210E_{s,2,0}E_{s,3,1}$
8	$C_{s,6,2}$	$E_{s,6,2} - 15E_{s,4,0}E_{s,2,2} - 20(E_{s,3,1})^2 + 30E_{s,4,0}(E_{s,2,0})^2 + 60E_{s,4,0}(E_{s,1,1})^2 + 240E_{s,3,1}E_{s,1,1}E_{s,2,0} + 90E_{s,2,2}(E_{s,2,0})^2 - 90(E_{s,2,0})^4 - 540(E_{s,2,0})^2(E_{s,1,1})^2$

8	$C_{s,5,3}$	$E_{s,5,3} - 5E_{s,4,0}E_{s,3,1} - 30E_{s,3,1}E_{s,2,2} + 90E_{s,3,1}(E_{s,2,0})^2 + 120E_{s,3,1}(E_{s,1,1})^2 + 180E_{s,2,2}E_{s,1,1}E_{s,2,0} + 30E_{s,4,0}E_{s,2,0}E_{s,1,1} - 270\,(E_{s,2,0})^3E_{s,1,1} - 360(E_{s,1,1})^3E_{s,2,0}$
8	$C_{s,4,4}$	$E_{s,4,4} - (E_{s,4,0})^2 - 18(E_{s,2,2})^2 - 16(E_{s,3,1})^2 - 54(E_{s,2,0})^4 - 144(E_{s,1,1})^4 - 432(E_{s,2,0})^2(E_{s,1,1})^2 + 12E_{s,4,0}(E_{s,2,0})^2 + 96E_{s,3,1}E_{s,1,1}E_{s,2,0} + 144E_{s,2,2}(E_{s,1,1})^2 + 72E_{s,2,2}(E_{s,2,0})^2 + 96E_{s,3,1}E_{s,2,0}E_{s,1,1}$

Selecting higher order moments and cumulants are expected to be very useful in distinguishing modulation schemes of communication signals [20]. In this study, even order moments and cumulants are used for the classification of modulation types to be detected.

CHAPTER 5

IMPLEMENTATION OF AUTOMATIC MODULATION CLASSIFIER

5.1 Introduction

The main purpose of this chapter is to show the implementation of the automatic modulation classifier and then to demonstrate the simulation of the algorithmic functions of the automatic classifier using specific examples of digital signals passing through wireless communication system. Before, discussing the details of the implementation of the automatic modulation classifier, details of the implementation of the wireless communication system model are given. Also, since digital signals are the main menu for the wireless system, the details of generation and use of digital signal are discussed. Then, details of generating modulated signals out of the basic random signals are presented. Further, the effect of noise communication in the modulation scheme as well as on the process of classification of modulation scheme from the signal received, are discussed. Finally, the process of the classification of the modulation scheme by setting appropriate threshold values for making decision to the group the modulated signals according to its statistical features are discussed. All these implementations were made using user developed subroutines of the MATLAB® program and MATLAB® Communication Toolbox. Separate MATLAB® functions were written to code the details of the various mathematical formulations of the moments and cumulant expressions described in the previous chapters. The implementation of the wireless communication system model are described first.

5.2 Implementation of Wireless Communication System

A basic wireless communication system consisting of a transmitter, channel and receiver is implemented in MATLAB® to serve as a framework for developing the automatic modulation classifier. The pertinent models of the transmitter, channel, and receivers,

shown in Figure 30. The transmitter model contains a random digital signal generator and digital signal modulator. The channel model contains models of the AWGN channel, multipath Rayleigh fading channel and multipath Ricean fading channel. The receiver model contains statistical signal analyzer and the automatic classification algorithm, which identifies the modulation scheme of the signal. Therefore, input to the wireless communication system is basically a digital modulated signal using a specific modulation scheme, and the output is the identified modulation scheme in the signal captured that is distinguished without *a priori* knowledge of the modulation scheme used in the input signal.

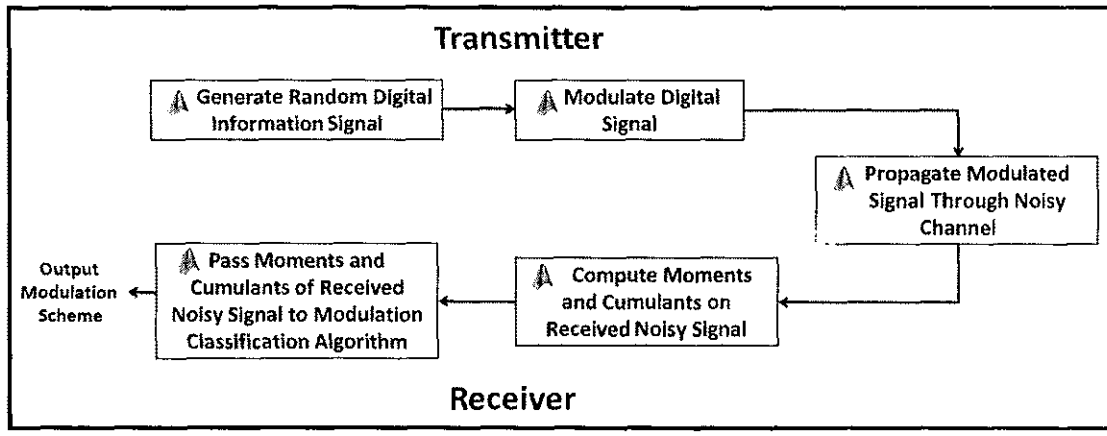

Figure 30: Block Diagram of MATLAB® Model.

5.3 Generation of Random Digital Signals and Modulation of the Signals

Communication signals are random and fluctuate in time. The digital message signal was generated using integer stream of data points by using a MATLAB® function called "randi". In this study, 20,000 bits of random data were generated to represent the information signal. This random vector of data had zero mean, and the size of digital vector was 1 x 20,000. In the simulation studies, the modulated random signals were passed through the transmitter, the channel and the receiver system, iteratively, 1,000 times, to test the capability of the automatic modulation to correctly identify the modulation scheme.

This stream of random data bits were then modulated using one of the MATLAB® modulation functions for each of the modulation schemes. For example, the BPSK modulator uses "comm.BPSKModulator" and the 4-PSK modulator uses the function "comm.PSKModulator" from the MATLAB® Communication Toolbox. Figure 31 shows an example of the MATLAB® code used to model the 4-PSK modulation scheme in the wireless communication system. In this example, a random signal with 20,000 data points is modulated using 4-PSK. Inputs for the PSK function are modulation size, phase offset and symbol mapping scheme. The modulation size for PSK function is of size 4 or 8. For the 4-PSK modulation scheme, the modulation size is set to 4. In PSK modulation, the phase offset variable defines the which phases of the carrier signal should contain the message information. In 4-PSK, the phase offset is set to $\frac{\pi}{4}$ such that the digital information are mapped onto $\frac{\pi}{4}, \frac{3\pi}{4}, \frac{5\pi}{4}, \frac{7\pi}{4}$ intervals of the phases of the original carrier signal. The symbol mapping variable is set to "gray" so that Gray coding is using to encode the message signal into adjacent bits on the constellation diagram. As shown in Figure 31, once the signal passes through the PSK function, the output signal will be modulated with 4-PSK. After modulation, each bit of the random message signal is of the form $s = a + jb$. Similarly, the other modulation functions are scripted and are called as needed to generated various types of modulated signal.

```
%% 4PSK Modulation AWGN
clear all
clc
close all
for j = 1:1000;
M = 4;                    % Modulation alphabet size
phOffset = pi()/4;        % Phase offset
symMap = 'gray';          % Symbol mapping
hMod = comm.PSKModulator(M,phOffset,'SymbolMapping',symMap);
modData = step(hMod,randi([0 3],20000,1));
noise(j) = randi([0 25],1);        %Generate random noise data in the range of 0dB to 25dB
hAWGN = comm.AWGNChannel('SNR',noise(j),'BitsPerSymbol',4);
channelOutput = step(hAWGN, modData);
scatterplot(modData)
scatterplot(channelOutput)
end
```

Figure 31: MATLAB® Model of the Wireless Communication System for 4-PSK Modulated Signal Passed Through AWGN Channel.

5.4 Model of the Noisy Communication Channel

The modulated signal was passed through the communication channel. The channel functions available in the MATLAB® Communication Toolbox were used to simulate the propagation of a random signal through the communication medium. The communication channel was simulated with either a AWGN channel, multipath Rayleigh fading channel with AWGN, or multipath Ricean fading channel with AWGN at various levels of SNR. The AWGN channel is implemented using the "comm.AWGNChannel" function from the MATLAB® Communication toolbox. The AWGN function adds noise to the modulated random signal. The inputs to this function are the signal to noise ratio and the number of bits per symbol. Each of the message symbols were mapped onto four bits per symbol. The SNR levels of the channel were randomly generated as an integer value within the range of 0 dB to 25 dB to propagate signals through high noise channels. Similarly, for low noise channels, integer values of the SNR were randomly chosen within the range of 50 dB to 100 dB. This random generation of the SNR was implemented by using the "randi" function in MATLAB®. The implementation of the AWGN function in MATLAB® is shown in Figure 31.

The multipath Rayleigh fading channel with AWGN was implemented using the "rayleighchan" function from the MATLAB® Communication Toolbox. The Rayleigh channel model constructs a multiple fading channel that has multiple discrete signal paths. The inputs to this function are sample time of the input signal, signal path delay, average path gain and frequency of the Doppler shift. The Rayleigh fading channel was assumed to have two multipath delays of 0 seconds and 1e-7 seconds [22], respectively. The average path gain was zero and the signal sample time used was 1e-5 seconds. There was no Doppler shift considered in the Rayleigh fading scenario; therefore, this parameter was set to zero. AWGN was added to the Rayleigh fading channel using the "comm.AWGNChannel" function. The implementation of the Rayleigh fading with AWGN channel for random signals modulated with 4-PSK is shown in Figure 32.

```
%% 4PSK Modulation Rayleigh Channel With AWGN
clear all
clc
close all
for j = 1:1000;
M = 4;                    % Modulation alphabet size
phOffset = pi()/4;        % Phase offset
symMap = 'gray';          % Symbol mapping (either 'binary' or 'gray')
hMod = comm.PSKModulator(M,phOffset,'SymbolMapping',symMap);
modData = step(hMod,randi([0 3],20000,1));
ts = 1e-5;        % sample time
fd = 0;           % maximum Doppler shift in Hz
tau = [0 1e-7];   % path delays
pdb = [0 0];      % average path gains
c1 = rayleighchan(ts, fd, tau, pdb); %Pass the modulated bits through Rayleigh channel
channelOutput = filter(c1, modData);
noise(j) = randi([0 25],1);          %Generate random noise data in the range
hAWGN = comm.AWGNChannel('SNR',noise(j),'BitsPerSymbol',4);
channelOutput = step(hAWGN, channelOutput);  %Pass the modulated bits through AWGN channel
scatterplot(modData)
scatterplot(channelOutput)
end
```

Figure 32: MATLAB® Model of the Wireless Communication System for 4-PSK Modulated Signal Passed Through Rayleigh Channel with AWGN.

The multipath Ricean fading channel with AWGN was implemented using the "rayleighchan" function from the MATLAB® Communication Toolbox. The Ricean channel model constructs a multiple fading channel that has multiple discrete signal paths. The inputs to this function are sample time of the input signal, signal path delay, Ricean *k* factor, average path gain and frequency of the Doppler shift. The Ricean fading channel was assumed to have two multipath delays of 0 seconds and 10^{-7} seconds [22], respectively. The average path gain was zero and the signal sample time used was 10^{-5} seconds. There was no Doppler shift considered in the Rayleigh fading scenario; therefore, this parameter was set to zero. The Ricean *k* factor used was 3 dB. AWGN was added to the Ricean fading channel using the "comm.AWGNChannel" function. The implementation of the Ricean fading with AWGN channel for random signals modulated with 4-PSK is shown in Figure 33.

```
%% 4PSK Modulation AWGN
clear all
clc
close all
for j = 1:1000;
M = 4;                    % Modulation alphanet size
phOffset = pi()/4;        % Phase offset
symMap = 'gray';          % Symbol mapping (either 'binary' or 'gray')
hMod = comm.PSKModulator(M,phOffset,'SymbolMapping',symMap);
modData = step(hMod,randi([0 3],20000,1));
ts = 1e-5;                % sample time
fd = 0;                   % maximum Doppler shift in Hz
tau = [0 1e-7];           % path delays
pdb = [0 0 ];             % average path gains
k = 3;                    % Ricean k factor in dB
c1 = ricianchan(ts, fd, k, tau, pdb); % Pass modulated bits through Ricean Channel
channelOutput = filter(c1, modData);
noise(j) = randi([0 25],1);          %Generate random noise data in the range of SNR
hAWGN = comm.AWGNChannel('SNR',noise(j),'BitsPerSymbol',4);
channelOutput = step(hAWGN, channelOutput);  %Pass the modulated bits through AWGN channel
scatterplot(modData)
scatterplot(channelOutput)
end
```

Figure 33: MATLAB® Model of the Wireless Communication System for 4-PSK Modulated Signal Passed Through Ricean Channel with AWGN.

5.5 The Receiver, Signal Statistical Analyzer and Classifier

At the receiver end of the wireless communication system, the modulated signal that was generated by the transmitter and passed though the noisy communication channel is received. The primary functions implemented in the receiver model are statistical computational algorithm, which computes all the moments and cumulants of the received signal. Also, the receiver has an automatic modulation classification algorithm. The statistical computational algorithm passes the higher order statistics of the signal to the modulation classification algorithm, which identifies the modulation scheme of the signal based on predefined statistical thresholds. Figure 30 showed the block diagram representation of the receiver model.

The message signal after modulation was of the form $s = a + jb$. The real and the imaginary portions of the modulation signal were separated to feed into the moment and cumulant expressions (shown in Table 1 through Table 4 of Chapter 4) to compute the higher order statistics of the signal. Figure 34 shows the MATLAB® code which computes the signal moments. The second, fourth and sixth order cumulant implementations of the user written function in the MATLAB® code are shown in Figure 35. Figure 36 shows the eighth order cumulant expressions in the MATLAB®.

```
a = real(channelOutput);
b = imag(channelOutput);
p_out = sum(abs(channelOutput).^2)/20000;
%second order moments
e20(j) = mean(a.^2-b.^2);
e11(j) = mean(a.^2+b.^2);
%fourth order moments
e40(j) = mean(a.^4+b.^4-(6*a.^2.*b.^2));
e31(j) = mean(a.^4-b.^4);
e22(j) = mean(a.^4+b.^4+(2*a.^2.*b.^2));
%sixth order moments
e60(j) = mean(a.^6-b.^6+(15.*a.^2.*b.^4)-(15.*a.^4.*b.^2));
e51(j) = mean(a.^6-(5.*a.^4.*b.^2)-(5.*a.^2.*b.^4)+b.^6);
e42(j) = mean(a.^6+a.^4.*b.^2-a.^2.*b.^4-b.^6);
e33(j) = mean(a.^6 + 3.*a.^4.*b.^2+3.*a.^2.*b.^4+b.^6);
%eight order moments
e80(j) = mean(a.^8-28.*a.^6.*b.^2+70.*a.^4.*b.^4-28.*a.^2.*b.^6+b.^8);
e71(j) = mean(a.^8-(14.*a.^6.*b.^2)+(14.*a.^2.*b.^6)-b.^8);
e62(j) = mean(a.^8-(4.*a.^6.*b.^2)-(10.*a.^4.*b.^4)-(4.*a.^2.*b.^6)+b.^8);
e53(j) = mean(a.^8+(2.*a.^6.*b.^2)-(2.*a.^2.*b.^6)-b.^8);
e44(j) = mean(a.^8+(4.*a.^6.*b.^2)+(6.*a.^4.*b.^4)+(4.*a.^2.*b.^6)+b.^8);
```

Figure 34: MATLAB® Implementation of 2nd, 4th and 8th Order Moment Expressions.

```
%second order cumulant
c20(j) = e20(j);
c11(j) = e11(j);
%fourth order cumulant
c40(j) = e40(j)-3.*(e20(j)).^2;
c31(j) = e31(j)-3.*(e20(j)).*(e11(j));
c22(j) = e22(j)-(e20(j)).^2-2.*(e11(j)).^2;
%sixth order moment
c60(j) = e60(j)-15.*(e20(j)).*(e40(j))+30.*(e20(j)).^2;
c51(j) = e51(j)-10.*(e20(j)).*(e31(j))-5.*(e11(j)).*(e40(j))+30.*(e20(j)).^2.*...
    (e11(j));
c42(j) = e42(j)-e20(j).*(e40(j))-8.*(e11(j)).*(e31(j))-6.*(e20(j)).*(e22(j))+6.*...
    (e20(j)).^3+24.*(e11(j)).^2.*e20(j);
c33(j) = e33(j)-6.*(e20(j)).*(e31(j))-9.*(e11(j)).*(e22(j))+18.*(e20(j)).^2.*...
    (e11(j))+12.*(e11(j)).^3;
```

Figure 35: MATLAB® Implementation of 2nd, 4th and 8th Order Cumulant Expressions.

```
%eighth order moment
c80(j) = e80(j)-35.*(e40(j))^2-630.*(e20(j)).^4+420.*(e20(j)).^2.*(e40(j));
c71(j) = e71(j)-35.*(e40(j)).*(e31(j))-630.*(e20(j)).^3.*(e11(j))+210.*(e40(j)).*...
    (e20(j)).*(e11(j))+210.*(e20(j)).*(e31(j));
c62(j) = e62(j)-15.*(e40(j)).*(e22(j))-20.*(e31(j)).^2+30.*(e40(j)).*(e20(j)).^2+...
    60.*(e40(j)).*(e11(j)).^2+240.*(e31(j)).*(e11(j)).*(e20(j))+90.*(e22(j)).*...
    (e20(j)).^2-90.*(e20(j)).^4-540.*(e20(j)).^2.*(e11(j)).^2;
c53(j) = e53(j)-5.*(e40(j)).*(e31(j))-30.*(e31(j)).*(e22(j))+90.*(e31(j)).*...
    (e20(j)).^2+120.*(e31(j)).*(e11(j)).^2+180.*(e22(j)).*(e11(j)).*(e20(j))+...
    30.*(e40(j)).*(e20(j)).*(e11(j))-270.*(e20(j)).^3.*(e11(j))-360.*(e11(j)).^3.*(e20(j));
c44(j) = e44(j)-(e40(j)).^2-18.*(e22(j)).^2-16.*(e31(j)).^2-54.*(e20(j)).^4-...
    144.*(e11(j)).^4-432.*(e20(j)).^2.*(e11(j)).^2+12.*(e40(j)).*(e20(j)).^2+...
    96.*(e31(j)).*(e11(j)).*(e20(j))+144.*(e22(j)).*(e11(j)).^2+72.*(e22(j)).*...
    (e20(j)).^2+96.*(e31(j)).*(e20(j)).*(e11(j));
```

Figure 36: MATLAB® Implementation of 8th Order Cumulant Expression.

Moments and cumulants were computed for all the modulated signals passed through the AWGN channel with SNR levels at 0 dB, 3 dB, 5 dB, 6 dB, 7 dB, 8 dB, 10 dB, 15 dB, 20 dB, 40 dB, and 100 dB. The moments and cumulants were extracted at these SNR levels because the moments and cumulants showed to have significant statistical variations at these SNR levels. Based on extracted moments and cumulants at the various SNR levels, overall maximum and minimum higher order moment and cumulant ranges were computed in setting modulation decision thresholds for the automatic modulation classification algorithm.

It may be noted that one of the characteristics of the higher order moments and cumulants indicated that the magnitude of these higher order statistical values increase with the increasing order of the moments and cumulants. This characteristic resulted in forcing an artificially higher weight age on the higher order terms to influence the results from the classification scheme. In order to eliminate artificial weight age, the second order moments and cumulants were normalized with respect to the signal power. The fourth order moments and cumulants were normalized with respect to the square of the signal power. The third and fourth order moments and cumulants were normalized with respect to the cube and to the fourth power of the signal power, respectively. Normalizing the moments and cumulants in this way helped to even out the magnitude of moments and cumulants with increasing order. Figure 37 and Figure 38 show the MATLAB® code that normalizes the moments and cumulants to signal power.

```
% normalized
ne20 = e20/p_out;
ne11 = e11/p_out;
%
ne40 = e40/p_out^2;
ne31 = e31/p_out^2;
ne22 = e22/p_out^2;
%
ne60 = e60/p_out^3;
ne51 = e51/p_out^3;
ne42 = e42/p_out^3;
ne33 = e33/p_out^3;
%
ne80 = e80/p_out^4;
ne71 = e71/p_out^4;
ne62 = e62/p_out^4;
ne53 = e53/p_out^4;
ne44 = e44/p_out^4;
```

Figure 37: Normalization of Moments With Respect to Signal Power.

```
% normalized
nc20 = c20/p_out^2;
nc11 = c11/p_out^2;
%
nc40 = c40/p_out^2;
nc31 = c31/p_out^2;
nc22 = c22/p_out^2;
%
nc60 = c60/p_out^3;
nc51 = c51/p_out^3;
nc42 = c42/p_out^3;
nc33 = c33/p_out^3;
%
nc80 = c80/p_out^4;
nc71 = c71/p_out^4;
nc62 = c62/p_out^4;
nc53 = c53/p_out^4;
nc44 = c44/p_out^4;
```

Figure 38: Normalization of Cumulants With Respect to Signal Power.

The moment and cumulants were computed for the modulated signal that was transmitted through the communication medium; they were then passed on to the automatic modulation classifier to identify the modulation scheme at the receiver end. The implementation and design of the modulation classification algorithm are described in Section 5.6.

5.6 Automatic Modulation Classification Algorithm

The automatic classification modulation algorithm identifies the modulation scheme of the signal by evaluating whether the statistical features of a modulated signal lie within the predefined cumulant range thresholds. The cumulant threshold ranges for the classifier were determined by evaluating the moments and cumulants of modulated signals that were transmitted through an AWGN channel at various levels of high and low SNRs. In this research, signals were modulated using BPSK, 4-PSK, 8-PSK, 2-FSK, 4-FSK, 8-FSK, 8-QAM, 16-QAM, 64-QAM and 256-QAM. The modulation algorithm

defines a preset cumulant threshold range for each of the modulation scheme evaluated in this study.

The modulation classification algorithm identifies the modulation scheme of the received signal by evaluating whether the eighth order cumulants lie within one of the preset cumulant threshold ranges of a particular modulation scheme. If the cumulants of the noisy signal do not meet the threshold criteria, then the signal is identified as not belonging to the modulation scheme associated with that statistical feature. On the other hand, if the cumulants of the noisy signal does meet the threshold criteria, then the classification tree identifies that only the certain modulation scheme is associated with the statistical features.

The cumulant thresholds for the modulation classification algorithm were determined by evaluating the higher order statistics of each of the modulated signals transmitted through an AWGN channel at low and high levels of SNRs. Table 5 provides the moments and cumulants of signals that were modulated using BPSK, 4-PSK, 8-PSK, 2-FSK, 4-FSK, 8-FSK, 8-QAM, 16-QAM, 64-QAM and 256-QAM and passed over an noiseless channel (SNR = ∞). The moments and cumulant values shown in Table 5 were computed based on moments and cumulant expressions, that were provided in Table 1 throughTable 3 in Chapter 4 and cumulant expressions provided in Table 4 of Chapter 4. Similarly, the moments and cumulants of modulated signals were extracted for noisy channels at SNR levels at 0 dB, 3 dB, 5 dB, 6 dB, 7 dB, 8 dB, 10 dB, 15 dB, 20 dB, and 40 dB. The moments and cumulants were also extracted for a noiseless channel with SNR level of 100 dB. The moments and cumulants for the modulated signals at these SNRs were exported to Microsoft® Excel to evaluate statistical threshold values for each of the modulation schemes.

Table 5: Simulated Moments and Cumulants Simulated Without Disturbance.

	BPSK	4PSK	8PSK	2FSK	4FSK	8FSK	8QAM	16QAM	64QAM	256QAM
SNR	∞	∞	∞	∞	∞	∞	∞	∞	∞	∞
Es20	1	0.00	0.00	0.00	0.00	0.00	0.67	0.00	0.00	0.01
Es11	1	1.00	1.00	1.00	1.00	1.00	1.00	1.00	1.00	1.00
Es40	1	-1.00	0.00	0.00	0.00	0.00	0.33	-0.68	-0.62	-0.61
Es31	1	0.00	0.00	0.00	0.00	0.00	1.11	0.00	0.00	0.01
Es22	1	1.00	1.00	1.00	1.00	1.00	1.44	1.32	1.38	1.39
Es60	1	0.00	0.00	0.00	0.00	0.00	-0.81	0.00	0.01	0.00
Es51	1	-1.00	0.00	0.00	0.00	0.00	0.63	-1.32	-1.31	-1.29
Es42	1	0.00	0.00	0.00	0.00	0.00	1.85	0.00	-0.01	0.01
Es33	1	1.00	1.00	1.00	1.00	1.00	2.33	1.95	2.24	2.28
Es80	1	1.00	-1.00	0.00	0.00	0.00	-3.23	2.19	1.95	1.84
Es71	1	0.00	0.00	0.00	0.00	0.00	-1.35	0.00	0.02	0.00
Es62	1	-1.00	0.00	0.00	0.00	0.00	1.07	-2.46	-2.79	-2.81
Es53	1	0.00	0.00	0.00	0.00	0.00	3.07	0.00	-0.01	0.02
Es44	1	1.00	1.00	1.00	1.00	1.00	3.84	3.09	4.00	4.17
Cs20	1	0.00	0.00	0.00	0.00	0.00	0.11	0.00	0.00	0.00
Cs11	1	1.00	1.00	1.00	1.00	1.00	0.17	0.10	0.02	0.01
Cs40	-2	-1.00	0.00	0.00	0.00	0.00	-1.00	-0.68	-0.62	-0.61
Cs31	-2	0.00	0.01	0.00	0.00	0.00	-0.89	-0.01	0.00	-0.01
Cs22	-2	-1.00	-1.00	-1.00	-1.00	-1.00	-1.00	-0.68	-0.62	-0.61
Cs60	16	0.00	0.00	0.00	0.00	0.00	-1.93	0.04	0.00	0.07
Cs51	16	4.00	0.00	0.00	0.00	0.00	4.92	2.09	1.79	1.75
Cs42	16	0.00	-0.03	0.00	0.00	0.00	4.77	0.04	0.00	0.06
Cs33	16	4.00	4.00	4.00	4.00	4.00	4.92	2.10	1.78	1.75
Cs80	-244	-34.00	-1.00	0.00	0.00	0.00	-69.77	-14.09	-11.54	-11.13
Cs71	-244	0.00	0.01	0.00	0.00	0.00	-129.03	-0.54	0.13	-0.76
Cs62	-244	-46.00	0.00	0.00	0.00	0.00	-29.14	-29.92	-27.15	-26.61
Cs53	-244	0.00	0.28	0.00	0.00	0.00	-9.73	-0.27	-0.07	-0.15
Cs44	-244	-18.00	-17.00	-17.00	-17.00	-17.00	-2.62	16.99	24.44	25.46

Based on the moments and cumulants evaluated at each of the SNR levels, an overall maximum and minimum 2^{nd} order moment, 4^{th} order moment, 6^{th} order moment and 8th order moment were extracted for each of the modulation schemes. Similarly, an overall maximum and minimum 2^{nd}, 4^{th}, 6^{th} and 8^{th} order cumulants were extracted for each of the modulation schemes evaluated in this study. Appendix A provides the overall maximum and minimum moments and cumulant tables for each of the modulated signals transmitted through an AWGN channel over a range of low and high SNR levels. The modulation scheme cumulant decision thresholds were determined by analyzing the maximum and minimum moments and cumulants ranges. A decision threshold for an modulation scheme was chosen based on the unique maximum and minimum statistical range which did not overlap with other maximum and minimum statistical modulation ranges.

Table 6 shows the eighth order maximum and minimum cumulant ranges. Analysis of this table shows that signals modulated with modulated with BPSK, 4-PSK, 8-PSK and 8-QAM have unique non overlapping cumulant ranges. For example, in Table 6, it can be seen that BPSK has a eight order cumulant range that does not overlap the cumulant range for any of the other modulation schemes. Therefore, signals modulated with BPSK, 4-PSK, 8-PSK and 8-QAM can be identified by using the higher order eighth order cumulants, C_{s80}. These eighth order cumulant ranges were used as decision thresholds in the modulation classification algorithm to evaluate whether the transmitted was modulated specifically with BPSK, 4-PSK, 8-PSK or 8-QAM. The modulation classification algorithm evaluates the received signal's moments and cumulants to clearly distinguish the modulation scheme of signal types "BPSK", "4-PSK", "8-PSK", and "8-QAM" if the signal's statistical features satisfy the preset moment and cumulant threshold range.

Modulation schemes 2-FSK, 4-FSK and 8-FSK have overlapping maximum and minimum eighth order cumulant (C_{s80}) ranges or ranges with values that lie within close proximity. Therefore, eight order cumulant threshold range for 2-FSK, 4-FSK and 8-FSK are grouped together such that the classifier will identify the signals modulated with FSK as "M-FSK". Also based on the cumulant ranges given in Table 6, it was analyzed

that signals modulated with 16-QAM, 64-QAM or 256-QAM can be identified with eighth order cumulant (C_{s44}) ranges. However, modulation schemes 16-QAM, 64-QAM and 256-QAM have maximum and minimum eighth order cumulant (C_{s44}) ranges that overlap each other or are in close proximity. Therefore, the eighth order cumulant threshold ranges for 16-QAM, 64-QAM and 256-QAM are grouped together such that the classifier will identify these modulated signals as "M-QAM".

Table 6: Eighth Order Cumulant Range for Modulated Signals Passed Through AWGN Channel.

	Cs80		Cs71		Cs62		Cs53		Cs44	
	max	min	max	min	max	min	max	min	max	min
BPSK	-98.55	-244	-86.23	-244	-73.49	-244	-61.44	-244	-56.53	-244
4PSK	-14.36	-34	0.2327	-0.7535	-28.12	-46	0.1751	-0.4187	22.84	-18
8PSK	-0.379	-1	0.012	-0.0442	0.3692	-0.155	0.2866	-0.0846	23.128	-17
2FSK	0.0053	-0.021	0.0372	-0.0075	0.2552	-0.027	0.1644	-0.0452	56.068	-17
4FSK	0.0064	-0.029	0.0119	-0.0382	0.0481	-0.242	0.2855	-0.0591	56.577	-17
8FSK	0.0084	-0.065	0.0178	-0.0078	0.0979	-0.386	0.0541	-0.2526	56.384	-17
8QAM	-58.81	-69.77	-113.9	-129.03	-20.08	-29.14	1.4958	-9.7297	10.089	-2.621
16QAM	-12.84	-14.1	-0.456	-0.5526	-28.51	-29.92	-0.209	-0.3117	20.653	16.992
64QAM	-11.27	-11.54	0.1776	0.0762	-26.82	-27.16	-0.013	-0.1041	25.244	24.444
256QAM	-11.05	-11.14	-0.727	-0.816	-26.49	-26.61	-0.141	-0.1695	25.598	25.452

Communication signals are random and fluctuate in time. Therefore, the moments and cumulants of these signals will also vary. Even though 1,000 random signals were generated, modulated and transmitted through a communication channel to extract an overall unique statistical range for each modulation scheme, these ranges are not definite. Therefore, tolerances were built into the eighth order cumulant ranges that were used to identify the modulation scheme of the received signal. In order to evaluate variations in moments and cumulants ranges for different communication channels, other than on an AWGN channel, tables similar to the ones shown in Appendix A were constructed for a multipath Rayleigh fading channel with AWGN and multipath Ricean fading channel with AWGN. Overall maximum and minimum moment and cumulant ranges for a Rayleigh fading channel at the various levels of SNRs evaluated in this study are shown

in Appendix B. Appendix C shows the overall maximum and minimum moment and cumulant ranges for Ricean fading channel, evaluated at the various levels of SNRs.

From analysis of eighth order cumulant values from Table 6, eighth order cumulant decision threshold ranges with tolerances were chosen to evaluate the received signal's modulation scheme. Therefore, the classification algorithm will identify the modulation scheme of a random signal as "BPSK" if the eighth order cumulant C_{s80} of the intercepted signal lies in between -1e12 to -80. The classification algorithm will identify the modulation scheme of a random signal as "4-PSK" if the eighth order moment E_{s80} of the intercepted signal lies in between -35 and -3. The classification algorithm will identify the modulation scheme of a random signal as "8-PSK" if the eighth order cumulant C_{s80} of the intercepted signal lies in between -2 and 0.1. The classification algorithm will identify the modulation scheme of a random signal as "M-FSK" if the eighth order cumulant C_{s80} of the intercepted signal lies in between -0.5 and 0.25. The classification algorithm will identify the modulation scheme of a random signal as "8-QAM" if the eighth order cumulant C_{s80} of the intercepted signal lies in between -78 and -20. The classification algorithm will identify the modulation scheme of a random signal as 8-QAM if the eighth order cumulant C_{s80} of the intercepted signal lies in between -78 and -20. The classification algorithm will identify the modulation scheme of a random signal as "16-QAM, 64-QAM or 256-QAM" if the eighth order cumulant C_{s44} of the intercepted signal lies between 15 and 1e12. A flowchart diagram of the modulation classification algorithm is shown in Figure 39.

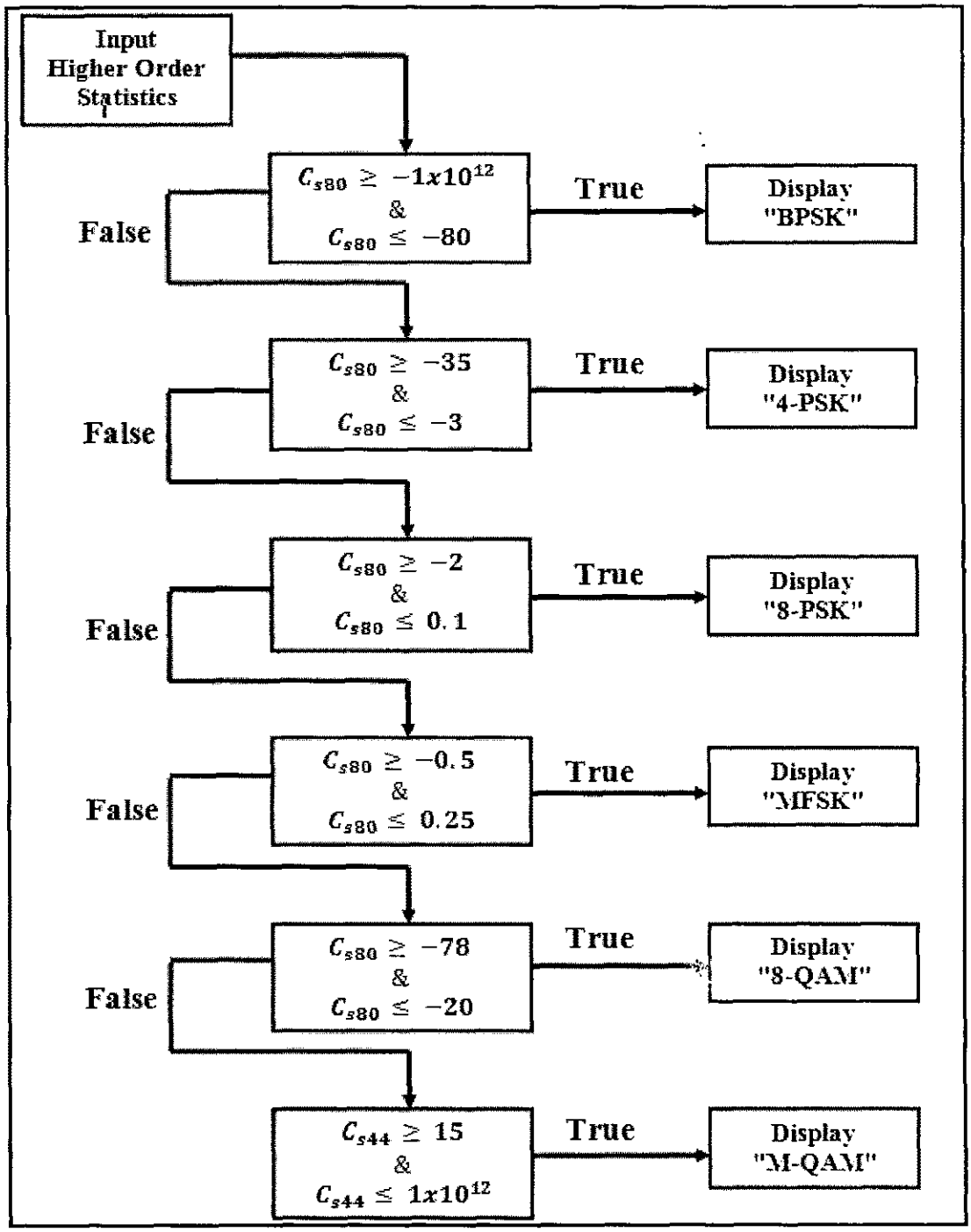

Figure 39: Block Diagram of Modulation Classification Algorithm.

The robustness of the modulation classification algorithm is evaluated by examining its ability to detect the modulated scheme transmitted signal passed through AWGN channel, multipath Rayleigh fading channel and multipath Ricean fading channel. Chapter 6 discusses the results of the ability of the classification modulation algorithm to detect the modulation scheme of a distorted signal.

CHAPTER 6

SIMULATION RESULTS AND DISCUSSION

6.1 Introduction

In this chapter, wireless communication system simulation results are presented with a focus on results from the automatic modulation classifier system. Simulation results are presented in two parts. First, basic simulations results which describe the benefits of an automatic modulation classifier over conventional modulation identifier are presented. Second, the results from the modulation classification algorithm developed in this study as it currently operating in the wireless communication system designed are presented. Section 6.2 through Section 6.3 present basic simulations of the wireless communication system are presented where results show how the effect of channel noise on the signals detected at the receiver. In these sections, simulations performed compare the performance and tradeoffs between two types of modulation schemes 1) M-PAM and 2) M-PSK. The results show how M-PAM and M-PSK signals passed over a channel with AWGN to analyze the bit error rate impact the signal's detection at the receiver. Finally, the results from the successful classification or detection of modulation schemes as identified by the classification algorithm developed in this research are presented in Section 6.4.

6.2 Simulations Examining Effect of AWGN on M-PAM and M-PSK Modulation

Eight distinct computer simulation experiments were performed to show the effect of Additive White Gaussian Noise channel (AWGN) on four modulation schemes: 2-PAM, 4-PAM, QPSK and 8-PSK. In these experiments, the amplitude of the signal and noise variances were changed to see the effect of variations of these to analyze the decoding issues on signals at the receiver end.

The first experiment was performed with the 2-PAM modulation scheme. In this experiment, the signal is characterized by a vector of random numbers with a defined noise variance given by the parameter σ^2. In Experiment 1A, a message signal is modulated using the 2-PAM scheme with signal amplitude of 1. The modulated signal is then passed over various AWGN channels with noise variances of 0.1, 0.04, 0.1 and 0.25. In Experiment 1B, the message signal is modulated using 2-PAM with signal amplitude increased to 2 and is passed over a channel with noise variance of 0.25. At the receiver end, the signal bits or symbols are observed. Based on the observed bits (or symbols) from Experiments 1A and Experiment 1B, an analysis was made to determine how the modulation scheme could be modified to reduce the signal error detected at the receiver.

The second experiment was performed with the 4-PAM modulation scheme. In Experiment 2A, the information signal was modulated using 4-PAM modulation scheme with signal amplitudes of 2 and 4. The modulated signal was then passed over various channels with noise variances of 0.1, 0.04, 0.1 and 0.25. In Experiment 2B, the message signal was modulated using 4-PAM with increased signal amplitudes of 4 and 8. The digitally modulated analog signal was then passed over a channel with noise variance of 0.25. Based on the results obtained from Experiments 2A and Experiment 2B an analysis was made to determine how the modulation scheme could be modified to reduce the detection error at the receiver end.

The third experiment was performed with the QPSK modulation scheme. In Experiment 3A, QPSK modulation is studied with noise variance just like in previous experiments but with a signal amplitude of 1. In Experiment 3B, the message signal is modulated using QPSK with signal amplitudes increased to 1, 2, 3 and 4, and signal transmitted with noise variance of 0.25. The signal bits or symbols are observed At the receiver end. Based on the observed bits (or symbols) from Experiments 3A and Experiment 3B, an analysis was made to determine how the modulation scheme could be modified to reduce the signal error detected at the receiver.

Finally, the fourth experiment was performed with the 8-PSK modulation scheme. In Experiment 4A, 8-PSK modulation is studied for which signals with amplitude of 1 are passed with various noise variances just like before. In Experiment 4B, the message

signal modulated using 8-PSK with signal amplitudes increased to 1, 2, 3 and 4 noise variance of 0.25. Based on the observed bits (or symbols) from Experiments 4A and 4B, an analysis was made to determine how the modulation scheme could be modified to reduce the signal error detected at the receiver.

The following sub-sections discuss the results from these simulation analyses.

6.2.1. Experiment 1A: Modulation With 2-PAM With Constant Amplitude and Varying Noise Level

Figure 40 throughFigure 44 show the 2-PAM signal constellation diagrams constructed after information was received from the noisy channel.

Figure 40 shows a 2-PAM signal constellation diagram with two signals transmitted with amplitudes of 1 and -1 with noise variance of 0.01. The digital modulator transmits an analog waveform with amplitude 1 that maps to a binary bit of 1, and analog waveform of amplitude of -1 that maps to a binary bit of 0. The receiver measures the amplitude of the received analog waveform and distinguishes whether a 1 or 0 binary digit was transmitted. The "o" in the plots corresponds to 1 binary bit received and "x" corresponds to 0 binary bit received at the receiver. (Note that both the digital modulator and the receiver know the mapping between the binary bits to the analog waveform). With noise variance of 0.01, the noise was clustered compactly around the actual transmitted waveform. The receiver can make a distinction between the binary bits, based on whether the amplitude of the received analog signal is positive or negative. Positive signal amplitude received can map to a 1 bit transmitted and negative signal amplitude received can map to a 0 bit transmitted.

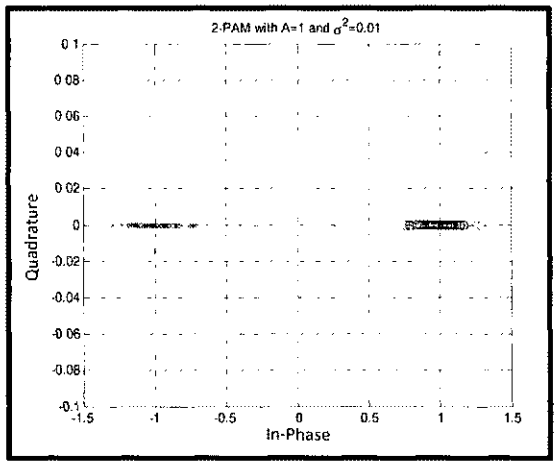

Figure 40: 2-PAM with A = 1, σ^2 = 0.01.

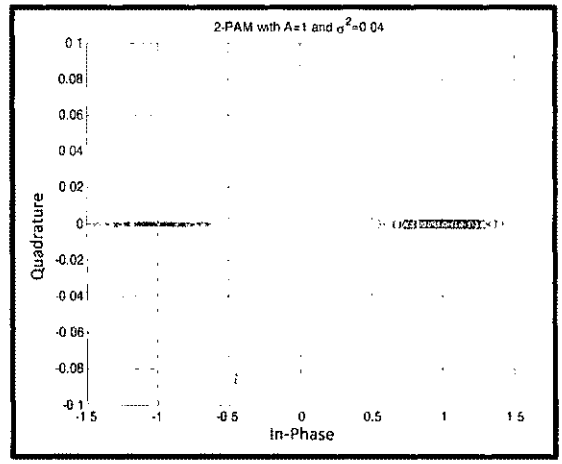

Figure 41: 2-PAM with A = 1, σ^2 = 0.04.

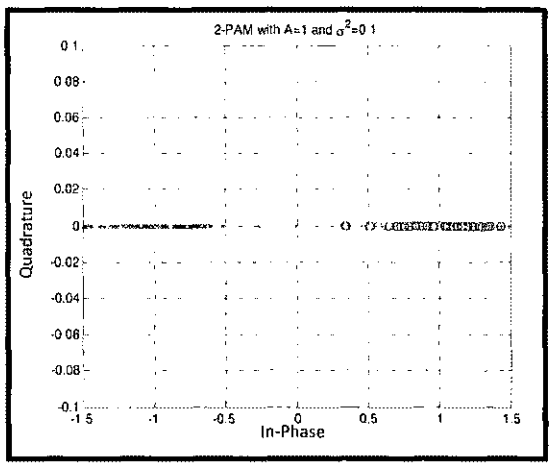

Figure 42: 2-PAM with A = 1, σ^2 = 0.1.

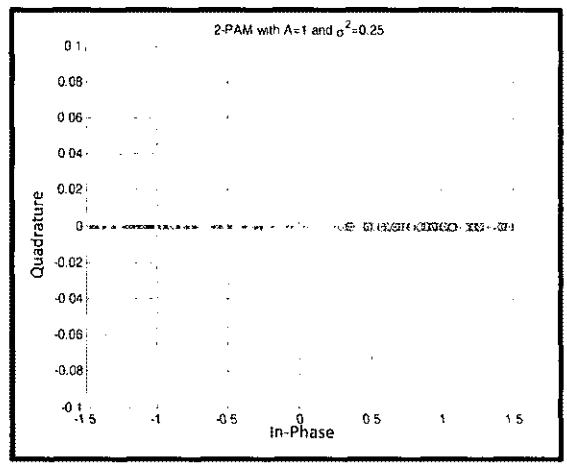

Figure 43: 2-PAM with A = 1, σ^2 = 0.25.

Figure 41 shows a 2-PAM signal constellation diagram with two signals transmitted with amplitudes of 1 and -1 and with noise variance of 0.04. With noise variance of 0.04, received signal bits were scattered around more than with noise variance of 0.01. This makes it difficult for the receiver to measure the amplitude of the actual transmitted analog waveform containing the binary encoded information. However, since the two signals lie on the positive and negative sides of the axis, the receiver may be able to distinguish that positive received signal maps to a 1 bit transmitted and negative received signal maps to a 0 bit transmitted.

Figure 42 shows a 2-PAM signal constellation diagram with two signals transmitted at amplitudes 1 and -1 and noise variance of 0.1. With noise variance of 0.1, the received signal bits were spread apart more than with noise variance of 0.01 or 0.04. It may be difficult for the receiver to measure the amplitude of the actual transmitted signal. However, if the receiver can roughly determine that the signal waveform with the positive amplitude maps to 1 binary bit and signal waveform with the negative amplitude maps to 0 binary bit, then the transmitted information can be decoded.

Figure 43 shows a 2-PAM signal constellation diagram with two signals transmitted at amplitudes of 1 and -1 and noise variance of 0.25. With noise variance as great as 0.25, noise from transmitting the signal with amplitude of 1 (which maps to 1 binary bit transmitted), stretches into the negative region where only the signal with the amplitude of -1 (which maps to 0 binary bit transmitted) is supposed to lie. Noise from transmitting the signal with amplitude of -1 (which maps to 0 binary bit transmitted), stretches into the positive region where only the signal with the amplitude of 1 is supposed to lie. Since there is a great amount of noise, this becomes difficult or impossible for the receiver to decode the transmitted signal.

6.2.2. Experiment 1B: Increasing Amplitude Level in 2-PAM Modulation

Figure 44 shows a 2-PAM signal constellation diagram with two signals transmitted with amplitudes of -2 and 2 with noise variance of 0.25. Notice that in Figure 43, a 2-PAM signal was transmitted with amplitudes of -1 and 1 with variance of 0.25. If the amplitude of the transmitted signals increases and the noise remains constant, the noise from the two signals transmitted do not interfere with each other and the therefore the receiver may be able to decode the received signal.

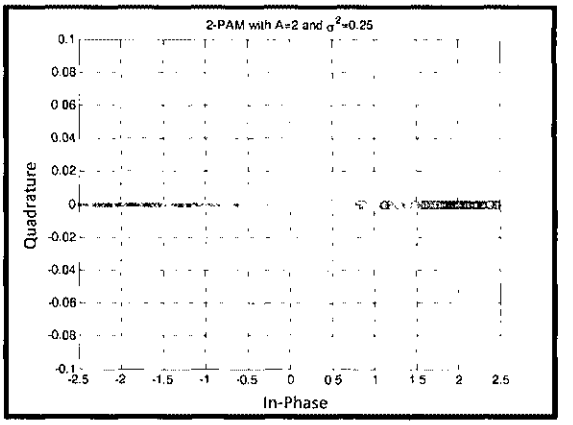

Figure 44: 2-PAM with A = 2, σ^2 = 0.25.

6.2.3. Conclusions on Experiments 1A and 1B

Each transmitted analog waveform with specified amplitudes carrying the digital information contains a certain amount of energy. If the amplitude of the analog waveform is larger, then the waveform transmitted will have more energy. The Euclidian distance between two signals in the signal representation, which depends upon the amplitude of the transmitted waveform, increases as the amplitude of the signal increases. If the energy of the analog waveform increases, then the distance between the two signals increases, decreasing the noise interference between the two signals.

If the noise variance is 0.01, 0.04, or 0.1 with signal amplitude of 1 or -1, then the receiver can distinguish whether binary bit 1 or 0 was transmitted based on whether the received signal waveform has a positive amplitude or negative amplitude. Positive signal amplitude received can map to a 1 bit transmitted and negative signal amplitude received can map to a 0 bit transmitted. If the noise variance is 0.25, then the signal amplitude should be greater than 1 in order to minimize the noise interference between the two signals transmitted.

6.2.4. Experiment 2A: Modulation With 4-PAM With Constant Amplitude, Varying Noise Level

Figure 45 throughFigure 49 show the 4-PAM signal constellation diagrams constructed from the signals at the receiver.

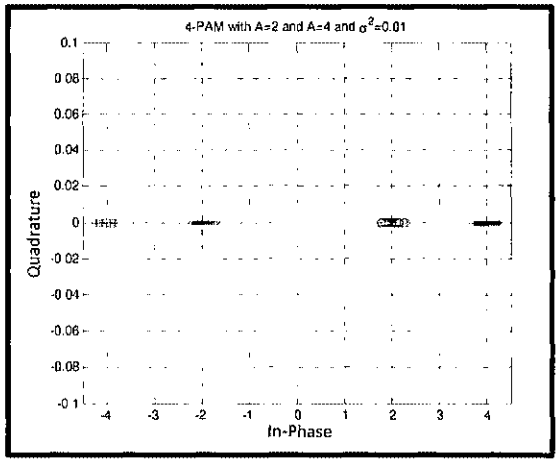

Figure 45: 4-PAM with A = 2 & A = 4, σ^2 = 0.01.

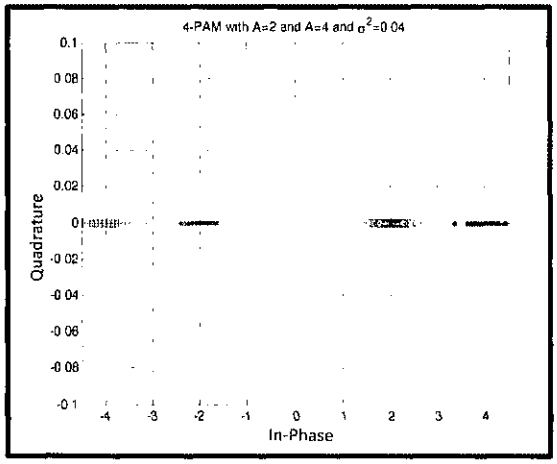

Figure 46: 4-PAM with A = 2 & A = 4, σ^2 = 0.04.

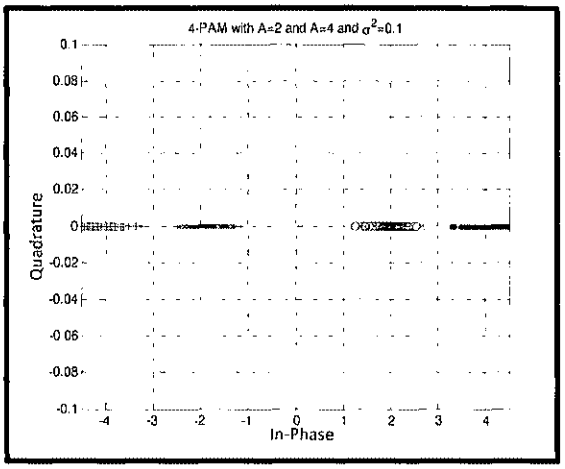

Figure 47: 4-PAM with A = 2 & A = 4, σ^2 = 0.1.

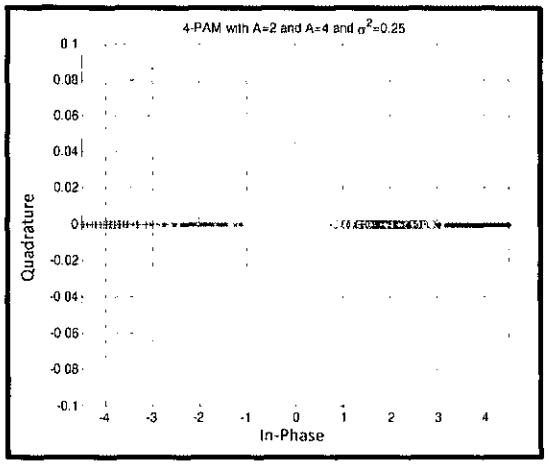

Figure 48: 4-PAM with A = 2 & A = 4, σ^2 = 0.25.

Figure 45 shows a 4-PAM signal constellation diagram with four signals transmitted with amplitudes of 2, -2, 4 and -4 with noise variance of 0.01. The digital modulator transmits

an analog waveform, with amplitude of -4 mapping to 00 binary bit, amplitude of -2 corresponding to 01 binary bit, amplitude of 2 mapping to 11 binary bit and amplitude of 4 mapping to 10 binary bit. The receiver measures the amplitude of the received analog waveform and distinguishes whether a 00, 01, 11 or 10 binary bit was transmitted. The "+" in the plots corresponds to 00 binary bit received, "x" corresponds to 01 binary bit received, "o" corresponds to 11 binary bit received and "." corresponds to binary bit 10 received at the receiver. With noise variance of 0.01, the noise was clustered compactly around the actual transmitted waveform. The receiver makes distinction of whether 00, 01, 11 or 10 binary bit was received by measuring the average amplitude of the signal signals received. Also, the receiver makes a distinction between the binary bits based on whether the amplitude of the analog signal received is positive or negative. Positive signal amplitude received can map to either 11 or 10 bit transmitted and negative signal amplitude received can map to 00 or 10 bit transmitted.

Figure 46 shows a 4-PAM signal constellation diagram with four signals transmitted with amplitudes of 2, -2, 4, and -4 and noise variance of 0.04. With noise variance of 0.04, noise was scattered around than with noise variance of 0.01. Figure 47 shows 4-PAM signal constellation diagram with four signals transmitted with amplitudes 2, -2, 4, and -4 and noise variance of 0.1. With noise variance of 0.1, noise was spread apart more than with noise variance of 0.01 or 0.04. This makes it difficult for the receiver to measure the amplitude of the actual transmitted analog waveform containing the binary encoded information. However, since two out of the four signals lie on the positive and negative sides of the axis, the receiver may be able to distinguish that positive signal received maps to either 11 or 10 bit transmitted and negative signal received maps to a 00 or 01 bit received. Also the receiver may be able to approximately measure the amplitude of the signal transmitted by determining the average amplitude of the signals with the noise, and map it to a binary bit.

Figure 48 shows a 4-PAM signal constellation diagram with four signals transmitted with amplitudes of 2, -2, 4, and -4 and noise variance of 0.25. With noise variance as great as 0.25, noise from transmitting the signal with amplitude of 2 (which maps to 11 binary bit transmitted), stretches into the region where only the signal with the amplitude of 4 (which maps to 10 binary bit transmitted) is supposed to lie (and vice versa). Noise from

transmitting the signal with amplitude of -2 (which maps to 01 binary bit transmitted), stretches into the region where only the signal with the amplitude of -4 (which maps to 00 binary bit transmitted) is supposed to lie (and vice versa). Since there is great amount of noise, this becomes difficult or impossible for the receiver to determine decode the transmitted signal.

6.2.5. Experiment 2B: Increase Amplitude Level in 4-PAM Modulation

Figure 49 shows a 4-PAM signal constellation diagram with four signals transmitted with amplitudes of 4, -4, 8, and -8 with noise variance of 0.25. Notice that in Figure 48 a 4-PAM signal was transmitted with amplitudes of 2, -2, 4, and -4 with variance of 0.25. If the amplitude of the signals transmitted increases and the noise remains constant, the noise from the two signals transmitted do not interfere with each other; therefore, the receiver may be able to decode the received signal.

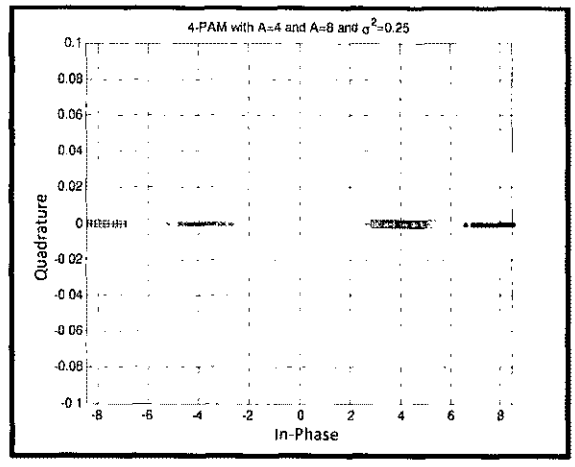

Figure 49: 4-PAM with A = 4 & A = 8, σ^2 = 0.25.

6.2.6. Conclusions on Experiments 2A and 2B

Each transmitted analog waveform with specified amplitudes carrying the digital information, contains a certain amount of energy. If the amplitude of the analog waveform is larger, then the waveform transmitted will have more energy. The Euclidian

distance between two signals in the signal representation, which depends upon the amplitude of the transmitted waveform, increases as the amplitude of the signal increases. If the energy of the analog waveform increases, then the distance between the two signals increases, decreasing the noise interference between the two signals.

The main issue with PAM is that symbols are transmitted with different amplitudes and some symbols are more error-prone than others. Also, some signals may incur more error depending on the noise. If the variance of the noise is high or comparable to the energy of the analog waveform carrying the digital information, then the signal received will always be affected by an error. Therefore, it is preferred that signals transmitted have the same energy for all waveforms.

If the noise variance is 0.01, 0.04, or 0.1 with signal amplitudes of 2, -2, 4, or -4 , then the receiver can distinguish whether binary bits 00, 01, 11 or 10 was transmitted based on whether the received signal waveform has a positive amplitude or negative amplitude and also by measuring the average signal amplitude.

If the noise variance is high (0.25) or is comparable to energy of the signal transmitted (2, -2, 4, or -4), then the amplitude (energy) of the signal should be increased in order to minimize the noise interference between the signals transmitted.

Also, note that if larger amounts of bits are encoded (increase k), the lower the average error rate will be of decoding the received waveform at the receiver.

6.2.7. Experiment 3A: Modulation With QPSK Constant Amplitude With Varying Noise Level

Figure 50 through Figure 57 show the QPSK signal constellation diagrams constructed at the receiver after information is transmitted over a noisy channel. In this experiment, noise is characterized by a vector of random numbers with a defined noise variance given by the parameter σ^2.

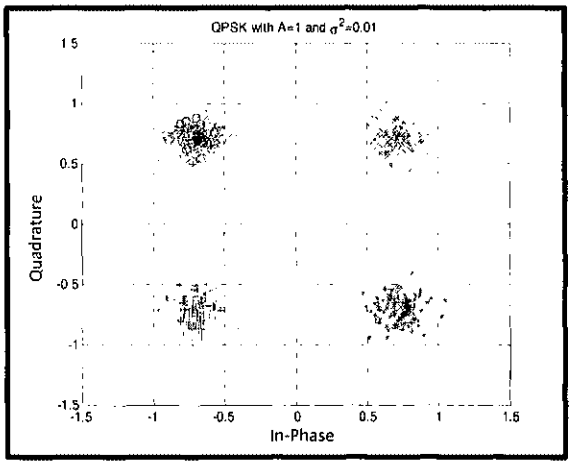

Figure 50: QPSK with A = 1, σ^2 = 0.01.

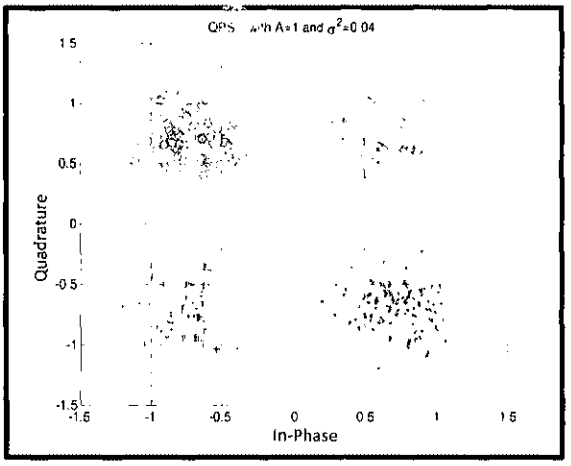

Figure 51: QPSK with A = 1, σ^2 = 0.04.

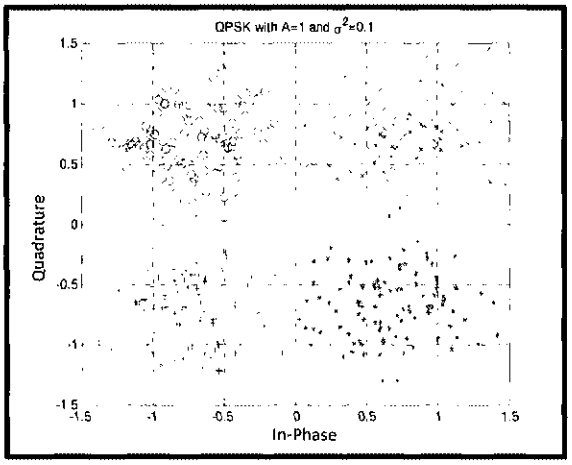

Figure 52: QPSK with A = 1, σ^2 = 0.1.

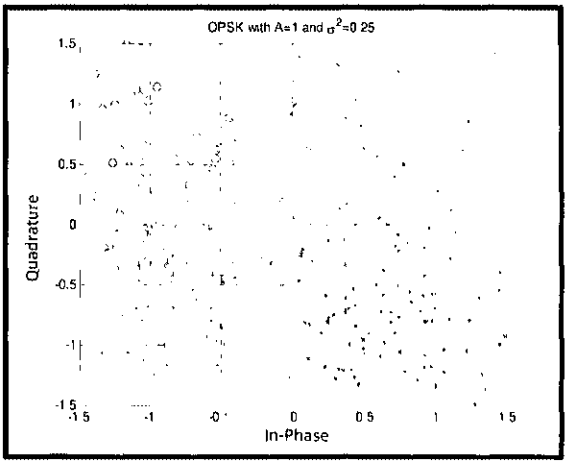

Figure 53: QPSK with A = 1, σ^2 = 0.25.

Figure 50 shows a QPSK signal with four signals transmitted each with amplitudes of 1 and noise variance of 0.01. Each signal transmitted is distinguished by phase angles $\frac{\pi}{4}, \frac{3\pi}{4}, \frac{5\pi}{4}$ and $\frac{7\pi}{4}$. The digital modulator transmits an analog waveform, with phase angle of $\frac{\pi}{4}$ mapping to 00 binary bit, phase angle of $\frac{3\pi}{4}$ mapping to 01 binary bit, phase angle of $\frac{5\pi}{4}$ mapping to 11 binary bit and phase angle of $\frac{7\pi}{4}$ mapping to 11 binary bit. The receiver measures the phase angle of the received analog waveform and distinguishes whether a 00, 01, 11 or 10 binary bit was transmitted. The "x" in the plot corresponds to 00 binary bit, "o" corresponds to 01 binary bit, "+" in the plot corresponds to 11 binary

bit, and "*" corresponds to 10 binary bit received at the receiver. With noise variance of 0.01, the noise is clustered compactly around the actual transmitted waveform. The receiver may make a distinction of whether a 00, 01, 11 or 10 binary bit was received based on whether the phase angle of the analog signal received is located in the first, second, third or fourth quadrant of the signal constellation diagram.

Figure 51 shows a QPSK signal with four signals transmitted each with amplitudes of 1 and noise variance of 0.04. Each signal transmitted is distinguished by phase angles $\frac{\pi}{4}, \frac{3\pi}{4}, \frac{5\pi}{4}$ and $\frac{7\pi}{4}$. With noise variance of 0.04, noise was scattered around than with noise variance of 0.01. This makes it difficult for the receiver to measure the phase angle of the actual transmitted analog waveform containing the binary encoded information. However, since the four signals each lie within the four quadrants of the constellation, the receiver may be able to distinguish that signals are received. Those with the phase angles which lie in the first quadrant map to a 00 bit, signals received with phase angles which lie in the second quadrant map to 01 bit, signals received with phase angles which lie in the third quadrant map to 11 bit, and signals received with phase angles which lie in the fourth quadrant map to 10 bit received.

Figure 52 shows a QPSK signal with four signals transmitted each with amplitudes of 1 and noise variance of 0.1. Each signal transmitted is distinguished by phase angles $\frac{\pi}{4}, \frac{3\pi}{4}, \frac{5\pi}{4}$ and $\frac{7\pi}{4}$. With noise variance of 0.1, noise was spread apart more than with noise variance of 0.01 or 0.04. It may be difficult for the receiver to measure the phase angle of the actual transmitted signal. However, if the receiver can roughly make a distinction as to which signal waveforms lie in which quadrants of the constellation, then the transmitted information can be decoded.

Figure 53 shows a QPSK signal with four signals transmitted each with amplitudes of 1 and noise variance of 0.25. Each signal transmitted is distinguished by phase angles $\frac{\pi}{4}, \frac{3\pi}{4}, \frac{5\pi}{4}$ and $\frac{7\pi}{4}$. With noise variance as great as 0.25, noise from transmitting the signal with phase angle of $\frac{\pi}{4}$ (which maps to 00 binary bit transmitted) stretches into the region where only the signal with the phase angle of $\frac{3\pi}{4}, \frac{5\pi}{4}$ and $\frac{7\pi}{4}$ (which maps to 01, 11, and 10 binary bit transmitted, respectively) is supposed to lie (and vice versa for each of the

phase angles). Since there is a great amount of noise, it becomes difficult or impossible for the receiver to determine decode the transmitted signal.

6.2.8. Experiment 3B: Increase Amplitude in QPSK

Figure 54 throughFigure 57 show a QPSK signal with four signals transmitted with amplitudes of 1, 2, 3 and 4 (respectively) and each with noise variance of 0.25. If the amplitude of the signals transmitted increases and the noise remains constant, the noise from the four signals transmitted does not interfere with each other; therefore, the receiver may be able to decode the received signal.

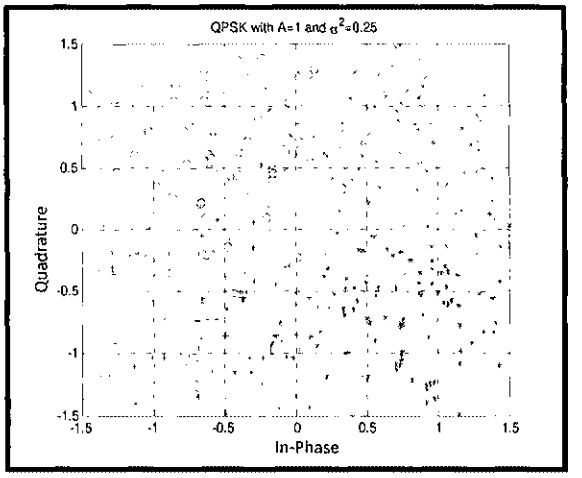

Figure 54: QPSK with A = 1, σ^2 = 0.25.

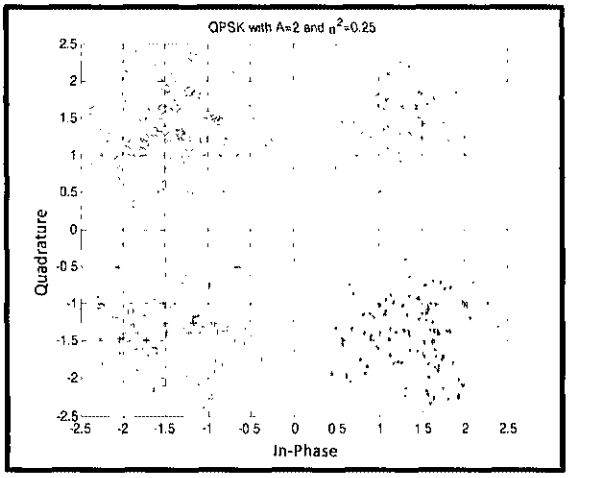

Figure 55: QPSK with A = 2, σ^2 = 0.25.

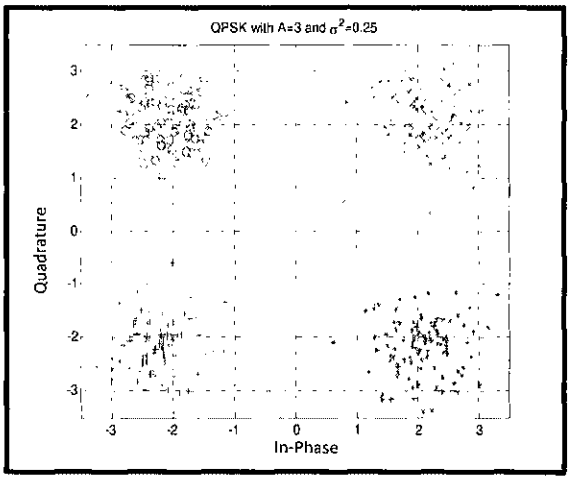

Figure 56: QPSK with A = 3, σ^2 = 0.25.

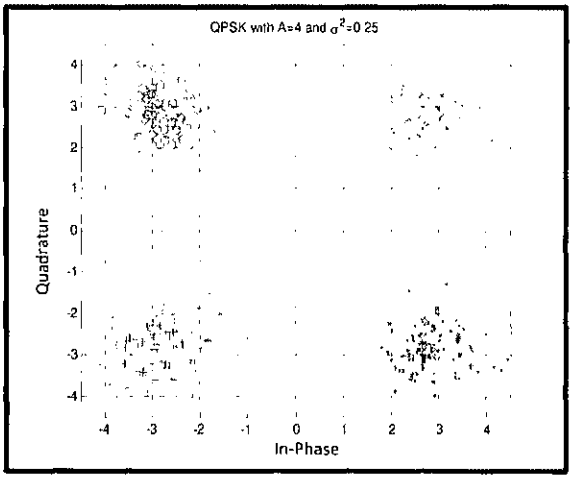

Figure 57: QPSK with A = 4, σ^2 = 0.25.

Each transmitted analog waveform with specified amplitudes carrying the digital information, contains a certain amount of energy. If the amplitude of the analog waveform is larger, then the waveform transmitted will have more energy. Additionally, the distance between signals in the signal representation, which is depends upon the amplitude of the transmitted waveform, increases as the amplitude of the signal increases. If the energy of the analog waveform increases, then the distance between the signals increases, decreasing the noise interference between the signals. If the variance of the noise is high or comparable to the energy of the analog waveform carrying the digital information, then the signal received will always be affected by an error. Therefore, it is preferred that signals transmitted have the same energy for all waveforms.

6.2.9. Conclusions from Experiment 3A and 3B

If the noise variance is 0.01, 0.04, or 0.1 with signal amplitude of 1, then the receiver can distinguish whether binary bit 00, 01, 10, and 11 was transmitted based on whether the received signal waveform lies within the first, second, third or fourth quadrant of the constellation. Signals with phase angles lying in between phase angles 0 to $\frac{\pi}{2}$, can map to

a signal which was transmitted with phase angle $\frac{\pi}{4}$, which maps to the 00 bit of digital information. Signals with phase angles lying in between phase angles $\frac{\pi}{2}$ to π, can map to a signal which was transmitted with phase angle $\frac{3\pi}{4}$, which maps to the 01 bit of digital information. Signals with phase angles lying in between phase angles π to $\frac{3\pi}{2}$, can map to a signal which was transmitted with phase angle $\frac{5\pi}{4}$, which maps to the 11 bit of digital information. Signals with phase angles lying in between phase angles $\frac{3\pi}{2}$ to 2π, can map to a signal which was transmitted with phase angle $\frac{7\pi}{4}$, which maps to the 10 bit of digital information. If the noise variance is 0.25, then the signal amplitude should be greater than 1 in order to minimize the noise interference between the four signals transmitted.

6.2.10. Experiment 4A: Modulation With 8-PSK With Constant Amplitude and Varying Noise Level

Figure 58 throughFigure 61 show the 8-PSK signal constellation diagrams constructed at the receiver after information is transmitted over a noisy channel.

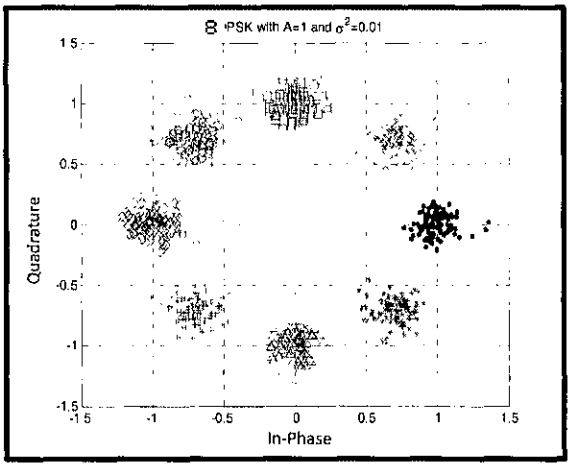

Figure 58: 8-PSK with A = 1, σ^2 = 0.01.

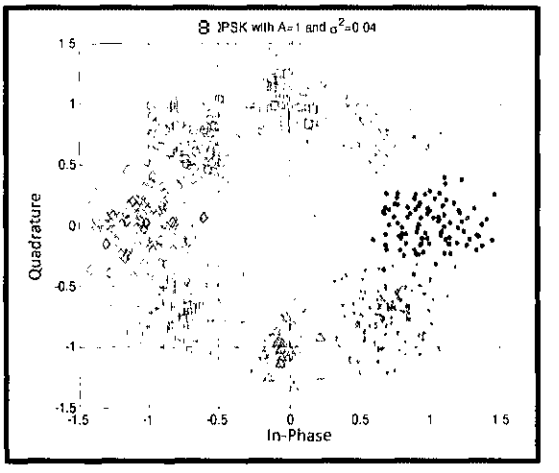

Figure 59: 8-PSK with A = 1, σ^2 = 0.04.

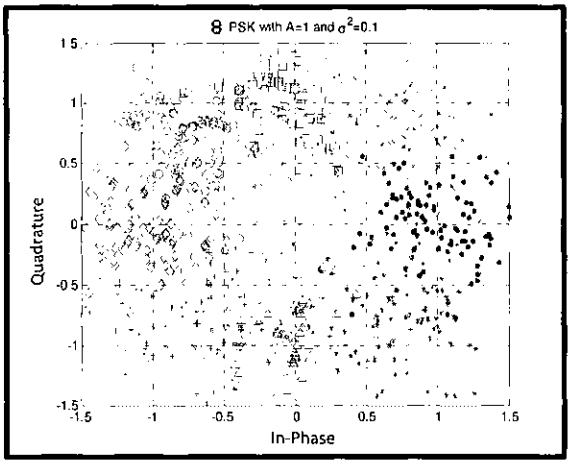

Figure 60: 8-PSK with A = 1, σ^2 = 0.1.

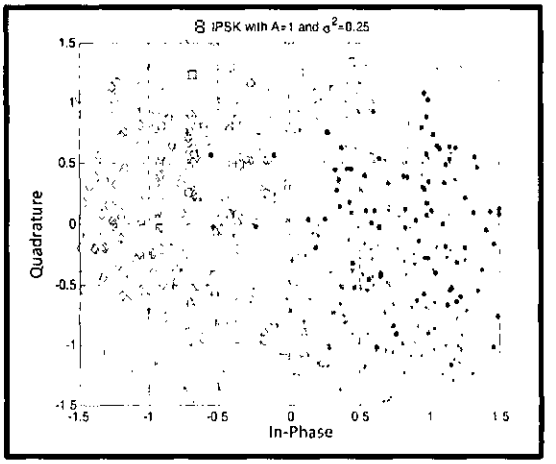

Figure 61: 8-PSK with A = 1, σ^2 = 0.25.

Figure 58 shows an 8-PSK signal constellation diagram with eight signals transmitted each with amplitude of 1 and noise variance of 0.01. The digital modulator transmits the analog waveform in the following manner: (a) Signals with phase angle of 0 map to a 000 binary bit, (b) those with phase angle of $\frac{\pi}{4}$ map to a 001 binary bit, (c) those with phase angle of $\frac{\pi}{2}$ map to a 011 binary bit, (d) those with phase angle of $\frac{3\pi}{4}$ map to 010 binary bit, (e) those with phase angle of π map to 110 binary bit, (f) those with phase angle of $\frac{5\pi}{4}$ map to 111 binary bit, (g) those with phase angle of $\frac{3\pi}{2}$ map to 101 binary bit, and (h) those with phase angle of $\frac{7\pi}{4}$ map to 100 binary bit. The receiver measures the amplitude of the received analog waveform and distinguishes whether 000, 001, 011, 010, 110, 111, 101, 100 binary bit was transmitted. The "x" in the plots corresponds to 000 binary bit received, "o" corresponds to 001 binary bit received, "+" corresponds to 011 binary bit received, "*" corresponds to 010 binary bit received, "." corresponds to 110 binary bit received, "■" corresponds to 111 binary bit received, "◊" corresponds to 101 binary bit received and "Δ" corresponds to "100" binary bit received at the receiver. With noise variance of 0.01, the noise is clustered compactly around the actual transmitted waveform. The receiver may make a distinction of whether 000, 001, 011, 010, 110, 111, 101, 100 binary bit was received by distinguishing between the average phase angle of

the signals received. Also, the receiver may make a distinction between the binary bits based on whether the phase angle of the analog signal received lies within the first, second, third or fourth quadrant or on the axes of the signal constellation diagram. Additionally, because of Grey encoding, error in detecting the encoded binary bit may be limited to one bit, since the neighboring bits are different by one bit.

Figure 59 shows an 8-PSK signal constellation diagram with eight signals transmitted each with amplitude of 1 and noise variance of 0.04. Each signal transmitted is distinguished by the phase angles $0, \frac{\pi}{4}, \frac{\pi}{2}, \frac{3\pi}{4}, \pi, \frac{5\pi}{4}, \frac{3\pi}{2}$ and $\frac{7\pi}{4}$. With noise variance of 0.04, noise is scattered around more than with noise variance of 0.01. This makes it difficult for the receiver to measure the phase angle of the actual transmitted analog waveform containing the binary encoded information. However, most of the four (out of the eight) signals lie within the four quadrants of the constellation. Hence, the receiver may be able to distinguish that the signals received with the phase angles which lie in the first quadrant map to a 001 bit, signals received with phase angles which lie in the second quadrant map to 010 bit, signals received with phase angles which lie in the third quadrant map to 111 bit and signals received with phase angles which lie in the fourth quadrant map to 100 bit received. Most of the other four out of the eight signals lie on the axes of the signal constellation, and the receiver may be able to distinguish that signals with phase angles that average out to 0, $\frac{\pi}{2}, \pi$ or $\frac{3\pi}{2}$ map to 000, 001, 110, or 101 binary bits respectively. Note that Grey coding is used to limit error by one bit.

Figure 60 shows an 8-PSK signal with eight signals transmitted each with amplitude of 1 and noise variance of 0.1. With noise variance of 0.1, noise is spread apart more than with noise variance of 0.01 or 0.04. It may be difficult for the receiver to measure the phase angle of the actual transmitted signal.

Figure 61 shows an 8-PSK signal with eight signals transmitted each with amplitude of 1 and noise variance of 0.25. With noise variance as great as 0.25, noise from transmitting a signal stretches into regions where other signals are supposed to lie. Since there is a great amount of noise, it becomes difficult or impossible for the receiver to decode the transmitted signal.

6.2.11. Experiment 4B: Increasing Amplitude in 8-PSK

Figure 62 throughFigure 65 show 8-PSK signal with eight signals transmitted with amplitudes of 1, 2, 3 and 4, respectively and each with noise variance of 0.25. If the amplitude of the signals transmitted increases and the noise remains constant, the noise from the eight signals transmitted does not interfere with each other; therefore, the receiver may be able to decode the received signal.

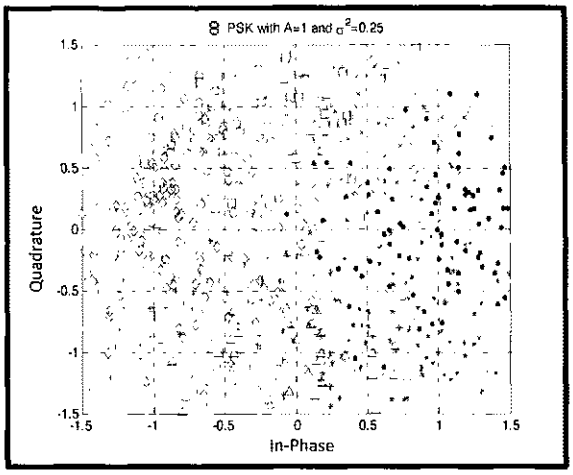

Figure 62: 8-PSK with A = 1, σ^2 = 0.25.

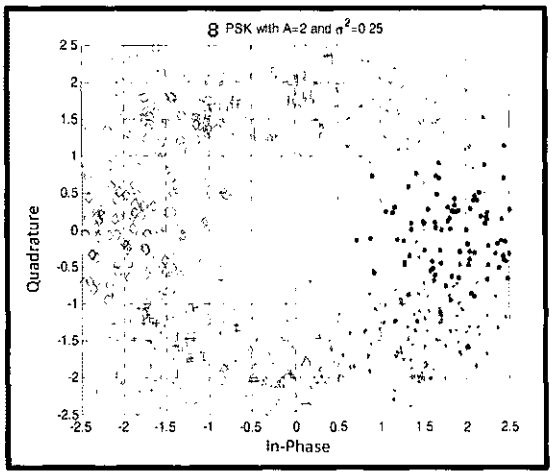

Figure 63: 8-PSK with A = 2, σ^2 = 0.25.

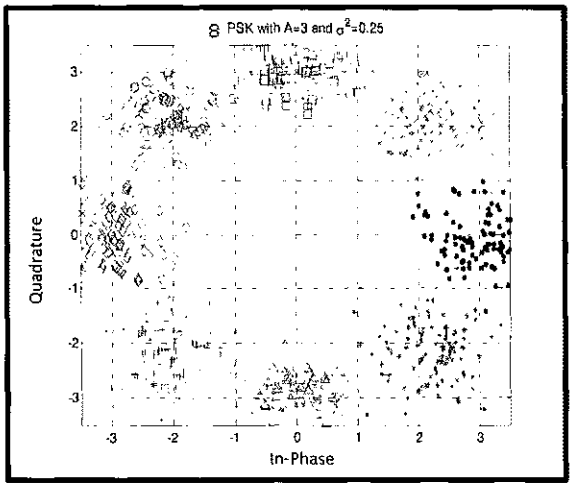

Figure 64: 8-PSK with A = 3, σ^2 = 0.25.

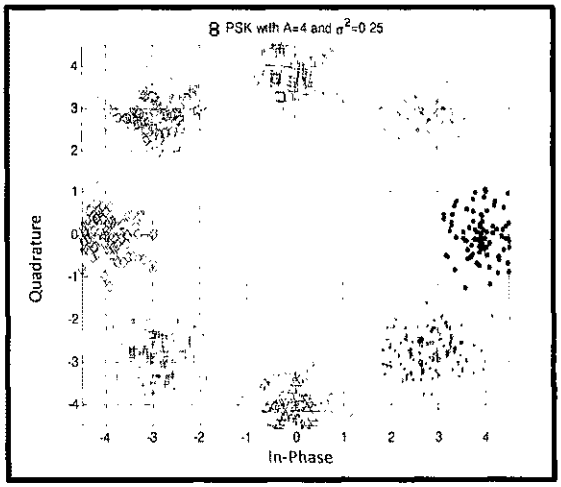

Figure 65: 8-PSK with A = 4, σ^2 = 0.25.

Each transmitted analog waveform with specified amplitudes carrying the digital information, contains a certain amount of energy. If the amplitude of the analog waveform is larger, then the waveform transmitted will have more energy. Additionally, the distance between signals in the signal representation, which depends upon the amplitude of the transmitted waveform, increases as the amplitude of the signal increases. If the energy of the analog waveform increases, then the distance between the signals increases, decreasing the noise interference between the signals. If the variance of the noise is high or comparable to the energy of the analog waveform carrying the digital information, then the signal received will always be affected by an error. Therefore, it is preferred that signals transmitted have the same energy for all waveforms.

6.2.12. Conclusions from Experiment 4A and 4B

If the noise variance is 0.01, 0.04, or 0.1 with signal amplitude of 1, then the receiver can distinguish whether binary bit 000, 001, 011, 010, 110, 111, 101, 100 was transmitted based on whether the received signal waveform lies within the first, second, third or fourth quadrant or on the axes of the constellation. Signals with phase angles lying in between phase angles 0 to $\frac{\pi}{2}$, can map to a signal which was transmitted with phase angle $\frac{\pi}{4}$, which maps to the 001 bit of digital information. Signals with phase angles lying in between phase angles $\frac{\pi}{2}$ to π, can map to a signal which was transmitted with phase angle $\frac{3\pi}{4}$, which maps to the 010 bit of digital information. Signals with phase angles lying in between phase angles π to $\frac{3\pi}{2}$, can map to a signal which was transmitted with phase angle $\frac{5\pi}{4}$, which maps to the 111 bit of digital information. Signals with phase angles lying in between phase angles $\frac{3\pi}{2}$ to 2π, can map to a signal which was transmitted with phase angle $\frac{7\pi}{4}$, which maps to the 100 bit of digital information. Signals with phase angles lying close to phase angle of 0, can map to a signal which was transmitted with phase angle 0, which maps to the 000 bit of digital information. Signals with phase angles lying close to phase angle of $\frac{\pi}{2}$, can map to a signal that was transmitted with

phase angle $\frac{\pi}{2}$, which maps to the 011 binary bit of information. Signals with phase angles lying close to phase angle of π, can map to a signal that was transmitted with phase angle π, which maps to the 110 binary bit of information. Signals with phase angles lying close to phase angle of $\frac{3\pi}{2}$, can map to a signal which was transmitted with phase angle $\frac{3\pi}{2}$, which maps to the 101 binary bit of information. If the noise variance is 0.25, then the signal amplitude should be greater than 1 in order to minimize the noise interference between the four signals transmitted.

6.3 Conclusions on the Effect of AWGN on M-PAM and M-PSK Modulation Schemes

Computer simulations showed that the existence of noise in communication channels will certainly affect the detectability of the transmitted signal at the receiver. Simulation results showed that when the noise level increased for a given signal energy, the error of detecting the correct bit at the receiver was increased. When the noise level of a channel increased signal points on the signal constellation over lapped making it difficult for the receiver to distinguish between the different types of transmitted signals. The results showed that energy of the transmitted signal can be increased in order to keep the probability of symbol error minimum. However, increasing the energy of the signal may not be desired since it may increase the power level and complexity of the communication system hardware. In general, as the energy of the signal increased, the BER decreased and vice versa. Computer simulations assumed perfect carrier signal and perfect synchronization. In practice, carrier and bit synchronization algorithms should be implemented into simulation calculations. The performance of these algorithms will vary with physical realization and will affect the resultant BER performance. A wireless system should use a modulation scheme best suited for the channel characteristics in order to provide optimal results when interpreting the received data. Therefore, it is beneficial to have an receiver that can demodulate a range of modulation schemes.

6.4 Success Results of the Automatic Modulation Classifier

Sections 6.2.1 through 6.2.12 presented the results of a conventional demodulator which attempted to identify the message embedded within the known modulation scheme of the transmitted signal that was distorted due to the noise in the communication channel. A receiver which uses an automatic modulation classifier will not have a priori knowledge of the modulation scheme used in the incoming signals. An automatic modulation classifier identifies the modulation scheme of the transmitted signal based on statistical analysis of the signal. In order identify the modulation schemes code into incoming signals, over 1,000 random message signals were generated and modulated using BPSK, 4-PSK, 8-PSK, 2-FSK, 4-FSK, 8-FSK, 8-QAM, 16-QAM, 64-QAM and 256-QAM schemes. Each modulated signal was taken to propagate through a noisy communication channel. The noisy communication channels were modeled with AWGN, multipath Rayleigh fading with AWGN, and multipath Ricean fading with AWGN. The noise levels of the communication channel were varied from low noise level to high noise levels. Noisy channels had signal to noise ratio in the range of 0 dB to 100 dB. The SNR levels were randomly generated as an integer value within the range of 0 dB to 25 dB to propagate signals through high noise channels. Low noise channels had SNR levels within the range of 50 dB to 100 dB. Integer values of the SNR were similarly chosen for low noise channels to be within the range of 50 dB to 100 dB.

Table 7 throughTable 12 show the results from the successful classification of signal using the modulation algorithm for identifying random signals that were pre-modulated, but the modulation scheme was kept hidden while analyzing the results from the automatic classifier. A study of these tables shows that under various noise and multipath fading channel conditions, the classification modulation algorithm was able to successfully identify the modulation scheme of the transmitted signals at 79.21% of the trial run. This percentage of the successful identification of transmitted signal was computed by averaging the successful classification of data shown in Table 7 throughTable 12. If the signal was modulated with BPSK, the classification algorithm successfully identified the modulation scheme at 67.56% of the trial run, under all AWGN noise and fading channels. If a random signal was modulated with 4-PSK, the

classification algorithm was successful in classifying the modulation scheme 67.76% of the time as reflected by the classification success averages of the 4-PSK modulation types. If a random signal was modulated with 8-PSK, the classifier selected the correct modulation scheme as 8-PSK 88.28% of the time. If the signal was modulated via 2-FSK, 4-FSK or 8-FSK, the classification algorithm correctly selected M-FSK 100% of the time for communication channel that had high and low SNR levels. If the signal was modulated using 8-QAM the classification algorithm correctly identified the modulation type as 8-QAM 83.4% of the time. If the signal was generated using 16-QAM, 64-QAM or 256-QAM, the classifier identified the modulation as the general case of the M-QAM signal type 69.24% of the time.

Sections 6.5 through 6.7 discuss the each of the successes for modulation classifier after the signals were transmitted through AWGN channel, multipath Rayleigh fading with AWGN channel and multipath Ricean fading with AWNG multipath channel. Each of these channels were evaluated for low and high noise levels. Since the eighth order cumulants of BPSK, 4-PSK, 8-PSK and 8-QAM were unique and non-overlapping, the classification modulation algorithm was able to identify these specific variations of the signal's modulation scheme. On the other hand, since the higher order statistics of 2-FSK, 4-FSK and 8-FSK all had cumulants within the same range, it was not possible to identify and distinguish these modulation types one from the other. Signals that were modulated using any of the FSK types were identified therefore as M-FSK modulation type by the classifier. Similarly, signals with 16-QAM, 64-QAM and 256-QAM were identified as M-QAM modulation types by the classification modulation algorithm.

6.5 Results from Classification of Modulated Signals Transmitted Through AWGN Channel

The classification modulation algorithm had great success in identifying the modulated signals that were transmitted through AWGN channel at both high and low levels of SNR. Table 7 and Table 8 show the classification percent success of modulated signals propagated through AWGN channel at both low and high noise levels. Table 7 and

Table 8 show that for high noise levels (SNR range: 0 dB to 25 dB) and for low noise levels (SNR range: 50 dB to 100 dB) the classifier was able to correctly identify the modulation scheme of the transmitted signal in 100 % of all trial runs. This classification percent success was calculated by computing the average of the elements in the main diagonal elements of Table 7 and Table 8. For example, the percent success was calculated as follows:

$$\begin{aligned} &Classification\ Percent\ Success \\ &\quad = (BPSK + 4PSK + 8PSK + 2FSK + 4FSK + 8FSK + 8QAM \\ &\quad + 16QAM + 64QAM + 256QAM)/10{,}000 * 100. \end{aligned} \tag{6.1}$$

Notice that for some of the modulation types, the classifier identified the modulation scheme to be of multiple types of modulation schemes. For example, in Table 7, even though 1,000 random signals were tried during the identification of the signal with 8-PSK modulation type, the classifier identified the signal to be of M-QAM modulation type 116 times in these trials. This is because some of the cumulants of the randomly generated signal modulated with 8-PSK were in the overlapped cumulant threshold detection range of the M-QAM type signal. Even though some margins were built into the cumulant threshold detection range, the randomness in the communication signal still caused some of modulated signal's cumulants to overlap into the threshold detection range of other modulation schemes. Nevertheless, the classification modulation algorithm successfully identified all the modulation schemes of a signal that was transmitted through an AWGN channel.

Table 7: Classifier Success Results for AWGN Channel at High Noise Level.

Classification Rate 100%		Modulation Schemes Detected In The Trial						
		BPSK	4-PSK	8-PSK	M-FSK	8-QAM	M-QAM	Total
Trial Cases Transmitted	BPSK	1000	0	0	0	0	0	1000
	4-PSK	0	1000	0	0	0	0	1000
	8-PSK	0	0	1000	0	0	116	1116
	2-FSK	0	0	0	1000	1000	0	2000
	4-FSK	0	0	0	1000	0	0	1000
	8-FSK	0	0	0	1000	0	0	1000
	8-QAM	0	0	0	0	1000	0	1000
	16-QAM	0	1000	0	0	0	1000	2000
	64-QAM	0	1000	0	0	0	1000	2000
	256-QAM	0	0	0	0	0	1000	1000
Classification Modulation Algorithm Success Results AWGN Channel, 1000 Trials, SNR Range: 0 dB to 25 dB (High Noise)								

Table 8: Classifier Success Results for AWGN Channel at Low Noise Level.

Classification Rate 100%		Modulation Schemes Detected In The Trial						
		BPSK	4-PSK	8-PSK	M-FSK	8-QAM	M-QAM	Total
Trial Cases Transmitted	BPSK	1000	0	0	0	0	0	1000
	4-PSK	0	1000	0	0	1	44	1045
	8-PSK	0	0	1000	0	0	0	1000
	2-FSK	0	0	0	1000	1000	0	2000
	4-FSK	0	0	0	1000	0	0	1000
	8-FSK	0	0		1000	0	0	1000
	8-QAM	0	0	0	0	1000	0	1000
	16-QAM	0	0	0	0	0	1000	1000
	64-QAM	0	1000	0	0	0	1000	2000
	256-QAM	0	0	0	0	0	1000	1000
Classification Modulation Algorithm Success Results AWGN Channel, 1000 Trials, SNR Range: 50 dB to 100 dB (Low Noise)								

Figure 66 shows an excerpt of the MATLAB® code which shows 1,000 random signals being modulated using 8-PSK and transmitted over a communication channel with high noise. Figure 67 shows the output of the classification algorithm in 1,000 random trials on 8-PSK type modulation signals where the classifier identified the modulation scheme of the signal to be of M-QAM type 116 times in the trials. Figure 68 and Figure 69 show

examples of signal constellation diagrams of 4-PSK modulated signal with noise levels of 10 dB and 90 dB, respectively.

```
%% 8PSK Modulation
clear all
clc
close all
for j=1:1:1000;
M = 8;                      % Modulation alphabet size
phOffset = pi()/8;          % Phase offset
symMap = 'gray';            % Symbol mapping
hMod = comm.PSKModulator(M,phOffset,'SymbolMapping',symMap);
modData = step(hMod,randi([0 7],20000,1));
noise(j) = randi([0 25],1); % Generate random noise in the range of 0 dB to 25 dB
hAWGN = comm.AWGNChannel('EbNo',noise(j),'BitsPerSymbol',4);
channelOutput = step(hAWGN, modData);
```

Figure 66: Communication Model Showing Input of 8-PSK Modulated Signal.

```
Command Window
INPUT: 8-PSK
OUTPUT: DETECTED MODULATION SCHEME
CHANNEL: AWGN CHANNEL, HIGH NOISE

BPSK

count_BPSK =

     0

4PSK

count_4PSK =

     0

8PSK

count_8PSK =

     1000

MFSK

count_MFSK =

     0

8QAM

count_8QAM =

     0

MQAM

count_MQAM =

     116

Total =

     1116
```

Figure 67: Output of Classifier Algorithm for 8-PSK Input Signal Passed Over AWGN Channel (High Noise).

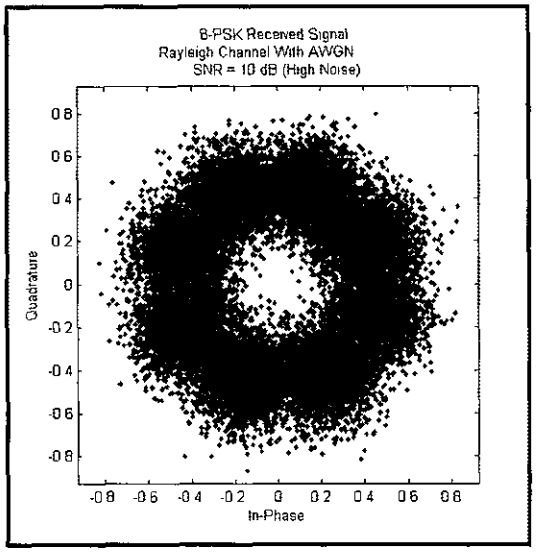

Figure 68: 8-PSK Received Signal Over AWGN Channel with SNR = 10 dB.

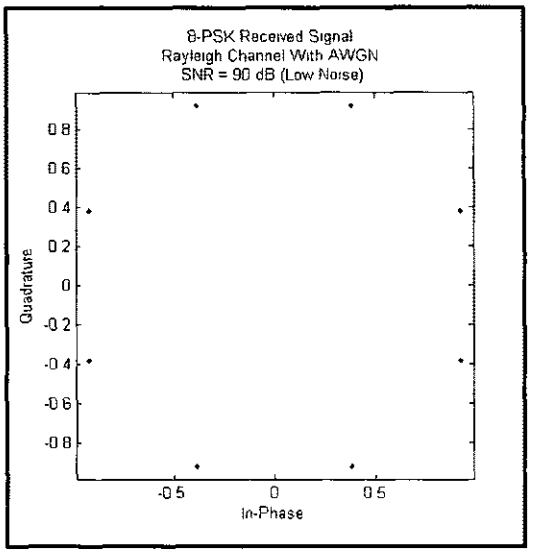

Figure 69: 8-PSK Received Signal Over AWGN Channel with SNR = 90 dB.

6.6 Results from Classification of Modulated Signals Transmitted Through Rayleigh Channel

The classification modulation algorithm designed was again used for simulations of the wireless communication system to evaluate its ability to correctly identify the modulation scheme of signals transmitted through multipath Rayleigh fading channels with AWGN at low and high noise levels. Table 9 and Table 10 show the classification percent success of modulated signals propagated through the multipath Rayleigh fading channel. Table 9 shows that for high noise (SNR range: 0 dB to 25 dB) the classifier was able to correctly identify the modulation scheme of the transmitted signal in 68.59% of all trial runs. Table 10 shows that for low noise (SNR range: 50 dB to 100 dB) the classifier was able to correctly identify the modulation scheme of the transmitted signal 76.68% of the time. Again, these classification percents were determined by computing the averages of the successes in the main diagonals of the table.

The classification algorithm was able to correctly identify all the 1,000 signals that were modulated using one of the FSK types as M-FSK with a percent success of 100%. These

signals were transmitted through Rayleigh fading channel at both high and low levels of SNR. The FSK had unique cumulant ranges that did not overlap with the threshold detection range of the other modulation scheme. Hence, the FSK modulated signals had the greatest level of success when initially chosen.

The modulation classification algorithm does not have a priori knowledge of the signal modulation scheme or the characteristics of the propagation channel used in the transmission. The thresholds for the modulation classification algorithm were based on evaluations of moments and cumulants ranges of modulated signals that were passed through AWGN channel. The same modulation classification algorithm was used to evaluate its ability on classifying the modulation scheme of signals that were transmitted through Rayleigh channel at both high and low noise levels. At high noise levels (SNR range: 0 dB to 25 dB), the modulation classification algorithm was able to identify 68.59% of modulated types correctly. At low noise levels (SNR range: 50 dB to 100 dB), the modulation classification algorithm was able to identify 76.68% of the modulation types correctly. For some modulation schemes, the classifier identified the modulated signal as both the correct modulation type and in some cases as belonging to other modulation types. For example, in Table 9, signals that were modulated using either 16-QAM, 64-QAM or 256-QAM and passed through a very noisy channel were correctly identified as M-QAM, on average, 449 times. The remaining signals were identified as BPSK, 4-PSK, 8-PSK, M-FSK or 8-QAM signal types. This is because some of the cumulants for the M-QAM signal overlapped the threshold detection range for the modulation thresholds set within the classifier. For example, from Table 6 in Chapter 5, the maximum end range (21.07) of the 16-QAM eighth order cumulant (C_{s44}) range that is close to the eighth order cumulant (C_{s44}) range (22.83) of the 4-PSK scheme. Therefore, if random signals are modulated with a 16-QAM signal and are transmitted in various levels of noisy channels, the cumulants for the 16-QAM can intersect with the cumulants of 4-PSK signal causing confusion for the classifier to correctly identify the modulation scheme of the transmitted signal. Appendix B shows the overall maximum and minimum moments and cumulant tables for each of the modulated signals that were transmitted through an multipath Rayleigh fading channel with AWGN at low and high SNR levels.

Table 28 in Appendix B also shows that the maximum end range (24.17) of the 16-QAM eighth order cumulant (C_{s44}) range is close to the eighth order cumulant (C_{s44}) range (26.33) of the 4-PSK scheme.

Table 9: Classifier Success Results for Rayleigh Channel at High Noise Level.

Classification Rate 68.59%		Modulation Schemes Detected In The Trial						
		BPSK	4-PSK	8-PSK	M-FSK	8-QAM	M-QAM	Total
Trial Cases Transmitted	BPSK	398	109	307	236	109	0	1159
	4-PSK	91	617	108	498	92	0	1406
	8-PSK	0	0	935	126	0	0	1061
	2-FSK	0	0	0	1000	0	0	1000
	4-FSK	0	0	0	1000	0	0	1000
	8-FSK	0	0	0	1000	0	0	1000
	8-QAM	117	441	109	234	562	194	1657
	16-QAM	189	108	418	406	102	449	1672
	64-QAM	117	118	396	267	117	547	1562
	256-QAM	147	361	219	29	141	351	1248
Classification Modulation Algorithm Success Results Rayleigh Channel with AWGN, 1000 Trials, SNR Range: 0 dB to 25 dB (High Noise)								

Table 10: Classifier Success Results for Rayleigh Channel at Low Noise Level.

Classification Rate 76.68%		Modulation Schemes Detected In The Trial						
		BPSK	4-PSK	8-PSK	M-FSK	8-QAM	M-QAM	Total
Trial Cases Transmitted	BPSK	663	71	135	104	89	0	1062
	4-PSK	107	428	282	224	135	124	1300
	8-PSK	7	18	833	155	4	0	1017
	2-FSK	0	0	0	1000	0	0	1000
	4-FSK	0	0	0	1000	0	0	1000
	8-FSK	0	0	0	1000	0	0	1000
	8-QAM	134	15	51	416	651	94	1361
	16-QAM	431	113	245	176	133	680	1778
	64-QAM	587	86	185	141	96	794	1889
	256-QAM	121	394	119	87	47	619	1387
Classification Modulation Algorithm Success Results Rayleigh Channel with AWGN, 1000 Trials, SNR Range: 50 dB to 100 dB (Low Noise)								

Figure 70 shows the output of the classification algorithm, in 1,000 random trials on 8-PSK type modulated signals which were passed over a Rayleigh channel with AWGN at a low level of SNR. The classification algorithm identified the signal as 8-PSK 935 times and M-FSK 126 times. Figure 71 and Figure 72 show examples of signal constellation diagrams of 2-PSK modulated signal with noise levels of 15 dB and 75 dB, respectively.

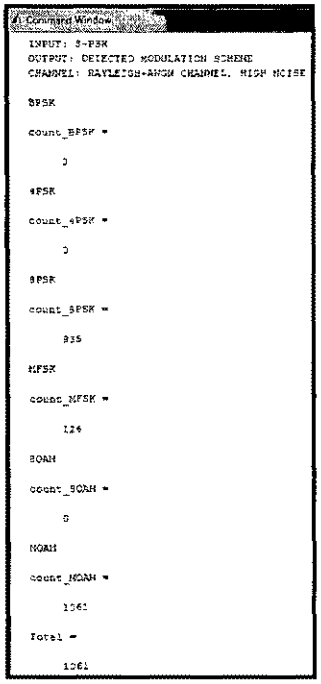

Figure 70: Output of Classifier Algorithm for 8-PSK Input Signal Passed Over Rayleigh Channel With AWGN (High Noise).

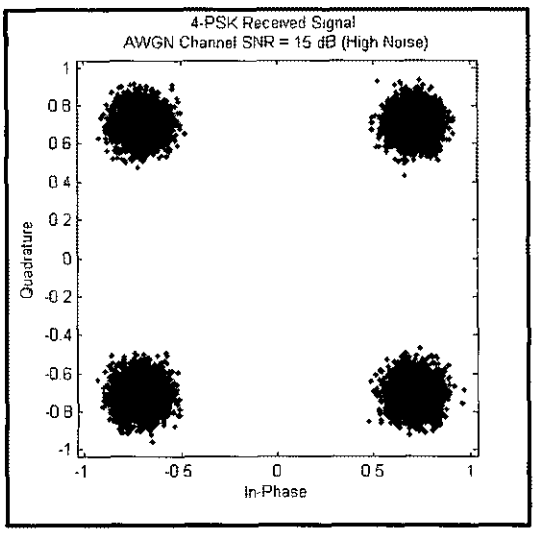

Figure 71: 4-PSK Received Signal Over Rayleigh Channel with SNR = 15 dB.

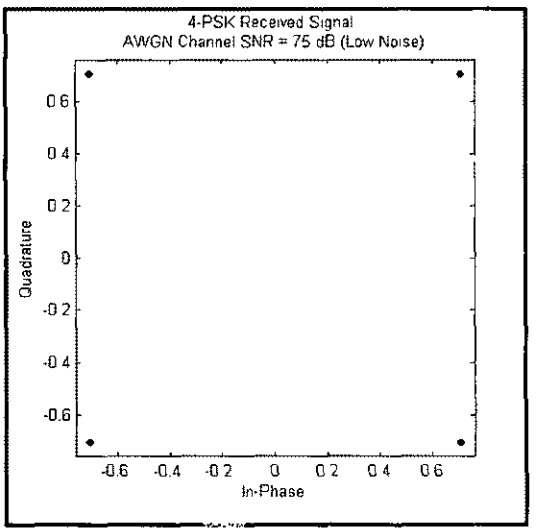

Figure 72: 4-PSK Received Signal Over AWGN Channel with SNR = 75 dB.

6.7 Results from Classification of Modulated Signals Transmitted Through Ricean Channel

Random signals were modulated and transmitted through a multipath Ricean fading channel with AWGN in order to determine the ability of the classification algorithm to correctly identify the modulation scheme of the received signal. Table 11 and Table 12 show the classification success of modulated signals propagated through multipath Ricean fading channel with AWGN noise at various low SNR levels (SNR range: 0 dB to 25 dB) and high SNR levels (SNR range: 50 dB to 100 dB). At low SNR levels (high noise), the percent success of the classifier dropped to 67.06% for modulated signals that were propagated through the Ricean fading channel. At high SNR levels (low noise), the classifier was able to identify the modulation scheme of the signal 76.52% of the time. The classifier success for the Ricean fading channel was determined by computing the average across the main diagonals of Table 11 and Table 12.

On average, the classification algorithm identified fewer modulation schemes correctly for signals propagated through the Ricean fading channel at low SNR than for signals propagated through the Rayleigh fading channel at low SNR. For some modulation

schemes, the classifier identified the modulated signal as both the correct modulation type and as other modulation types. For example, in Table 11 the classifier was able to correctly identify the modulation scheme of 8-QAM signal that was propagated through a noisy channel 927 times. However, the remaining 211 signals were identified as either BPSK, 4-PSK, M-FSK, or M-QAM. For low noise levels some of the cumulants for the 8-QAM overlapped with the cumulant decision thresholds for the other modulation schemes, confusing the classifier and making it unable to correctly identify the modulation type of the transmitted signal.

For example, from Table 6 in Chapter 5, the maximum range end (-58.81) of the 8-QAM eighth order cumulant (C_{s80}) range that is close to the minimum range end of the eighth order cumulant (C_{s80}) range (-34) of the 4-PSK scheme. Therefore, if random signals are modulated with the 8-QAM signal and are transmitted in various levels of noisy channels, the cumulants for the 8-QAM can intersect with the cumulants of 4-PSK signal causing confusion for the classifier and making it unable to correctly identify the modulation scheme of the transmitted signal. Appendix C shows the overall maximum and minimum moments and cumulant tables for each of the modulated signals that were transmitted through an multipath Ricean fading channel with AWGN at low and high SNR levels.

Table 36 in Appendix C also shows that the maximum end range (-58.72) of the 8-QAM eighth order cumulant (C_{s80}) range is close to the eighth order cumulant (C_{s80}) range (-10.18) of the 4-PSK scheme.

Table 11: Classifier Success Results for Ricean Channel at High Noise Level.

Classification Rate 67.06%		Modulation Schemes Detected In The Trial						
		BPSK	4-PSK	8-PSK	M-FSK	8-QAM	M-QAM	Total
Trial Cases Transmitted	BPSK	332	110	353	283	107	4	1189
	4-PSK	142	561	207	442	101	28	1481
	8-PSK	24	86	589	570	37	57	1363
	2-FSK	0	0	0	1000	0	0	1000
	4-FSK	0	0	0	1000	0	0	1000
	8-FSK	0	0	0	1000	0	0	1000
	8-QAM	57	81	0	9	927	64	1138
	16-QAM	170	276	0	67	120	398	1031
	64-QAM	92	364	15	28	113	471	1083
	256-QAM	126	333	216	11	100	428	1214

Classification Modulation Algorithm Success Results
Ricean Channel with AWGN, 1000 Trials, SNR Range: 0 dB to 25 dB (High Noise)

Table 12: Classifier Success Results for Ricean Channel at Low Noise Level.

Classification Rate 76.52%		Modulation Schemes Detected In The Trial						
		BPSK	4-PSK	8-PSK	M-FSK	8-QAM	M-QAM	Total
Trial Cases Transmitted	BPSK	661	53	161	116	75	0	1066
	4-PSK	276	460	190	205	115	0	1246
	8-PSK	0	4	940	959	0	0	1903
	2-FSK	0	0	0	1000	0	0	1000
	4-FSK	0	0	0	1000	0	0	1000
	8-FSK	0	0	0	1000	0	0	1000
	8-QAM	123	75	0	27	864	39	1128
	16-QAM	81	127	9	398	178	487	1280
	64-QAM	139	126	39	130	128	562	1124
	256-QAM	111	322	246	2	567	678	1926

Classification Modulation Algorithm Success Results
Ricean Channel with AWGN, 1000 Trials, SNR Range: 50 dB to 100 dB (Low Noise)

Figure 73 shows an excerpt of MATLAB® code which shows 1,000 random signals that were modulated using 8-QAM and transmitted over a Ricean channel with AWGN at a high level of SNR. Figure 74 shows the output of the classification algorithm which identified the modulated signals as 8-QAM 927 times and identified the modulation scheme of the signal as M-FSK 9 times, 4-PSK 81 times, BPSK 57 times, and M-QAM 64 times. Figure 75 and Figure 76 show examples of signal constellation diagrams of 2-PSK modulated signal with noise levels of 5 dB and 80 dB, respectively.

```
%% Create 8-QAM Ricean
clear all
clc
close all
for j = 1:1:1000;
M = 8;              % Modulation alphabet size
hMod = comm.RectangularQAMModulator('ModulationOrder',M);
modData = step(hMod,randi([0 7],20000,1));
noise(j) = randi([0 25],1);
hAWGN = comm.AWGNChannel('SNR',noise(j),'BitsPerSymbol',4);
channelOutput = step(hAWGN, modData);
ts = 1e-5;                  % sample time
fd = 0;                     % maximum Doppler shift in Hz
tau = [0 1e-7];             % path delays
pdb = [0 0];                % average path gains
k = 3; % dB
c1 = ricianchan(ts, fd, k, tau, pdb);
channelOutput = filter(c1,channelOutput);
```

Figure 73: Communication Model Showing Input of 8-QAM Modulated Signal.

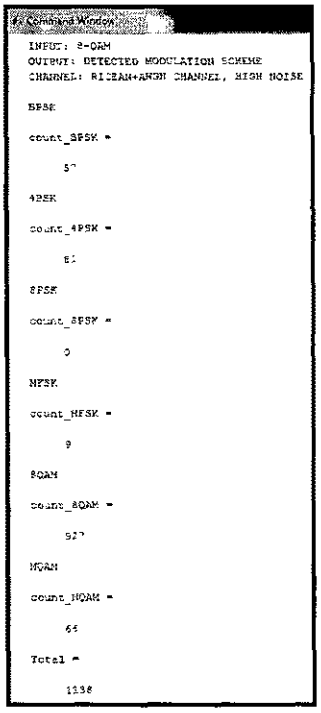

Figure 74: Output of Classifier Algorithm for 8-QAM Input Signal Passed Over AWGN Channel (High Noise).

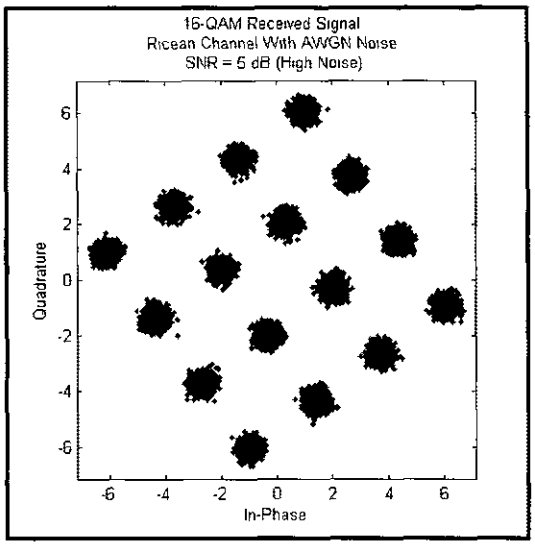

Figure 75: 16-QAM Received Signal Over Ricean Channel with SNR = 5 dB.

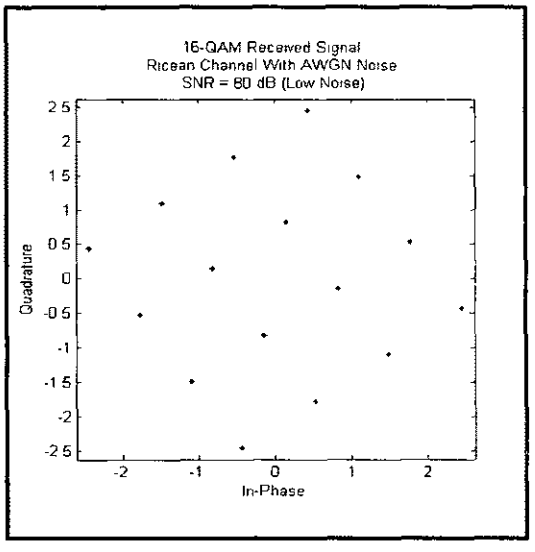

Figure 76: 16-QAM Received Signal Over Ricean Channel with SNR = 80 dB.

CHAPTER 7

CONCLUSIONS

7.1. Summary

The automatic classification of modulation schemes in the communication signals was recognized as an important issue in the development of a good wireless communication system. With the introduction of a large variety of modulation schemes in the signals, reliable detection of the modulation scheme has become important. The present research focused on modeling and simulation of an automatic modulation classifier, used the higher order statistical characteristics detected in the signals. This research began with an understanding of the commonly used digital modulation schemes, such as Phase Shift Keying (PSK), Frequency Shift Keying (FSK), and Quadrature Amplitude Modulation (QAM). Characteristics of commonly used modulation schemes were examined. A basic framework for a numerical modeling and simulation of a wireless communication system was developed to serve as a building block for the development of automatic modulation classifier. This research demonstrated that the higher order statistical features of a signal can effectively be used in the classification of the modulation scheme in a received signal. In the presence of noise, higher order moments and cumulants helped to identify the signal characteristics to enable classification of various modulation types. In the study, an classifier algorithm was developed to identify the modulation schemes used in the signals by using eighth order cumulants.

Numerical simulations were performed to demonstrate the working of an automatic modulation classifier. Communication channel models, including an AWGN channel, a multipath Rayleigh, and a Ricean fading with AWGN channels, were simulated and results were evaluated to show that the automatic modulation classifier identified the modulation scheme of a signal that was passed through these channels.

The modulation classification algorithm was able to identify the modulation scheme of the signals by evaluating whether the statistical features of the modulated signals lay within the predefined cumulant thresholds. The cumulant thresholds for the modulation classification algorithm were determined by evaluating the higher order statistics of each of the modulated signals transmitted through an AWGN channel at low and high levels of SNRs. The modulation classification algorithm was tested with 1,000 random signals modulated using BPSK, 4-PSK, 8-PSK, 2-FSK, 4-FSK, 8-FSK, 8-QAM, 16-QAM, 64-QAM and 256-QAM. Also, the automatic modulation classifier was tested for its ability to detect modulation schemes even with the multipath Rayleigh fading channel with AWGN and multipath Ricean fading channel with AWGN. The statistical moments and cumulants of the received noisy signal were computed correctly to identify the modulation scheme of the transmitted signal without a priori information about the modulation type of the transmittal signal. Simulation results were presented in two parts. First, basic simulation results were presented which helped to show the benefits of an automatic modulation classifier over a conventional modulation identifier. Simulations were performed to compare the performance and tradeoffs between two types of modulation schemes 1) M-PAM and 2) M-PSK. The results showed how the M-PAM and M-PSK signals, when passed over a channel with AWGN to analyze the Bit Error Rate (BER), had impacted the signal's detection at the receiver. Second, the results from the modulation classification algorithm developed in this study were presented and their operation in the wireless communication system implemented.

The designed automatic modulation classification algorithm was able to correctly identify all the modulation schemes of the transmitted signal that was taken to be transmitted through a AWGN channel at both low and high SNR levels. The classification percent success dropped further if the signal was transmitted through either a Ricean or Rayleigh channel. Under various noise and multipath fading channel conditions, the classification modulation algorithm was able to identify the modulation scheme of the transmitted signals with a success of 79.21% among all the trials signals passed through the system. Specifically, if the signal was modulated with BPSK with AWGN noise and fading channel conditions, the classification algorithm identified the modulation scheme with a success of 67.56% among all the trial runs. If a random signal was modulated with 4-

PSK, the classification algorithm was able to identify the modulation scheme with a success of 67.76% in all cases. If a random signal was modulated with 8-PSK, the classifier selected the correct modulation scheme in 88% of the cases. If the signal was modulated via 2-FSK, 4-FSK, or 8-FSK, the algorithm correctly selected M-FSK at 100% success with both high and low SNR levels. If the signal was modulated using 8-QAM the percent success was 83.4%. If the signal was generated using 16-QAM, 64-QAM or 256-QAM, the classifier identified the modulation as the general case of the M-QAM signal type 69.24% of the time.

7.2. Scope for Future Research Work

This thesis showed that higher order statistical features of a received signal can indeed be used to identify the modulation scheme of the original transmitted signal. This work is a small milestone of the research in this field of communication engineering and represents a unique contribution. However, future work will be needed to further improve the ability of the classification algorithm to reliably identify the modulation scheme of the transmitted signal. The design of the automatic modulation classifier used simple decision statistical thresholds to identify the modulation scheme of the signal. These statistical thresholds were based on signals that were passed through an AWGN channel. Additionally, the statistical thresholds could be considered for signals that were passed through various multipath channels. The complexity of the algorithm could be modified to use multiple statistical conditions to determine the modulation scheme.

Various modulation schemes were distinguishable at the eighth order cumulant. Further statistical computations could be made to determine if moments and cumulants of higher orders beyond eighth order might result in moments and cumulants ranges with no overlap. This would, in turn, improve the ability of the classifier to correctly identify the modulation scheme.

Further, utility of neural networks could be used to develop a receiver that could be trained to identify the modulation scheme of the transmitted signal. Additionally, the model could be extended to identify modern communication modulation schemes

including orthogonal frequency division multiplexing, cyclical shift keying, trellis coded modulation, and others. Finally, research could be carried out to evaluate the security aspects of an automatic modulation classifier. The automatic modulation classifier could be modified to detect a signal that was coded with frequency hopping spread spectrum to prevent jamming, which would improve security protection of the message signal.

REFERENCES

[1] B. Black, P. Dipiazza, and B. Ferguson, "Introduction"; "The Radio Link"; "Channel Characteristics"; "Digital Signaling Principles", in *Introduction to Wireless Systems*, 1st ed. Boston: Pearson Education, Inc. 2008.

[2] W. Juan-ping, H. Ying-zheng, Z. Jin-mei, and W. Hua-kui, "Automatic Modulation Recognition of Digital Communication Signals," in *2010 First International Conference on Pervasive Computing, Signal Processing and Applications*, Harbin, pp.590-593.

[3] D. Grimaldi, S. Rapuano, and L. De Vito, "An Automatic Digital Modulation Classifier for Measurement on Telecommunication Networks," *IEEE Transactions On Instrumentation and Measurement Society*, vol.56, no.5, pp.1711-1720, Oct. 2007.

[4] S. Taira, and E. Murakami, "Automatic Classification of Analogue Modulation Signals by Statistical Parameters," *MILCOM 1999 IEEE Military Communications Conference Proceedings*, vol.1, Atlantic City, NJ, pp.202-207.

[5] N. Geisinger, "Classification of Digital Modulation Scheme Using Linear and Nonlinear Classifiers," M.S. thesis, Naval Postgraduate School, Monterey, CA, March 2010.

[6] C. Le Martret and D. Boiteat, "Modulation Classification By Means Of Different Orders Statistical Moments," *IEEE Military Communications 1997,* vol.3, Monterey, CA, pp.256-258, Nov. 1997.

[7] P. Marchand, "Détection et Reconnaissance de Modulations Numériques a l'aide des Statistiques Cycliques d'ordre Supérieur", Ph.D. dissertation, Institut National Polytechnique de Grenoble, 1998.

[8] S.S. Soliman, and S.-Z. Hsue, "Signal Classification Using Statistical Moments," *IEEE Communications Society*, vol.40, no.5, pp.908-916, May 1992.

[9] O.A. Dobre, Y. Bar-Ness, and S. Wei, "Robust QAM Modulation Classification Algorithm Using Cyclic Cumulants," *WCNC 2004 IEEE Wireless Communications and Networking Conference*, vol.2, pp.745-748.

[10] O.A. Dobre, A. Abdi, Y. Bar-Ness, and W. Su, "Survey of Automatic Modulation Classification Techniques: Classical Approaches and New Trends," *IET Communications*, vol.1, no.2, pp.137-156, April 2007.

[11] V. Kalinin and D. Kavalov, "A SAW Neural Network Processor For Classification Of MSK and BPSK Modulations," *2002 IEEE Ultrasonics Symposium*, vol.1, pp.263-266.

[12] S.M. Baarrij, F. Nasir, and S. Masood, "A Robust Hierarchical Digital Modulation Classification Technique: Using Linear Approximations," *2006 IEEE International Symposium on Signal Processing and Information Technology*, pp.545-550.

[13] G. Hatzichristos, "Classification of Digital Modulation Types in Multipath Environments," MSEE thesis, Dept. Elect. Eng., Naval Postgraduate School, Monterey, CA, 2001.

[14] A. Young, "Classification of Digital Modulation Types in Multipath Environments," MSEE thesis, Dept. Elect. Eng., Naval Postgraduate School, Monterey, CA, 2008.

[15] J. Proakis and M. Salehi, "Introduction"; "Digital Transmission Through The Additive White Gaussian Noise Channel", in *Communication Systems Engineering*, 2nd ed. New Jersey: Prentice Hall, 2002.

[16] A. Goldsmith, "Digital Modulation and Detection", in *Wireless Communications*, 1st ed. New York: Cambridge University Press, 2005.

[17] A.M. Makowski, "On the Optimality of Uniform Pulse Amplitude Modulation," *IEEE Transactions On Information Theory*, vol.52, no.12, pp.5546-5549, Dec. 2006.

[18] M. Iqbal, L. Jeongseon, and K. Kiseon, "Performance Comparison Of Digital Modulation Schemes With Respect To Phase Noise Spectral Shape," *2000 Canadian Conference on Electrical and Computer Engineering*, vol.2, Halifax, NS, pp.856-860.

[19] T. Morsy and J. Gotze, "Near Optimum Maximum Likelihood Detector For Structured Communication Problems," *2012 Wireless Telecommunications Symposium (WTS)*, London, pp.1-6.

[20] G. Hatzichristos and M.P. Fargues, "A Hierarchical Approach to the Classification of Digital Modulation Types in Multipath Environments," *2001 Conference Record of the Thrity-Fifth Asliomar Conference on Signal, Systems and Computers*, vol.2, Pacific Grove, CA, pp.1494-1498.

[21] A. Papoulis and S. Unnikrishna Pillai, "Functions of One Random Variable", in *Probability, Random Variables and Stochastic Processes*, 4th ed. New York, 2002.

[22] D.C. Cox and R. Leck, "Distributions of Multipath Delay Spread and Average Excess Delay for 910-MHz Urban Mobile Radio Paths," *IEEE Transactions on Antennas and Propagation*, vol.23, no.2, pp.206-213, Mar 1975.

APPENDIX A: HIGHER ORDER STATISTICS OF SIGNAL THROUGH AWGN CHANNEL

Appendix A presents the overall maximum and minimum moments and cumulant tables for each of the modulated signals that were transmitted through an AWGN channel at low and high SNR levels. The modulation scheme decision thresholds were determined by analyzing the maximum and minimum moments and cumulants ranges. A decision threshold for a modulation scheme was chosen based on unique maximum and minimum statistical range which did not overlap with other maximum and minimum statistical modulation ranges. Analysis of these tables shows that lower order moments and cumulants have many overlapping ranges and, hence, cannot be used to identify a modulation scheme. Eighth order moments, on the other hand, have unique non overlapping cumulants which are used to identify the modulation scheme of a transmitted signal.

Table 13: Second Order Moment Range for Modulated Signals Passed Through AWGN Channel.

	Es20		Es11	
	max	min	max	min
BPSK	1	0.80108	1	1
4PSK	0.0047	-0.0013	1	1
8PSK	-0.0017	-0.0077	1	1
2FSK	0.0013	-0.0013	1.2487	1
4FSK	0.0011	-0.0005	1.2509	1
8FSK	0.0003	-0.0012	1.2495	1
8QAM	0.6674	0.64127	1	1
16QAM	0.0049	0.00381	1	1
64QAM	-0.0008	-0.0018	1	1
256QAM	0.0081	0.00727	1	1

Table 14: Fourth Order Moment Range for Modulated Signals Passed Through AWGN Channel.

	Es40		Es31		Es22	
	max	min	max	min	max	min
BPSK	1	0.6501	1.124	1	1.358	1
4PSK	-0.648	-1	0.005	-0.001	1.361	1
8PSK	0.0083	-0.003	3E-04	-0.013	1.36	1
2FSK	0.0033	-5E-04	0.003	-0.001	2.12	1
4FSK	0.001	-0.003	0.004	-7E-04	2.128	1
8FSK	0.0018	-0.006	6E-04	-0.004	2.124	1
8QAM	0.3334	0.3117	1.111	1.1023	1.487	1.442
16QAM	-0.651	-0.682	0.005	0.0035	1.349	1.316
64QAM	-0.613	-0.621	-0.002	-0.003	1.391	1.384
256QAM	-0.606	-0.608	0.01	0.0093	1.394	1.393

Table 15: Sixth Order Moment Range for Modulated Signals Passed Through AWGN Channel.

	Es60		Es51		Es42		Es33	
	max	min	max	min	max	min	max	min
BPSK	1	0.5395	1.183	1	1.928	1	2.279	1
4PSK	0.007	-0.02	-1	-1.17	0.009	-0.001	2.297	1
8PSK	0.008	-0.016	0.01	-0.008	0.003	-0.026	2.291	1
2FSK	0.01	-0.004	0.01	-0.001	0.008	-0.002	4.451	1
4FSK	0.006	-0.011	0.001	-0.012	0.014	-0.002	4.483	1
8FSK	0.009	-0.003	0.003	-0.014	8E-04	-0.011	4.466	1
8QAM	-0.71	-0.812	0.634	0.622	1.979	1.8454	2.568	2.325
16QAM	0.008	-0.005	-1.31	-1.319	0.005	0.0025	2.094	1.9476
64QAM	0.016	0.009	-1.3	-1.31	-0.003	-0.006	2.272	2.239
256QAM	-0	-0.005	-1.29	-1.291	0.015	0.0125	2.289	2.2836

Table 16: Eighth Order Moment Range for Modulated Signals Passed Through AWGN Channel.

	Es80		Es71		Es62		Es53		Es44	
	max	min	max	min	max	min	max	min	max	min
BPSK	1	0.4632	1.224	1	2.493	1	3.877	1	4.505	1
4PSK	1	0.3542	0.028	-0.04	-1	-2.456	0.016	-0.002	4.578	1
8PSK	-0.379	-1	0.009	-0.05	0.013	-0.021	0.011	-0.055	4.573	1
2FSK	0.006	-0.021	0.038	-0.01	0.052	-0.004	0.019	-0.005	11.02	1
4FSK	0.006	-0.028	0.012	-0.04	0.002	-0.058	0.063	-0.005	11.17	1
8FSK	0.009	-0.064	0.018	-0.01	0.007	-0.039	0.001	-0.027	11.09	1
8QAM	-2.714	-3.228	-1.315	-1.37	1.217	1.0679	3.705	3.068	4.751	3.842
16QAM	2.188	2.004	0.015	-0.01	-2.46	-2.614	0.006	6E-04	3.564	3.093
64QAM	1.953	1.8965	0.027	0.01	-2.79	-2.815	-0.003	-0.011	4.117	4.004
256QAM	1.837	1.8053	0.002	-0.01	-2.8	-2.812	0.021	0.017	4.188	4.169

Table 17: Second Order Cumulant Range for Modulated Signals Passed Through AWGN Channel.

	Cs20		Cs11	
	max	min	max	min
BPSK	1	0.6464	1	0.807
4PSK	1	-0.001	1	0.796
8PSK	1	-0.007	1	0.802
2FSK	1	-0.001	1.249	1
4FSK	1	-5E-04	1.251	1
8FSK	1	-0.001	1.249	1
8QAM	0.1663	0.102	0.166	0.159
16QAM	0.0995	0.0004	0.1	0.097
64QAM	0.0239	-4E-05	0.024	0.024
256QAM	0.0059	4E-05	0.006	0.006

Table 18: Fourth Order Cumulant Range for Modulated Signals Passed Through AWGN Channel.

	Cs40		Cs31		Cs22	
	max	min	max	min	max	min
BPSK	-1.958	-2.025	-1.964	-2.026	-1.971	-2.027
4PSK	1E-07	-1.024	0.0028	-0.01	-0.993	-1.009
8PSK	0.0097	-0.004	0.0135	0.0051	-0.991	-1.008
2FSK	0.0033	-5E-04	0.0037	-0.001	-0.998	-1.002
4FSK	0.001	-0.003	0.0009	-8E-04	-0.998	-1.001
8FSK	0.0018	-0.006	0.0018	-5E-04	-0.997	-1.002
8QAM	-0.893	-1.009	-0.891	-0.901	-1.001	-1.01
16QAM	-0.009	-0.689	-0.008	-0.011	-0.681	-0.689
64QAM	0.0012	-0.621	0.0025	0.0006	-0.614	-0.618
256QAM	-0.013	-0.609	-0.012	-0.014	-0.607	-0.608

Table 19: Sixth Order Cumulant Range for Modulated Signals Passed Through AWGN Channel.

	Cs60		Cs51		Cs42		Cs33	
	max	min	max	min	max	min	max	min
BPSK	16.001	8.262	16	8.177	16	8.1945	16	8.201
4PSK	0.0472	-0.016	3.9706	-3E-04	0.052	-0.016	4	2.044
8PSK	0.0086	-0.016	0.0099	-0.034	-0.02	-0.048	4	2.051
2FSK	0.0105	-0.004	0.0019	-0.011	0.006	-0.019	4.012	3.987
4FSK	0.0058	-0.011	0.0064	-0.006	0.004	-0.005	4.013	3.988
8FSK	0.0093	-0.003	0.0212	-0.008	0.003	-0.01	4.011	3.983
8QAM	-1.743	-1.927	4.9112	4.338	4.771	4.2112	4.918	4.343
16QAM	0.0553	0.036	2.0939	0.044	0.048	0.0379	2.1	1.952
64QAM	0.0035	-0.006	1.795	-0.004	-0	-0.01	1.782	1.751
256QAM	0.0701	0.064	1.7525	0.058	0.063	0.0562	1.748	1.742

Table 20: Eighth Order Cumulant Range for Modulated Signals Passed Through AWGN Channel.

	Cs80		Cs71		Cs62		Cs53		Cs44	
	max	min	max	min	max	min	max	min	max	min
BPSK	-98.55	-244	-86.23	-244	-73.49	-244	-61.44	-244	-56.53	-244
4PSK	-14.36	-34	0.2327	-0.7535	-28.12	-46	0.1751	-0.4187	22.84	-18
8PSK	-0.881	-1.03	0.0307	-0.0394	0.1743	-1.504	0.8749	-1.0838	55.818	-17.02
2FSK	0.0053	-0.021	0.0372	-0.0075	0.2552	-0.027	0.1644	-0.0452	56.068	-17
4FSK	0.0064	-0.029	0.0119	-0.0382	0.0481	-0.242	0.2855	-0.0591	56.577	-17
8FSK	0.0084	-0.065	0.0178	-0.0078	0.0979	-0.386	0.0541	-0.2526	56.384	-17
8QAM	-58.81	-69.77	-113.9	-129.03	-20.08	-29.14	1.4958	-9.7297	10.089	-2.621
16QAM	-12.64	-14.11	-0.077	-0.4805	-28.28	-29.94	-0.136	-0.1828	21.07	17.45
64QAM	-11.27	-11.54	0.1776	0.0762	-26.82	-27.16	-0.013	-0.1041	25.244	24.444
256QAM	-11.05	-11.14	-0.727	-0.816	-26.49	-26.61	-0.141	-0.1695	25.598	25.452

APPENDIX B: HIGHER ORDER STATISTICS OF SIGNAL THROUGH RAYLEIGH CHANNEL

Appendix B presents the overall maximum and minimum moments and cumulant tables for each of the modulated signals that were transmitted through a multipath Rayleigh fading channel with AWGN at low and high SNR levels. Analysis of these tables shows that lower order moments and cumulants have many overlapping ranges and, hence. cannot be used to identify a modulation scheme. Eighth order moments, on the other hand, have unique non overlapping cumulants which are used to identify the modulation scheme of a transmitted signal.

Table 21: Second Order Moment Range for Modulated Signals Passed Through Rayleigh Channel with AWGN.

	Es20		Es11	
	max	min	max	min
BPSK	0.8869	0.77594	1	1
4PSK	-0.0002	-0.0042	1	1
8PSK	0.0926	0.08861	1	0.763
2FSK	0.0004	-0.0007	0.9057	0.498
4FSK	-0.0009	-0.002	1.18	0.778
8FSK	0.0009	-0.0006	0.7945	0.387
8QAM	-0.5086	-0.571	1	1
16QAM	0.0012	1.2E-05	1	1
64QAM	0.0054	0.00437	1	1
256QAM	0.0003	-0.0003	1	1

Table 22: Fourth Order Moment Range for Modulated Signals Passed Through Rayleigh Channel with AWGN.

	Es40		Es31		Es22	
	max	min	max	min	max	min
BPSK	0.7373	0.5608	1.083	1.0391	1.356	1.164
4PSK	-0.359	-0.465	-0.004	-0.01	1.391	1.179
8PSK	0.0014	-0.024	0.161	0.1003	1.624	0.781
2FSK	0.0007	-0.004	-2E-04	-0.006	1.584	0.436
4FSK	0.0029	-0.001	-0.001	-0.005	2.508	0.932
8FSK	0.0015	-0.002	0.003	-1E-04	1.245	0.281
8QAM	0.2096	0.1693	-0.982	-1.014	1.639	1.531
16QAM	-0.431	-0.459	-0.001	-0.004	1.379	1.343
64QAM	0.5952	0.5798	0.013	0.0103	1.398	1.388
256QAM	0.2908	0.2897	0.002	0.0007	1.398	1.396

Table 23: Sixth Order Moment Range for Modulated Signals Passed Through Rayleigh Channel with AWGN.

	Es60		Es51		Es42		Es33	
	max	min	max	min	max	min	max	min
BPSK	0.566	0.3904	1.015	0.99	1.842	1.375	2.266	1.5333
4PSK	-0	-0.069	-0.64	-0.668	-0.007	-0.026	2.419	1.5854
8PSK	0.148	0.0993	0.017	-0.077	0.358	0.1341	3.56	0.9824
2FSK	0.04	-0.005	0.002	-0.015	-0.002	-0.038	4.053	0.5323
4FSK	0.009	-0.013	0.021	-0.005	0.001	-0.017	7.521	1.4643
8FSK	0.034	-0.002	0.009	-0.01	0.01	0.0007	2.89	0.2926
8QAM	0.295	0.1848	0.442	0.407	-1.945	-2.214	3.444	2.8098
16QAM	0.047	0.0324	-0.89	-0.913	-0.006	-0.015	2.226	2.0626
64QAM	0.005	-0.003	1.265	1.245	0.029	0.0214	2.308	2.2615
256QAM	-0.02	-0.022	0.62	0.617	0.009	0.005	2.306	2.2957

Table 24: Eighth Order Moment Range for Modulated Signals Passed Through Rayleigh Channel with AWGN.

	Es80		Es71		Es62		Es53		Es44	
	max	min	max	min	max	min	max	min	max	min
BPSK	0.386	0.269	0.904	0.828	2.1	1.4702	3.675	2.017	4.456	2.24
4PSK	-0.108	-0.296	-0.008	-0.23	-0.96	-1.424	-0.014	-0.072	5.009	2.381
8PSK	0.127	-0.143	0.598	0.17	0.074	-0.272	0.929	0.209	9.785	1.454
2FSK	0.139	-0.04	0.292	-0.01	2E-04	-0.071	-0.008	-0.254	13.58	0.827
4FSK	0.102	-0.06	0.026	-0.12	0.124	-0.069	0.051	-0.051	28.93	2.823
8FSK	0.009	-0.044	0.124	-0.01	0.072	-0.04	0.048	0.002	8.86	0.394
8QAM	-0.083	-0.289	0.72	0.459	1.23	0.8776	-4	-5.681	8.522	5.705
16QAM	-0.055	-0.086	0.099	0.056	-1.8	-1.884	-0.014	-0.039	3.995	3.451
64QAM	1.788	1.695	0.025	0.002	2.747	2.7318	0.067	0.043	4.251	4.09
256QAM	-1.029	-1.036	-0.031	-0.04	1.355	1.3455	0.034	0.022	4.24	4.205

Table 25: Second Order Cumulant Range for Modulated Signals Passed Through Rayleigh Channel with AWGN.

	Cs20		Cs11	
	max	min	max	min
BPSK	0.3057	0.2349	0.345	0.303
4PSK	0.3262	-0.001	0.376	0.326
8PSK	0.5895	0.0522	0.59	0.45
2FSK	0.9057	-7E-04	0.906	0.498
4FSK	1.18	-0.002	1.18	0.778
8FSK	0.7945	-6E-04	0.794	0.387
8QAM	0.2795	-0.18	0.316	0.279
16QAM	0.0664	8E-07	0.068	0.066
64QAM	0.0232	0.0001	0.023	0.023
256QAM	0.0036	-1E-06	0.004	0.004

Table 26: Fourth Order Cumulant Range for Modulated Signals Passed Through Rayleigh Channel with AWGN.

	Cs40		Cs31		Cs22	
	max	min	max	min	max	min
BPSK	-1.245	-1.264	-1.244	-1.26	-1.245	-1.26
4PSK	0.0002	-0.359	0.0051	-0.005	-0.608	-0.619
8PSK	-0.022	-0.111	-0.11	-0.116	-0.385	-0.392
2FSK	0.0007	-0.004	-7E-04	-0.004	-0.057	-0.06
4FSK	0.0029	-0.001	0.0026	-6E-04	-0.276	-0.279
8FSK	0.0015	-0.002	0.0017	0.0004	-0.017	-0.02
8QAM	0.5439	-0.611	0.5495	0.5439	-0.62	-0.625
16QAM	-0.006	-0.438	-0.003	-0.006	-0.621	-0.625
64QAM	0.5832	-0.003	-0.002	-0.004	-0.599	-0.602
256QAM	0.2907	0.0015	0.0017	0.0012	-0.601	-0.602

Table 27: Sixth Order Cumulant Range for Modulated Signals Passed Through Rayleigh Channel with AWGN.

	Cs60		Cs51		Cs42		Cs33	
	max	min	max	min	max	min	max	min
BPSK	-0.668	-1.109	11.687	7.864	11.68	7.8644	11.68	7.863
4PSK	-0.03	-0.083	1.6878	8E-04	0.02	-0.037	2.975	1.902
8PSK	0.3101	0.253	0.3665	0.099	0.391	0.3665	1.015	1.007
2FSK	0.0403	-0.005	0.0035	-0.002	0.002	-0.002	0.064	0.058
4FSK	0.0088	-0.013	0.0058	-0.002	0.008	-0.005	0.601	0.585
8FSK	0.0344	-0.002	0.0034	-0.004	7E-04	-0.002	0.011	0.008
8QAM	5.1789	3.673	3.3742	-2.267	-2.27	-3.289	3.424	2.356
16QAM	0.0541	0.036	1.3838	0.028	0.03	0.0166	1.974	1.813
64QAM	-0.036	-0.047	0.007	-1.711	0.009	0.0045	1.765	1.722
256QAM	-0.018	-0.023	-0.0048	-0.834	-0	-0.005	1.732	1.723

Table 28: Eighth Order Cumulant Range for Modulated Signals Passed Through Rayleigh Channel with AWGN.

	Cs80		Cs71		Cs62		Cs53		Cs44	
	max	min	max	min	max	min	max	min	max	min
BPSK	-97.22	-164.9	-169.9	-261.5	-71.74	-148.2	-57.96	-142.02	-52.1	-139.7
4PSK	-4.644	-7.854	0.2716	-0.2864	-15.46	-20.63	0.2111	-0.4563	26.339	2.9113
8PSK	0.0437	-0.18	1.7969	0.9047	-0.415	-1.426	6.1802	-0.0673	51.937	6.695
2FSK	0.1383	-0.04	0.2922	-0.0116	0.0148	-0.163	-0.013	-0.5405	58.61	4.1177
4FSK	0.1019	-0.061	0.0272	-0.1174	0.23	-0.127	0.0212	-0.4323	139.41	15.663
8FSK	0.0088	-0.044	0.1238	-0.0107	0.0995	-0.065	0.125	0.00059	36.731	1.799
8QAM	-24.53	-39.98	138.67	100.14	1.7119	-11.62	-12.93	-31.284	48.278	24.845
16QAM	-6.59	-7.443	0.0113	-0.0626	-18.83	-20.1	-0.243	-0.4132	24.174	20.182
64QAM	-10.06	-10.61	0.4245	0.3313	26.058	25.372	0.5375	0.4081	26.091	24.976
256QAM	-3.966	-3.988	-0.037	-0.0566	12.702	12.662	0.1806	0.09773	26.295	26.065

APPENDIX C: HIGHER ORDER STATISTICS OF SIGNAL THROUGH RICEAN CHANNEL

Appendix C presents the overall maximum and minimum moments and cumulant tables for each of the modulated signals that were transmitted through a multipath Ricean fading channel with AWGN at low and high SNR levels. Analysis of these tables shows that lower order moments and cumulants have many overlapping ranges and, hence, cannot be used to identify a modulation scheme. Eighth order moments, on the other hand, have unique non overlapping cumulants which are used to identify the modulation scheme of a transmitted signal.

Table 29: Second Order Moment Range for Modulated Signals Passed Through Ricean Channel with AWGN.

	Es20		Es11	
	max	min	max	min
BPSK	-0.0533	-0.0601	1	0.509
4PSK	0.0027	-0.0037	1	1
8PSK	0.0042	-0.0099	1.2542	1
2FSK	0.0006	-0.001	1.2496	1
4FSK	0.0008	-0.0005	1.2498	1
8FSK	0.0014	-0.0004	1.2488	1
8QAM	0.6689	0.64277	1	1
16QAM	-0.0032	-0.0052	1	1
64QAM	-0.0007	-0.0016	1	1
256QAM	0.0066	0.00591	1	1

Table 30: Fourth Order Moment Range for Modulated Signals Passed Through Ricean Channel with AWGN.

	Es40		Es31		Es22	
	max	min	max	min	max	min
BPSK	-0.011	-0.047	-0.061	-0.158	2.004	0.486
4PSK	-0.323	-0.545	0.003	-0.007	1.685	1.401
8PSK	0.0169	-0.029	0.004	-0.016	2.138	1
2FSK	0.0036	-0.003	8E-04	-0.003	2.126	1
4FSK	0.0014	-0.003	0.002	-6E-04	2.121	1
8FSK	0.0025	-0.002	0.002	-0.001	2.123	1
8QAM	0.334	0.3163	1.108	1.1002	1.482	1.439
16QAM	-0.641	-0.675	-0.003	-0.006	1.353	1.324
64QAM	-0.615	-0.624	0.002	0.0005	1.388	1.381
256QAM	-0.617	-0.62	0.009	0.0072	1.397	1.395

Table 31: Sixth Order Moment Range for Modulated Signals Passed Through Ricean Channel with AWGN.

	Es60		Es51		Es42		Es33	
	max	min	max	min	max	min	max	min
BPSK	0.022	-0.149	-0.07	-0.22	-0.094	-0.681	6.144	0.6764
4PSK	-0.03	-0.094	-0.92	-1.044	0.028	-0.018	3.865	2.4649
8PSK	0.122	-0.018	0.029	-0.109	0.005	-0.05	4.531	1
2FSK	0.003	-0.008	0.007	-0.008	9E-04	-0.014	4.475	1
4FSK	0.004	-0.008	0.003	-0.012	0.005	-0.001	4.451	1
8FSK	0.009	-0.004	0.01	-0.003	1E-03	-0.003	4.468	1
8QAM	-0.69	-0.807	0.631	0.612	1.965	1.8336	2.547	2.31
16QAM	0.012	-0.008	-1.3	-1.325	-0.002	-0.009	2.108	1.9747
64QAM	-0.01	-0.024	-1.29	-1.306	0.006	0.0035	2.256	2.2217
256QAM	0.003	-0.003	-1.31	-1.314	0.011	0.0088	2.302	2.2921

Table 32: Eighth Order Moment Range for Modulated Signals Passed Through Ricean Channel with AWGN.

	Es80		Es71		Es62		Es53		Es44	
	max	min	max	min	max	min	max	min	max	min
BPSK	3.126	0.0351	0.073	-2.42	0.095	-1.425	-0.186	-4.274	25.9	1.241
4PSK	0.597	0.0835	0.008	-0.33	-2.32	-3.347	0.182	-0.05	11.14	5.171
8PSK	-0.977	-1.038	0.469	-0.03	0.05	-0.394	0.005	-0.183	11.42	1
2FSK	0.039	-0.005	0.013	-0.02	0.012	-0.032	0.001	-0.056	11.12	1
4FSK	0.003	-0.104	0.007	-0.01	0.005	-0.059	0.016	-0.003	11.01	1
8FSK	0.039	-0.007	0.078	-0.01	0.044	-0.009	0.002	-0.029	11.11	1
8QAM	-2.662	-3.194	-1.284	-1.35	1.207	1.0567	3.658	3.036	4.689	3.801
16QAM	2.217	1.964	0.015	-0.02	-2.51	-2.612	1E-03	-0.012	3.605	3.164
64QAM	1.913	1.8464	-0.02	-0.04	-2.75	-2.774	0.014	0.008	4.06	3.946
256QAM	1.856	1.8471	0.007	-0.01	-2.84	-2.859	0.016	0.01	4.224	4.189

Table 33: Second Order Cumulant Range for Modulated Signals Passed Through Ricean Channel with AWGN.

	Cs20		Cs11	
	max	min	max	min
BPSK	1.2283	-0.074	1.228	0.625
4PSK	0.6632	-0.003	0.909	0.663
8PSK	1	-0.01	1.254	1
2FSK	1	-0.001	1.25	1
4FSK	1	-5E-04	1.25	1
8FSK	1	-4E-04	1.249	1
8QAM	0.1656	0.1021	0.166	0.159
16QAM	0.1007	-5E-04	0.101	0.098
64QAM	0.0237	-4E-05	0.024	0.024
256QAM	0.0058	3E-05	0.006	0.006

Table 34: Fourth Order Cumulant Range for Modulated Signals Passed Through Ricean Channel with AWGN.

	Cs40		Cs31		Cs22	
	max	min	max	min	max	min
BPSK	0.0069	-0.058	0.0249	0.0069	0.0009	-0.036
4PSK	-0.005	-0.334	0.0035	-0.005	-0.313	-0.319
8PSK	0.0168	-0.029	0.02	-0.009	-0.996	-1.008
2FSK	0.0036	-0.003	0.0019	-0.001	-0.997	-1.002
4FSK	0.0014	-0.003	0.001	-0.001	-0.998	-1.003
8FSK	0.0025	-0.002	0.0003	-0.004	-0.996	-1.001
8QAM	-0.899	-1.013	-0.897	-0.902	-1.007	-1.011
16QAM	0.009	-0.678	0.0101	0.0071	-0.673	-0.683
64QAM	0.0049	-0.626	0.006	0.0042	-0.618	-0.62
256QAM	-0.011	-0.62	-0.01	-0.011	-0.604	-0.605

Table 35: Sixth Order Cumulant Range for Modulated Signals Passed Through Ricean Channel with AWGN.

	Cs60		Cs51		Cs42		Cs33	
	max	min	max	min	max	min	max	min
BPSK	0.1054	-0.052	0.0363	-0.078	-0.02	-0.087	0.124	0.038
4PSK	-0.02	-0.085	1.6811	0.027	0.029	-0.011	1.853	0.705
8PSK	0.1207	-0.016	0.0732	-0.062	0.049	-0.11	4.07	3.977
2FSK	0.0033	-0.007	0.0139	-0.013	0.006	-0.01	4.013	3.983
4FSK	0.0039	-0.008	0.0081	-0.005	0.006	-0.006	4.014	3.99
8FSK	0.0092	-0.004	0.009	-0.006	0.017	-0.001	4.006	3.979
8QAM	-1.772	-1.934	4.9666	4.369	4.826	4.2652	4.971	4.404
16QAM	-0.034	-0.055	2.0537	-0.044	-0.03	-0.049	2.057	1.934
64QAM	-0.018	-0.037	1.8158	-0.025	-0.02	-0.03	1.796	1.762
256QAM	0.0591	0.056	1.7871	0.047	0.049	0.0462	1.735	1.725

Table 36: Eighth Order Cumulant Range for Modulated Signals Passed Through Ricean Channel with AWGN.

	Cs80		Cs71		Cs62		Cs53		Cs44	
	max	min	max	min	max	min	max	min	max	min
BPSK	3.0879	-0.073	1.8778	-0.0039	0.1319	-2.064	-1.008	-13.706	98.556	5.4927
4PSK	-3.565	-10.18	0.1409	-0.4277	-14.37	-23.56	0.3367	-0.2616	58.523	27.32
8PSK	-0.981	-1.068	0.5128	-0.0399	0.8875	-2.196	0.8807	-0.9322	57.152	-17
2FSK	0.0389	-0.006	0.0135	-0.0196	0.1933	-0.246	0.0476	-0.2941	56.643	-17
4FSK	0.0029	-0.105	0.0076	-0.0142	0.0761	-0.238	0.07	-0.0085	55.839	-17
8FSK	0.0384	-0.007	0.0792	-0.0095	0.1984	-0.115	0.0061	-0.1561	56.488	-17
8QAM	-58.72	-70.54	-114.4	-130.2	-20.75	-30.09	0.3992	-10.813	8.8171	-3.752
16QAM	-12.43	-13.75	0.5983	0.3701	-28.08	-29.61	0.3033	0.11471	21.038	17.823
64QAM	-11.4	-11.72	0.1968	0.1038	-26.87	-27.27	0.3364	0.24631	24.897	24.062
256QAM	-11.5	-11.61	-0.604	-0.6703	-26.97	-27.08	-0.12	-0.1583	25.924	25.675

VITA

Old Dominion University
Department of Electrical and Computer Engineering
Norfolk, VA 23529

Meena Sreekantamurthy received a Bachelor of Science with a major in electrical engineering from Virginia Commonwealth University in May 2011. Soon after college graduation she joined Huntington Ingalls Industries to begin her career as an electrical engineer specializing in modeling and simulation of electrical power and controls. Eager to attain a higher education in electrical engineering, Meena enrolled in Old Dominion University as a part time student and took several courses in digital and wireless communication engineering. Meena completed her Master of Science in electrical engineering in August 2015.